Analytical Study on Seismic Strengthening of Existing Reinforced Concrete Buildings by Implementation of Energy Absorbers

Pari Yaseen

Submitted to the
Institute of Graduate Studies and Research
in partial fulfillment of the requirements for the degree of

Master of Science
in
Civil Engineering

Eastern Mediterranean University
February 2022
Gazimağusa, North Cyprus

Approval of the Institute of Graduate Studies and Research

Prof. Dr. Ali Hakan Ulusoy
Director

I certify that this thesis satisfies all the requirements as a thesis for the degree of Master of Science in Civil Engineering.

Prof. Dr. Umut Türker
Chair, Department of Civil Engineering

We certify that we have read this thesis and that in our opinion it is fully adequate in scope and quality as a thesis for the degree of Master of Science in Civil Engineering.

Assoc. Prof. Dr. Mehmet Cemal Geneş
Supervisor

Examining Committee

1. Prof. Dr. Mahmood Hosseini
2. Assoc. Prof. Dr. Mehmet Cemal Geneş
3. Assoc. Prof. Dr. Rifat Reşatoğlu

ABSTRACT

When an earthquake phenomenon occurs, it destroys the weak members of the RC buildings, therefore, the damages during severe earthquakes stimulate nonlinear behavior of the structure. The structural and nonstructural damages caused by earthquakes are essentially due to the lateral acceleration and displacements. Accordingly, seismic load evaluation is significant for seismic design assessment and performance. One of the considerable challenges is to establish the optimal design to retrofit existing buildings against the effect of predicted earthquakes with minimal disturbance of the existing structure and the residents in a short time.

This research presents an analytical study of an energy dissipation system for seismic strengthening of existing Reinforced Concrete RC building. The proposed analytical study was conducted to investigate the implementation of SHARK energy absorber to the bracing system of existing building located in high seismic zones of Turkiye. The proposed system, which aims to provide high protection of the structure during severe ULS earthquakes, long-term reliability against wear and fatigue problems, high redundant safety level, easy visual inspection, and easy to replace at low cost along with preventing earthquake damages by controlling the maximum inter-story drifts. The SHARK system performs as a bilinear hysteretic device which consists of fixation plates and a dissipative core that dissipates the energy by a series of hysteretic lamellas.

To investigate the performance of the proposed design and configuration nonlinear time history analyses NLTHA was carried out by applying a pair of 11 selected earthquake records on 8- Story RC buildings. The main investigated parameters which are (i) Displacement, (ii) Inter Story Drift Ratio, acceleration, and Input Energy are studied according to the different configurations of energy dampers. The obtained results of SHARK damper implementation and the absorbed seismic energy showed that the seismic responses of the strengthened structures were significantly higher than the original structures. The maximum displacement and drift reduction values of the strengthened buildings are between 70% and 80% in comparison with their original buildings. Further The maximum acceleration reduction values of the strengthened buildings are between 4% and 20% in comparison with their original buildings. The levels of input energy decreased considerably the reduction is on average about 64% and 70%, as a result the structure was able to resist various earthquakes events.

Keywords: Nonlinear Time History analyses (NLTHA), Hysteretic Damper, Energy Dissipation Device, Seismic Risk

ÖZ

Bir deprem meydana geldiğinde betonarme binaların zayıf elemanlarına hasar verir, bu nedenle şiddetli depremler sırasında oluşan hasarlar yapının doğrusal olmayan davranışını tetikler. Depremlerin neden olduğu yapısal ve yapısal olmayan hasarlar, esas olarak yanal ivme ve yer değiştirmelerden kaynaklanmaktadır. Bundan dolayı sismik yük değerlendirmesi hem sismik tasarım değerlendirmesi ve hem de bina performansı için önemlidir. Önemli zorluklardan biri, mevcut yapıları ve içlerindeki sakinleri en kısa sürede ve minimum düzeyde rahatsız ederek, öngörülen depremlerin etkisine karşı mevcut binaları güçlendirmek için en uygun tasarımı oluşturmaktır.

Bu araştırma, mevcut bir betonarme binanın sismik etkilere karşı güçlendirilmesi için yenilikçi bir enerji sönümleme sisteminin (SHARK) analitik çalışmasını sunmaktadır. Önerilen analitik çalışma, Türkiye'nin depremselliği yüksek bölgelerinde bulunan mevcut binaların çapraz sistemine SHARK adı verilen enerji sönümleyicilerinin uygulamasını araştırmak için yapılmıştır. Önerilen sistem, maksimum katlar arası ötelenmeleri kontrol altında tutarak, şiddetli depremlerde yapının yüksek düzeyde korunmasını, aşınma ve yorulma sorunlarına karşı uzun süreli güvenilirlik, yüksek yedek güvenlik seviyesi, kolay görsel denetim ve düşük maliyetle değiştirilmesinin yanı sıra deprem hasarlarını da önlemeyi amaçlamaktadır. SHARK sistemi, sabitleme plakalarından ve enerjiyi bir dizi histeretik levha ile dağıtan ve enerjiyi tüketen çekirdekten oluşan çift doğrusal bir histeretik cihaz olarak çalışmaktadır.

Önerilen tasarım ve konfigürasyonun performansını araştırmak için doğrusal olmayan zaman tanım alanı analizleri (NLTHA), 8-katlı betonarme binalara seçilen bir çift 11 deprem kaydı uygulanarak gerçekleştirilmiştir. Araştırılan ana parametreler enerji sönümleyicilerin yerleştirilme konfigürasyonlarına bağlı olarak (i) Yer Değiştirme, (ii) Katlar Arası Ötelenme Oranı, ivme ve Girdi Enerjisidir.SHARK sönümleyici uygulamasının elde edilen sonuçları ve emilen sismik enerji, güçlendirilmiş yapıların sismik tepkilerinin orijinal yapılara göre önemli ölçüde daha yüksek olduğunu göstermiştir. Güçlendirilen yapıların maksimum deplasman ve ötelenme azaltma değerleri orijinal yapılarına göre %70 ile %80 arasındadır. Ayrıca Güçlendirilen binaların maksimum ivme azaltım değerleri orijinal binalarına göre %4 ile %20 arasındadır. Girilen enerji seviyeleri önemli ölçüde azaldı, azalma ortalama olarak yaklaşık %64 ve %70'dir, bunun sonucunda yapı çeşitli deprem olaylarına dayanabildi.

Anahtar Kelimeler: Doğrusal Olmayan Zaman-Tanım Alanı Analizleri (NLTHA), Histeretik Sönümleyici, Enerji Dağılım Cihazı, Sismik Risk

DEDICATION

This thesis is dedicated to my beloved parents and fiancé whose endless love, patience, and encouragement have inspired me to pursue and complete this study.

ACKNOWLEDGMENT

With deep gratitude, I express my sincere acknowledgment to all those who contributed to my research work such significant academic accomplishment wouldn't have been possible without their support. I am particularly grateful to my supervisor Assoc. Prof. Dr. Mehmet Cemal GENEŞ for his support, guidance, and helpful comments that he provided for me throughout this study and the duration of my dissertation, which I greatly appreciated. I would also like to acknowledge MAURER staff for their guidance specially, Engineer Dr. Emanuele Gandelli for his valuable information and guidance.

I am grateful to my beloved family, to my father Ihsan for his never-ending encouragement and love through my life, to my mother Majed who willingly accompanied my first steps and every step of the way in my life with all her love, care, and sacrifices. Also, to my siblings, Reema, Salar, for their loving support and specially to Fatimah my little sister for being a big part of my life and for being always there for me, and to my little nieces for their sweet smiles which motivated me through this tough time.

My greatest gratitude goes out to my man Ali for being my greatest blessing, for all the love, care, and patience he has given me throughout the years, and for always being my biggest supporter, best friend, and lifelong partner.

TABLE OF CONTENT

LIST OF TABLES

LIST OF FIGURES

LIST OF SYMBOLS AND ABBREVIATIONS

Δ_i	Story Displacements Difference
AFAD	Disaster and Emergency Management Presidency
ASCE	American Society of Civil Engineers
ATC	Applied Technology Council
BRB	Buckling Restrained Braces
d_{cd}	Displacement Capacity
dMCE	MCE Seismic Design Displacement
dSLS	SLS Design Displacement
EDB	Energy Dissipative Bracing
FE	Finite Element
FEMA	The Federal Emergency Management Agency
FMCE	MCE Max Force
FVD	Fluid Viscous Dampers
F_y	Yielding Force
H1	Is the Recorded Ground Motion in the First Direction
H2	Is the Other Ground Motion 90 Degrees from the Other Recorded
HD	Hysteretic Damper
ISDR	Inter Story Drift Ratio
K_{el}	Elastic Stiffness
K_{pl}	Plastic Stiffness
L	Length Pin to Pin
LDP	Linear Dynamic Procedure
LSP	Linear Static Procedure

MCE	Maximum Credible Earthquake
MS	MAURER SHARK
NDP	Nonlinear Dynamic Procedure
NSP	Nonlinear Static Procedure
PBFD	Performance-Based Force Design
PBSD	Performance-Based Seismic Design
R	Response Modification Factor
RC	Reinforce Concrete
RCED	Re-Centering Energy Dissipative
RC-MRBFs	Reinforced Concrete Moment-Resisting Braced Frames
SHARK	Short-Stroke Hysteretic Damper
SEAOC	Structural Engineers Association of California
SLS	Serviceability Limit State
STSED	Seismic Saw Type Dissipaters
TBEC	Turkish Building Earthquake Code
TEC	Turkish Earthquake Code
TMD	Tuned Mass Damper
ULS	Ultimate Limit State
W	Max Width in Both Lateral Directions
X-X X	Direction of the Building and X Direction of the Earthquake
X-Y X	Direction of the Building and Y Direction of the Earthquake
Y-X Y	Direction of the Building and X Direction of the Earthquake
Y-Y Y	Direction of the Building and Y Direction of the Earthquake
δ	Story Drift

Chapter 1

INTRODUCTION

1.1 General Background

General overview about seismic hazard and earthquakes occurrence in Turkiye, seismic effects on buildings and the damages caused by those earthquakes, seismic strengthening and retrofitting measures, problem statement, research aim, and objectives and outline is discussed briefly in the following sections.

1.2 Seismic Hazard and Earthquake Events in Turkiye

An earthquake is a phenomenon that occurs due to the shaking of the earth's surface developed from a sudden release of energy. The slow-moving of the tectonic plates are restrained at their edges due to friction, as the stress overcomes the friction on the edges, energy is released through the Earth's crust which creates an earthquake(Hu et al., 1996). When a severe earthquake occurs near residential areas, it can cause damages to the reinforced concrete (RC) buildings and result in life and property losses, therefore the buildings and structures are required to be strong enough to resist seismic effects. During severe earthquakes, the RC buildings experience nonlinear behavior. Furthermore, structural, and nonstructural damages are essentially due to lateral displacements and acceleration. (El-Betar, S. A. 2018).

There is a seismic activity zone in Turkiye that ranks second on the planet which is known as the Alpine-Himalayan Belt as demonstrated in Figure 1, The color red represents the highest level of seismic activity which is up to 0.8g There are no fault lines within the white area, which indicates the least seismic activity, and faults are indicated by black lines. The Peak Ground Acceleration (PGA) contour distribution within 50 years will probably exceed 10% (Aşıkoğlu et al., 2019).

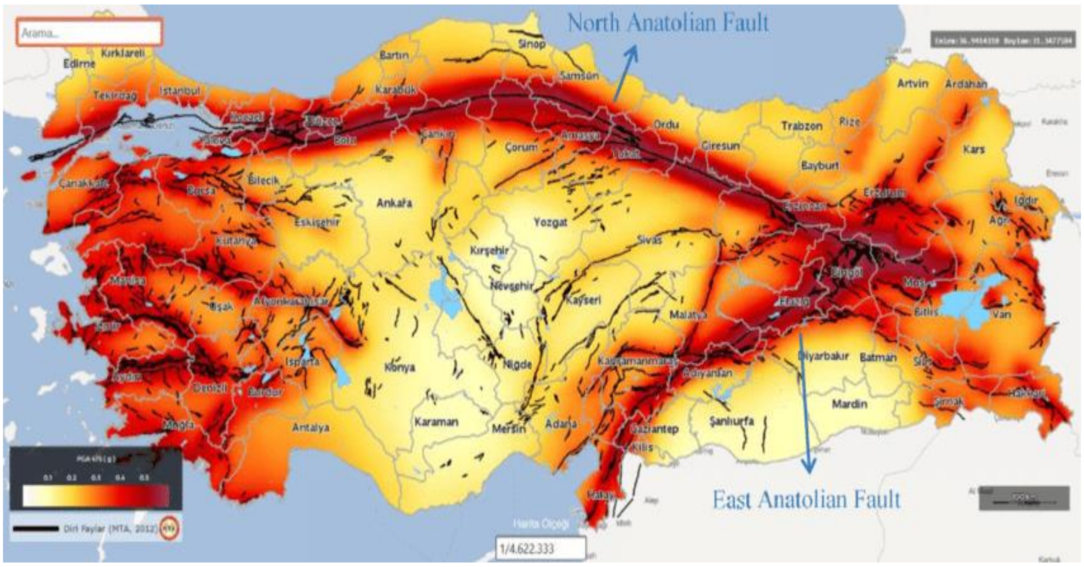

Figure 1. Seismic hazard map of Turkiye (Aşıkoğlu et al., 2019)

The major plate which Turkiye is in known as the Anatolian plate as shown in Figure 2 which it's bounded by two great strike-slip fault zones, the 550 km long East Anatolian Fault (EAF) and 1500 km long North Anatolian Fault (NAF) (Gökkaya, 2016). The fault in As a result of the collision, the Anatolian Plate was formed of the complicated zone between the Eurasian Plate and both the Arabian and African Plates as stated by (Isik et al., 2014).

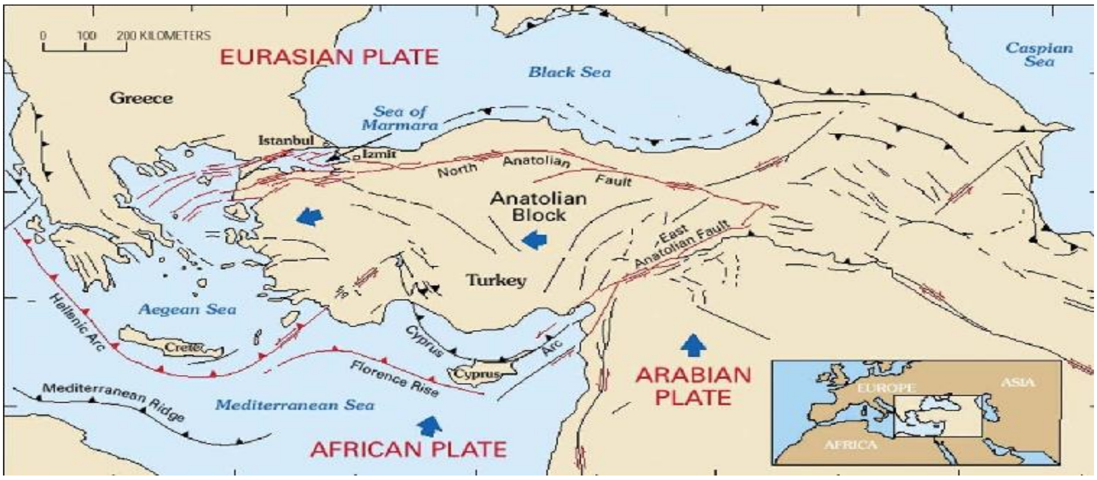

Figure 2. Tectonic map of Turkiye (Gökkaya, 2016)

Due to these faults ruptures more than 800 earthquakes with various magnitudes have occurred in the last 120 years in Turkiye as given in Table 1 according to the obtained data from the Disaster and Emergency Management Presidency, Earthquake Department (AFAD) (Code, 2018).

Table 1. Past earthquakes in Turkiye between 1900 and 2020 (Atmaca et al., 2020)

Earthquake Magnitude	$6 > M \geq 5$	$7 > M \geq 6$	$M > 7$
No. of Events	702	81	17
Return Interval (years)	0.2	1.5	7

Moreover, due to the continued convergence between Eurasian Plate and both the Arabian and African Plates, there is generated energy that is stored and can be released at any moment in the form of considerable earthquakes magnitude. Therefore at least one major earthquake of magnitude ≥ 7.0 can occur in the future (Bulut et al., 2019; Mojarab et al., 2015). The major earthquakes return period in Turkiye is around seven years according to AFAD (Code, 2018) which is a very short-term return interval for a major earthquake. In general, the earthquake magnitude between 7.0 and 7.9 is considered as a considerable earthquake that can cause severe damage or collapse of the buildings, injuries, as well as pose a risk to lives as can be shown in Table 2 from the earthquakes in Turkiye during the past century (Çağatay, 2005).

Table 2. Earthquakes in Turkiye during the past century (Çağatay, 2005)

Date	M_s	Location	Deads	Damaged buildings
1912	7.3	Murefte	216	5540
1928	7	Izmir-Torbali	50	2100
1930	7.2	Hakkari	2514	3000
1939	7.1	Izmir-Dikili	60	1235
1939	7.9	Erzincan	32962	116,720
1942	7	Niksar-Erbaa	3000	32,000
1943	7.2	Tosya-Ladik	2824	25,000
1944	7.2	Bolu-Gerede	3959	20,865
1944	7	Ayvalik-Edremit	27	1158
1949	7	Izmir-Karaburun	1	824
1949	7	Karliova	450	3000
1953	7.4	Yenice-Gonen	265	9670
1955	7	Aydin-Soke	23	470
1957	7.1	Fethiye	67	3100
1957	7.1	Bolu-Abant	52	4201
1964	7	Manyas	23	5398
1967	7.2	Adapazarı	89	5569
1970	7.2	Gediz	1086	9452
1976	7.2	Caldiran-Muradiye	3840	9552
1999	7.4	Kocaeli	15000	50,000
1999	7.3	Duzce	550	3000

1.3 Seismic Strengthening and Retrofit Measures

The existing buildings have much more crucial and seismic resistance problems in comparison to the buildings that have been designed according to seismic precautions. The buildings which have been constructed in high seismic zones if it’s designed to resist earthquakes according to seismic codes it can resist the earthquake adequately as stated by (El-Betar, 2018), (Pinho, 2000). Most of the buildings located in seismic areas demonstrate a failure to be resistant seismic loads due to several reasons indicated below.

The buildings have been designed according to older codes, which primarily focus on resisting gravity loads only. Moreover, the past forty years have witnessed a considerable increase of awareness about earthquake engineering that indeed modern structures do not anymore meet the requirements of constantly evolving codes. Therefore, several deficiencies can be found in existing structures as well as inadequate lateral stiffness, irregular structural configuration, and inappropriate member detailing for ductility.

However, the issue becomes more sophisticated when other aspects, beyond the reach of codes, are taken into consideration. Generally, it is usual for the owners of existing buildings to have structural modifications without any engineering consideration, which results in further obstruction of the structures which might already have low seismic resistance. Moreover, the construction quality may be poor because of deficient design and execution, which may lead to severe consequences, such as the destruction and human casualties in previous severe earthquakes in Turkiye (Pinho, 2000). Thus, the buildings that have seismic deficiencies may cause injuries and casualties besides an economic loss (Tsionis et al., 2014). Most of the existing buildings older than 30 years in Turkiye have been designed and constructed without or with weak methods of seismic resistance precautions therefore the buildings are most likely to experience severe damages even when mild earthquake events occur. To resist earthquakes and prevent failure and collapse of the structures, retrofit, and strengthening of both old buildings that have been designed according to old codes and new buildings but have insufficient seismic-resistant is critically needed.

A preliminary step in seismic strengthening is determining the essential construction characteristics of existing buildings as well as their earthquake resistance capacity. Rehabilitation performance objectives are set, and the seismic hazard level is determined accordingly.

However, it's not simple to work since complicated cooperation, needs to be considered between technical, economical, and social factors, specified for each region. The social factor is considered by the decision on the performance level of the building seismic appraisal and retrofitting. Once the structural features and performance characteristics of the existing building are estimated, under the considered input motion, a selection of a particular retrofitting process along with technical features, economical and social factors is required. According to engineering judgment, the most appropriate measures will be selected to improve the structure's behavior. In general, local evaluates are more suitable when some structure’s components have the inadequate capacity, while comprehensive measures are appropriate in case of major deformation, including irregularities and pounding. FEMA using seismic Techniques Rehabilitation of Existing Structures can be used as guidance for Seismic Assessment and Retrofit (Tsionis et al., 2014).

1.4 Problem Statement

When an earthquake occurs, it damages the weak elements of the RC building, consequently, the building encounters nonlinear behavior of the structure due to damages. The structural and nonstructural damages during earthquakes occurrence are due to the lateral displacements and acceleration of the building. Therefore, seismic load estimation is a significant consideration in assessment and performance-based seismic design. One of the significant challenges that face structural engineers in the present time is the optimal design to retrofit buildings against the impacts of predicted earthquakes in a short period and with minimum disturbance of the existing structural system and the residents as well as minimum seismic strengthening and building retrofit cost.

1.5 Research Aim

The main aim of this study is to introduce and recommend seismic control techniques for an existing RC building to withstand minor earthquakes and avoid major damage and collapse during a severe earthquake. A strengthening procedure involves technical interventions in a building's structure that increase its structural stiffness, strength, or/and ductility to increase its seismic resistance. Furthermore, increase awareness about earthquake impact on existing buildings in highly seismic areas of Turkiye and assure knowledge in design and seismic rehabilitation and strengthening of existing structures which assures to keep human life safe, and that occupants or pedestrian will not be crushed by a collapsed structure, and that the structure can be exited safely. Consequently, this study sought to achieve the following (i) To define a design procedure of seismic retrofitting of existing RC framed building using energy dissipation device based on hysteretic damping; (ii) To estimate the behavior resulting from the implementation of hysteretic Energy Dissipation Devices (EDBs) to the existing building.

1.6 Research Objectives

To accomplish the objectives of this study, it will be addressed as follows:

(i) Review the literature related to the evaluation of the seismic strengthening techniques and investigate the impacts of seismic forces on the buildings and the seismic-resistant design. Further, covering the building materials, plan, irregularities, location, and type of the applied control system.

(ii) Evaluate seismic strengthening of the buildings by the implementation of seismic control systems.

(iii) Develop an earthquake performance-based design model of existing RC building with 8 stories which was constructed 20 years ago or earlier by using ETABS computer software.

(iv) Analyze the buildings according to the codes and standards before and after strengthening against seismic loads through the implementation of an energy absorber.

The proposed study is carried out in two stages which include, collecting data and model analysis. Stage one is carried out to collect data about the selected building structure, seismic area, earthquake records, and MAURER energy absorber. The collected data is utilized in the second stage to develop and estimate accurate three-dimensional modeling and analysis through ETABS software, in which the buildings configurations were modeled, the contribution of earthquakes and their impact on the structure of the building were elaborately investigated under NLTHA considering and comparing the existing frames building and the strengthened frames building by the implementation of MAURER energy absorber.

1.7 Thesis Outline

The present research is implicitly organized into five distinct chapters.

First Chapter: A general overview of the applicable research methodology, a brief explanation of earthquakes in Turkiye and their impact on the existing structures as well as seismic strengthening and retrofit measures of the buildings is presented in this chapter.

Second Chapter: This chapter provides an overview of the most significant literature regarding earthquake-resistant structures and various control systems to resist earthquake loads of existing or new structures.

Third Chapter: An investigation is conducted for detailed explanations of earthquake record selection, scaling, and evaluation, the assessment of building seismic performance, and a method to strengthen buildings with diagonal energy dissipation to enhance their resistance against earthquake loads. Additionally, this chapter presents the details of methodologies and major terminologies.

Fourth Chapter: This chapter presents modeling and analysis results of the considered building and energy absorber using the ETABS program by conducting non-linear time history analysis to evaluate the building's seismic performance based on the earthquake records used as input. then models and analyses the properties of the considered buildings. Furthermore, in this chapter, the seismic response of strengthened buildings has been compared with those of original buildings.

Fifth Chapter: A summary of the most important aspects of the research is provided. In addition, a thorough discussion and conclusion of the main findings and a proposal for future research are provided in this chapter.

Chapter 2

LITERATURE REVIEW

2.1 Introduction

An inclusive overview and background of all the essential aspects of this study are provided throughout this chapter. First, those most used seismic control techniques in various countries and their components are described. Further, the behavior, deformation, stiffness, strength, drift ratio, and displacements are discussed. This chapter also provides an overview of the seismic performance of the buildings subjected to earthquake, including their control system, and the main factors influencing the behavior (i.e., with different plan dimensions, number of stories, concrete and steel quality, structural dynamic parameters, etc.).

2.2 General Overview

Many of the existing buildings in Turkiye have been designed and constructed without any seismic resistance precautions. Therefore, the buildings are most likely to experience severe damages even when mild earthquake events occur. Moreover, the buildings that have seismic deficiencies may cause injuries and casualties besides an economic loss as stated by (Perrone et al., 2019). To address these problems, seismic engineering researchers have focused significant attention on developing retrofit measures and seismic design concepts. Therefore, predicted structural response is no longer thought of as slightly preventing collapse but as accomplishing limited damages with predefined performance levels.

To achieve seismic design the probabilistic analysis is essential because of the large uncertainties associated with forces and structural responses (Benjamin & Cornell, 2014). Moreover, it is not possible to predict the earthquake's occurrence, its magnitude, the features of the rupture surface, and the structure's dynamic response with absolute certainty. Therefore, to evaluate the impact of these uncertainties on the performance of structures and seismic design, probabilistic and statistical methods are required. the other essential seismic engineering concept is that materials must be designed and be prepared to behave inelastically due to severe earthquake loading. The relationship between stress and strain is linear within Hooke's Law, but beyond this point, structural behavior becomes more complicated. Moreover, the Inelastic behavior of the structure was largely investigated using analytical and experimental techniques establish around the 1960s as stated by (Veletsos & Newmark, 1960).

Seismic design of buildings controls displacements and internal forces according to the specified limits to ensure structural safety and comfort. As a general rule, the seismic design of building structures consisted of increasing the earthquake resistance capabilities of the structures utilizing, for example, braced frames, shear walls, or moment-resistant frames. The traditional strengthening approaches can often result in large floor drifts for flexible buildings or large floor accelerations for rigid buildings. Consequently, the structural and nonstructural elements of the building can suffer considerable damages during a severe earthquake, regardless of whether the main structure remains intact. Other countries that experienced seismic events, for instance, Japan, have demonstrated that earthquake-related there can be reduced side effects if suitable A variety of design methods are employed, with an additional cost which is highly insignificant in comparison to the costs of repair and maintenance as a result of earthquake-induced damages. Therefore, in accordance with conventional the earthquake protection of buildings in earthquake-prone areas seismically active zones are required to meet the following requirements: **a.** The main system of the structure must have adequate resistance to be able to withstand medium intensity earthquakes without being damaged, which can impact the structure at least once. **b.** All the structure's elements should have ductility to decrease seismic input energy without collapse. This assures overcoming seismic events without plastic deformation and the safety of the residents. Modern structures can achieve these strengths and ductility benefits without anti-seismic devices if certain design and execution principles are adhered to. Conversely, buildings and structures built according to the old codes don't have high ductility, and even conventional strengthening techniques don't enhance the ductility as they are primarily focused on resistance in the elastic range. Therefore, to achieve a sufficient response to seismic activity or to reduce the structure's vulnerability, the energy can be dissipated through the implementation of the structural control system.

Therefore, to protect the structural and non-structural elements of the building during earthquakes, various innovative low-damage systems have been developed and put into the process to control the seismic response of buildings. One of the considered control systems is the implementation of a passive control system, be composed of Energy Dissipative systems that are attached to the frame of the structure. These regulations are differentiated by distinctive devices capable to considerable dissipate of seismic energy and reduce the inter-story drifts displacement by a significant amount (Constantinou et al., 1998; Marnani et al., 2021; Nikos, 2012; Providakis, 2008).

2.3 Seismic Performance Evaluation

Considering earthquakes occur at indiscriminate places and times with unpredictable frequencies and magnitudes, it's reasonable to evaluate the probabilistic performance of a structure. There are four steps in the performance assessment: seismic hazard assessment, facility response assessment, damage assessment, and loss assessment (Moehle & Deierlein, 2004; Yang et al., 2009).

1. By performing a seismic hazard assessment, the site's seismic vulnerability can be identified by determining which earthquakes magnitudes, distances and, fault mechanisms are more likely to occur at a specific site; this data then serves as a basis for determining records of ground motion which should be utilized for the dependent response analysis.
2. As a result of the seismic hazard analysis, records of ground motion are selected for the analysis of response step to quantify the responses of nonstructural and structural elements. By utilizing the chosen seismic intensity measure, the response statistics relate engineering demand parameters (drift, stress, etc.) to earthquake hazards encountered by the facility.
3. Damage analysis utilizes the observation acquired from laboratory tests, reported data, inspection reports post-earthquake, engineers' opinions, to determine the nonstructural and structural damage component based on an appropriate engineering demand parameter.
4. A loss assessment is performed in the final step to turn damage capacities into judgment variables which can be utilized by engineers, possessor, and other collaborators to determine management of risks. The calculation is conducted

based on repair times, repairs materials quantities, costs of labor, and casualties associated with damages specified through damage analysis.

2.4 Seismic Hazard & Accepted Risk

Since there are numerous amounts of buildings in Turkiye that must be retrofitted and strengthened Seismic Hazard & Accepted Risks must be considered to decide for seismic strengthening of existing buildings and which buildings are more important to start with. A seismic event occurs when tectonic plates move abruptly along the surface of the earth. There are different methods of representing seismic activity, such as site-specific and map-based methods. Under different hazard levels and site conditions, map-based methods determine seismic input by analyzing maps of peak ground accelerations (Fardis, 2005). A response spectrum can be applied to describe the ground movement of an earthquake at a given location using peak ground accelerations maps.

To reach the objectives of seismic retrofitting of existing buildings requires the definition of Identifying ground motions that represent seismic hazards is necessary. As a part of a seismic hazard analysis, a site's strong-motion parameters are estimated to design earthquake-resistant buildings or assess their seismic safety.

Seismic hazard analysis generally involves the use of "probabilistic" and "deterministic" methodologies:

i. The probabilistic method takes into account all the earthquakes that can be predictable to occur at various locations over a specified period, taking into account the uncertainties and random variables.

ii. Deterministic methods estimate the parameters for severe motions based on the maximum predictable earthquake, based on the distance from the site of interest of the maximally likely earthquake without taking into consideration the probability of it occurring within a particular exposure time.

According to the term, a serviceability earthquake is an earthquake that has a 50% probability of being exceeded at least once every 50 years. During the expected service life of the building, there is a good probability of no damage in seismic hazards at this level. A severe earthquake event also known as a maximum considered earthquake (MCE) at a 2% chance of exceeding every 50 years, could cause serious damage without causing collapse. The level of risk depends on the magnitude of the earthquake. The prescribed maximum considered earthquake is governed by the seismic zone and the site characteristics. Nevertheless, such a severe event is very unlikely to occur during the service life of a building. Although it is technically possible to design structures that would not be damaged or collapsed Even during the most destructive earthquakes, however, the process is extremely expensive and non-feasible. Therefore, the buildings have to be estimated as specified previously before strengthening any building. Figure 3 demonstrates an approximately proportional relationship between predictable damage and the level of an earthquake as proposed in design codes (Sahin, 2014).

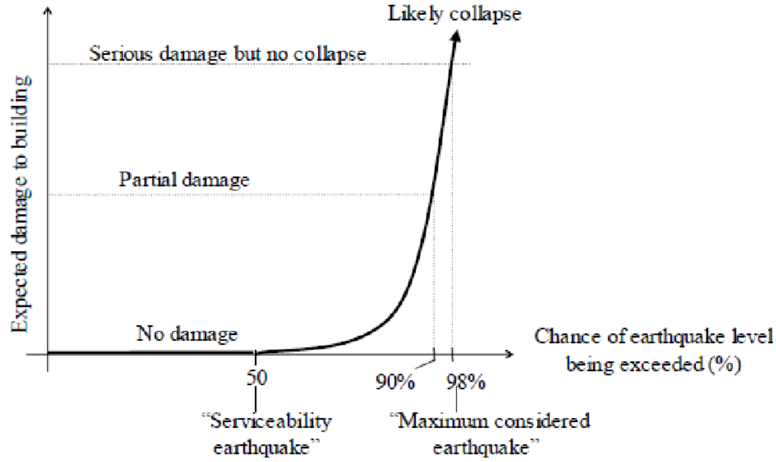

Figure 3. Estimated damage to buildings concerning earthquake intensity (Sahin, 2014)

According to NEHRP's Recommended Seismic Provisions, codes, standards, and industry standards relate to "acceptable risk"," in which the seismic-resistant construction cost is balanced against the potential for improper damages from earthquakes in the future (Abrahamson & Bommer, 2005; McGuire, 2008).

2.5 Seismic Design Procedure

In seismic design, two approaches can be distinguished: force-based seismic design and performance-based seismic design (Lagaros et al., 2006).

2.5.1 Force-Based Seismic Design Procedure

Currently designing for earthquakes in the United States and even in most countries around the globe follows force-based design guidelines Figure 4 below illustrates the process utilized in the codes to determine design base shear. Based on the assumed ductility of the structural system, R stands for the reduction factor of force, and I represents factor of occupancy for more important buildings to increase the design force to more significant structures (Priestley et al., 2007). In the design procedures, the elastic required forces are evaluated based on actual seismic ground motion strength then, the factor R is applied to reduce the elastic required forces (Newmark & Hall, 1969). Lateral forces at various floor levels along the height of the building are determined by using the formulas to measure the structure's dynamic characteristics. Deflection amplification factor Q is multiplied by calculated drift from elastic analysis to determine if the specified limits are met after member section design for strength. To meet the predictable ductility requirements, the detailing specifications must be followed. To prevent severe damages that leads to the collapse of the building, specific structural members, such as columns, are designed using a "partial design capacity process." (Goulet et al., 2007; Liao, 2010) The process is reiterated until the drift and strength demands are achieved.

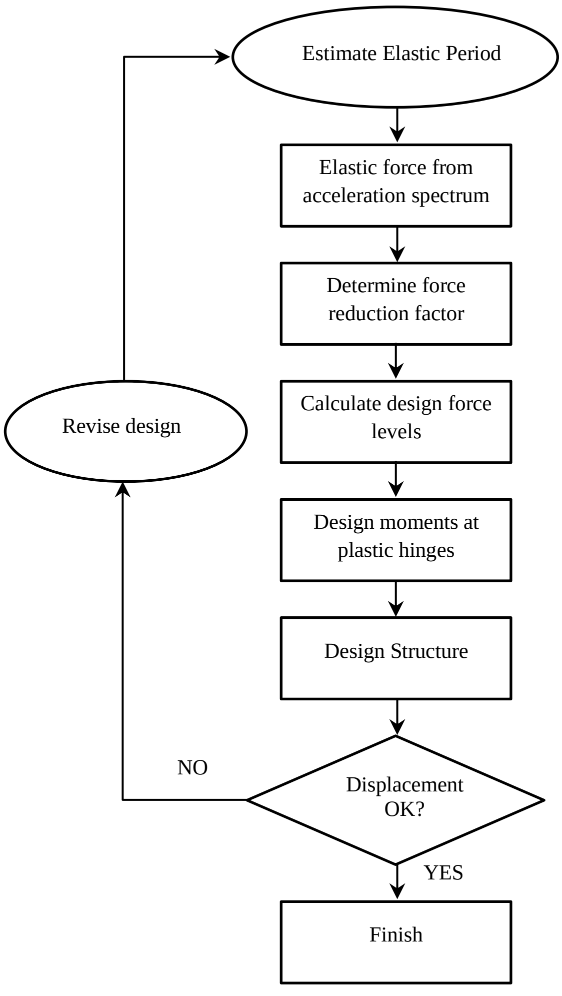

Figure 4. Force-based design (PBSD) flow chart (Priestley et al., 2007)

i. Assuming the increase of the design base shear could ensure safety or reduce damages of the structure: As a result of local column damage, the collapse has been observed in various previous earthquakes.

ii. According to elastic behavior, consider the design lateral force allocation through the height of the building: previous studies have shown that based on elastic behavior, the lateral force distribution along the building height could diverge significantly from what the nonlinear time-history dynamic analysis NLTHA as stated by (Chao et al., 2007). Hence, maximum inter-story drifts will not necessarily be uniform along with the height. The nonlinear dynamic analysis conducted by (Verde, 1991) also showed that lateral forces were distributed depending on the codes without taking into account that structures could become inelastic during severe earthquakes, this may be the primary reason for several upper stories collapses that occurred during the Mexico City quake in 1985.

iii. Using initial stiffness from an elastic analysis to proportion member sizes: Based on the proportional elastic stiffness of the members of the structure, the magnitude of member forces is determined from elastic analysis. However, some members become stiffer if they are subjected to severe earthquakes as the concrete cracks or the steel yields, while the stiffness of others may remain the same. As a result, the members of the structure then experience a different force allocation. To achieve the appropriate proportioning of structural members sizes, the force distribution needs to consider the predictable inelastic behavior.

iv. Predicting inelastic displacements with approximate factors and analysis behavior: various previous studies have found this to be unrealistic, particularly for structures where energy dissipation characteristic and hysteretic behavior degrade (Chao & Goel, 2006; Sabelli et al., 2003).

v. Eliminating yielding of the column by implementing an individual column-to-beam strength ratio: Various studies have found that traditional capacity design approaches cannot completely exclude the yield of moment frames in reinforced concrete structure (Dooley & Bracci, 2001; Kuntz & Browning, 2003). A column's moment demand is usually neglected because the columns are not only exposed to the moments imposed by their framing members but furthermore those imposed by their lateral displacements (Bondy, 1996).

2.5.2 Performance-Based Seismic Design Procedure

Performance-Based Seismic Design (PBSD) methods ensure that investors and users will meet their needs and goals with the structure's predetermined expected response to relatively minor and severe earthquakes Figure 5 below shows a flow chart of the main stages of the design process. Seismic Performance-based Design (SPBD) was initiated by the Structural Engineers Association of California (SEAOC), Federal Emergency Management Agency (FEMA), Applied Technology Council (ATC), and American Society of Civil Engineers (ASCE) with the primary goal of replacing the existing design with a new approach based on acceptable structural performance under a certain degree of earthquake load (Šipoš et al., 2018). A performance-based design process initiates the identification of performance objectives, follows by establishing a tentative formulation, testing how it meets the performance criteria, and eventually re-designing and reassessing it, if needed, until the desired performance level is achieved.

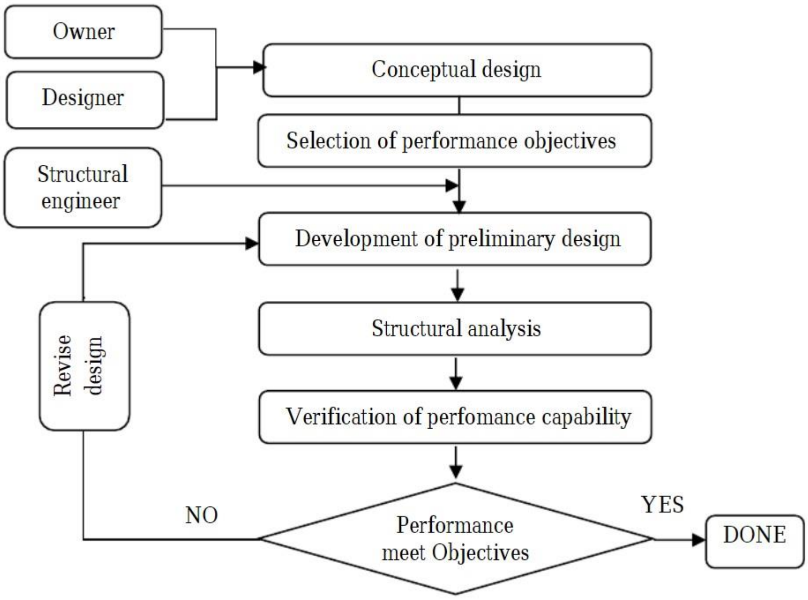

Figure 5. Performance-based seismic design (PBSD) flow chart (Šipoš et al., 2018)

According to ASCE 41-06, there are 4 analytical methods to analyze the performance-based design of a structure (ASCE, 2007):

- Linear Static Procedure (LSP).
- Linear Dynamic Procedure (LDP).
- Nonlinear Static Procedure (NSP).
- Nonlinear Dynamic Procedure (NDP).

According to the above list, both the complexity of the Cost of computation and procedure are primarily increasing. The simplest of all is the linear static procedure, while the nonlinear dynamic process is the most difficult one and requires the most computation power. Following ASCE 7-05 provisions for seismic activity, analysis of linear static or analysis of linear dynamics can be used to determine a structure's design forces but is not regularly precise compared to real earthquake loads. According to prevalent belief, engineers expect conservative results from nonlinear models when using linear limits on building response. ASCE 7-05 recommends designing structures so that they can withstand local stresses while remaining structurally stable in the long run (Ellingwood & Li, 2009) in this study the nonlinear dynamic procedure has been applied.

2.5.2.1 Nonlinear Dynamic Procedure (NDP)

The nonlinear dynamic procedure (NDP) demands the use of a model analyzed mathematically incorporating the components with nonlinear characteristics. Instead, determining the design displacements through target displacement based on the NSP, the calculations are performed by utilizing the time histories ground motion. Time histories of ground motion have to be specified according to the site of the structure. Due to the explicit simulation of nonlinear response, the internal forces should not be adjusted, furthermore, the displacements are capable of being immediately correlated to the requirements and a set of criteria for acceptance (Prestandard, 2000). According to TBEC eleven ground motions are required to analyze the model. In terms of its basis and modeling approach, the NDP is similar to the NSP. In cases of seismic loading, nonlinear dynamic techniques can provide the most accurate results. However, a time history analysis is not always carried out on all buildings due to time and engineering costs (Fema, 2012).

2.6 Seismic Strengthening Techniques of Existing Buildings

Seismic retrofitting that is effective requires it is critical to have an inclusive comprehension of the predictable response to a seismic event and all the deficiencies of the buildings that already exists. Considering the importance of both gravity load resistance and lateral stability, the retrofit emphasizes based on vertical alignment elements (e.g., columns, braces, walls, etc.). In contrast, the structure is insufficiently attached with each other for earthquake loads even though the columns and the walls are appropriate for gravity and seismic loads. Generally, improving the performance of existing buildings relies on increasing stiffness, strength, the capacity of deformation, and enhancing the connections with a total load path.

To assess whether retrofitting is necessary, the following technical issues need to be considered (NEHRP, 2006);

- Having a complete load path is essential.
- To comply with design standards, it should be strong and stiff.
- The system needs to be adaptable to lateral and gravitational forces systems already in place.

Several non-technical factors can significantly influence the chosen solution system. These are listed below (NEHRP, 2006);

- Retrofit methods will be significantly influenced by the seismic performance expectations of dominant authorities or objectives that intend to minimize damage or allow continued occupancy.
- In determining the retrofit methods, cost, or short-term disruption to building users, as well as contents that need to be protected seismically are always significant considerations.
- The functionality of the building over the long term is affected by adding members to the inside of the building which will constantly alter the functionality and decrease the flexibility of an existing building.
- As for aesthetics, historic properties impose limitations on performance objectives because of their preservation.

2.7 Seismic Structural Control Systems

A seismic design of structures uses an elastic design spectrum to determine the forces that will apply. The inelastic energy dissipation of the material is taken into account by utilizing a response modification factor (ASCE, 2014). Structures can sustain damage from severe earthquakes without collapsing because of the ductility of their members and the redundancy of their load paths. However, as a result of the inelastic behavior, the structural and non-structural members occasionally suffer significant damage and collapse. Therefore a significant development has been occurring over the last decade in methods and techniques for controlling structural behavior of buildings under dynamic loads due to earthquakes (Symans et al., 2008). This section describes the seismic control techniques intended to reduce the vulnerability of new or existing buildings that built-in seismic zones with medium to high activity. The earthquake-resistant design incorporates various types of seismic control systems to decrease the effects of seismic forces on the building's essential structural elements. In general, structural control systems are classified into four general types based on the device type they use: active, semi-active, hybrid, and passive (Castaldo, 2014).

2.7.1 Active Control System

The active system, which incorporates active, hybrid, and semi-active systems, is characterized by controllable force devices combined with controllers, sensors, and real-time information processing in which the structures are controlled or modified employing a control system based upon some external energy source (Soong & Costantinou, 2014). Electromechanical or electrohydraulic actuators are typically used to control the forces in active control systems based on feedback information from measurement responses, or feedforward information from external stimulation (Symans & Constantinou, 1997). Furthermore, structures with active control systems consist of (i) sensors mounted around the structure to monitor external excitations or structure response variables, or both; (ii) Active control devices can process the measured information and computing the required control forces according to a control algorithm; (iii) Extrinsic energy is frequently used to power actuators to generate the forces they need. The structure response is controlled by closed-loop control when it is monitored and used to correct the applied control forces because the structural response is continuously monitored and corrected as necessary throughout the process (Soong & Costantinou, 2014).

2.7.2 Passive Control System

A passive system includes various materials and devices available to increase structural strength, stiffness, and damping. Shock mitigation using passive seismic control is a concept that makes use of passive methods. There is no need to add any additional energy sources to the system to achieve mitigation. Rather, they use motion input from earthquakes to initiate seismic control. Passive control and the passive energy dissipation devices types such as Dynamic Oscillators, Base Isolation System, and Energy Dissipation Devices are briefly discussed (Housner et al., 1997; Soong & Dargush, 1999). In a seismic isolation system, earthquake energy is not absorbed, but rather deflected by the system's dynamics. A seismic isolator dampens seismic energy transmission to the buildings by reducing vibration frequency, it allows a building to displace or move, and reduces shock acceleration of the earthquake, therefore preventing the upper floors from moving more rapidly than the lower stories. Generally, those buildings that are isolated in this manner experience third to a fifth of the horizontal acceleration experienced by conventional structures during earthquake occurrence (Sadek et al., 1996).

Seismic control devices are at the moment, the most reliable and functional methods to reduce structure's seismic response. The effectiveness of these systems is highlighted through a detailed earthquake damage assessment, there can be a considerable reduction of seismic impacts on the main structure to be protected. Figure 6 illustrates how traditional seismic design and control systems design would affect the response of a building (Constantinou et al., 1998; Gkournelos et al., 2021).

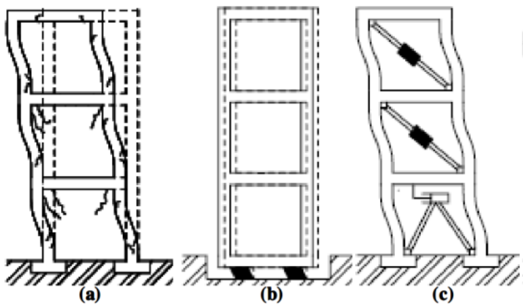

Figure 6. (a) Traditional seismic design, (b) seismic isolation system, and (c) energy dissipation devices (Gkournelos et al., 2021)

2.7.2.1 Seismic Isolation System

One of the main seismic isolation intentions is to distribute seismic energy dissipating it by decreasing the acceleration acquired by the structure as well as diverting the fundamental frequency of the structure from the predominant frequency of seismic ground motion and the fundamental frequency of the superstructure. The overall design approach aims to achieve this by isolating the structure from its supporting foundation, in the horizontal plane (Buckle & Mayes, 1990). Seismic base isolation is based on two main concepts, despite the wide differences in characteristics. In the first concept, using flexible supports, the impact of horizontal ground acceleration is minimized by ground isolation systems. Consequently, a structure with this fundamental frequency of a structure with a fixed base is much lower. The isolated structure's first dynamic mode only the isolation system is deformed, while the upper structure remains rigid. Deformation in the structure is caused by higher modes that are orthogonal to the initial mode and, subsequently, to the ground motion. Since these high modes don't contribute to the motion, at these higher frequencies, this energy cannot be transferred into the structure because it is high in the ground motion. With a friction surface between the base of a structure and the foundation, the second concept of an isolation system allows a structure to be more flexible. As a result, the transmission of shear force from the interface to the superstructure is limited. The shear force varies according to the friction coefficient and the weight of the superstructures, so the lower the friction's coefficient, the lower is the transmitted shear forces. Nevertheless, the friction force must be sufficient to withstand winds and slight earthquakes without sliding (Naeim & Kelly, 1999).

2.7.2.2 Base Isolation System

The technique of base isolation provides an isolation level is included between the foundation and superstructure to facilitate a greater range of variation in dynamic response characteristics than that of a fixed base configuration Figure 7. As seismic isolation systems are intended to dissociate the structure of the building from the earthquake input motion that causes damage. i.e., The superstructure of the building should be protected from seismic energy absorption to protect the structure from damage. All the superstructure's components must be supported on distinguished isolators with dynamic characteristics designed to isolate the shaking of the ground from the superstructure. The displacements and yields are concentrated in the isolation devices, and the structure behaves like a rigid body, Therefore, the natural frequency is decreased since the natural period of the structure is increased (Castaldo, 2014; Deb, 2004). As a result of the seismic energy being absorbed, the isolation device is composed primarily of a thin sliding surface, rubber bearings, or flexible members.

These techniques are highly effective at reducing the acceleration of responses and inter-story drifts, which result in a significant reduction of structural and non-structural damages. Both (Mokha et al., 1996) and (Pan et al., 2005) provide successful practical applications of the method. Nevertheless, they are very expensive solutions, and they can't be applied to general intend buildings (Skinner et al., 1993).

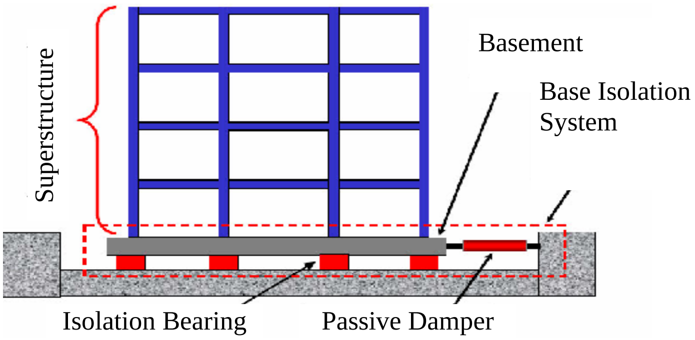

Figure 7. Base isolated structure overview (Skinner et al., 1993)

2.7.2.3 Dynamic Oscillators

A dynamic oscillator transforms seismic energy between vibrating modes when it encounters seismic waves. Tuned mass damper, better known as TMDs are common dynamic oscillators used in construction. TMD utilizes masses, as the structure moves when seismic force is applied to the structure, the control system partially absorbs the kinetic energy received by the structure as shown in Figure 8. A passive TMD is designed to reduce vibrations in flexible structures affected by long-term narrow band stimulation (Villaverde & Koyama, 1993).

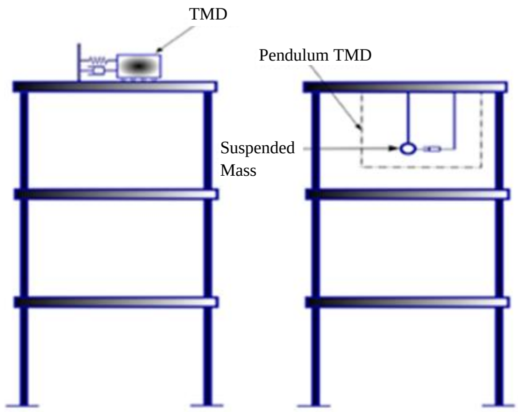

Figure 8. TMD at the top of the structure (Inaudi & Kelly, 1995; Sadhu & Narasimhan, 2012)

The reduction in TMD does not necessarily mean a reduction in the peak distortion demand in a structure subject to ground shaking, but it alleviates the corresponding damage level (Pinkaew et al., 2003; Sladek & Klingner, 1983) According to (Almazán et al., 2007) they study An alternative system for TMD, BH-TMDs, and more specifically, the bidirectional and homogeneous tuned mass damper, consist of a pendular mass attached to a friction damper that's oriented perpendicular to the direction of movement. The geometry of the device causes an energy dissipation increases quadratically with displacement amplitude (Inaudi & Kelly, 1995; Sadhu & Narasimhan, 2012).

2.7.2.4 Energy Dissipation Devices

The mechanical system linked to the building structure allows the building structure to withstand earthquake energy by absorbing a considerable amount of energy input from seismic activity, without deforming and yielding, therefore protecting the building structure from damage (Franco et al., 2010). There are different types of energy dissipation systems that are classified according to their ability to improve structural system dissipation energy.

The energy dissipating devices in framed structures are generally inserted in braces of steel between two sequent stories of the structure as shown in Figure 9. The inter-story drifts accommodated by the building when a seismic event occurs stimulate the energy dissipating devices before the essential members of the structure are involved in their inelastic behavior. Accordingly, the main objective of the current design strategy employed for energy dissipating devices is to substantially reduce the demands for ductility on structural members made of RC as stated by (Dolce et al., 2005). Thus, the system that supports gravity loads and the system that dissipates energy during an earthquake are discrete systems.

According to (Reinhorn et al., 1995) It has been shown that the implementation of energy dissipation devices greatly improves the overall capacity of old seismic codes or RC frame structures designed to bear gravity loads. The energy dissipating devices initially depends on the Most plastic hinges developed for columns have low energy dispersal capacity and rapidly deteriorate in rigidity and strength. accordingly, it's observed that structural vibrations have been significantly reduced (Aiken et al., 1993).

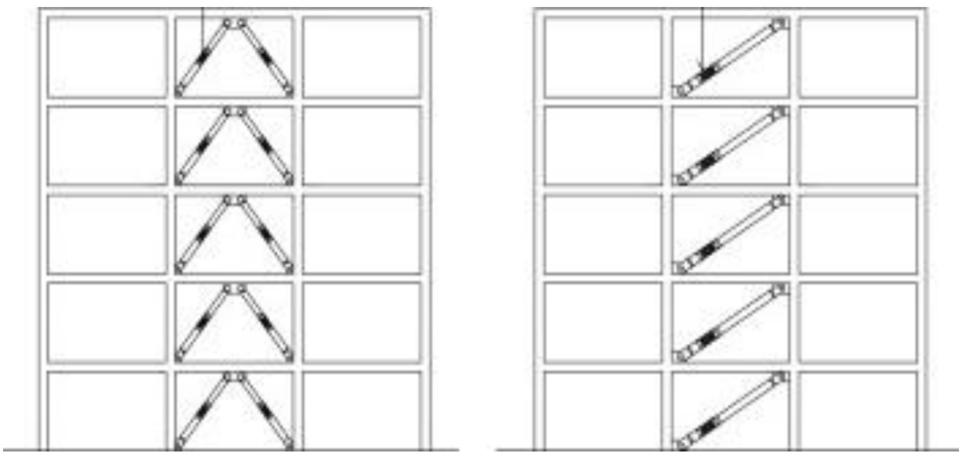
Figure 9. Energy dissipation system in structure (Aiken et al., 1993)

2.7.2.5 Seismic Energy Dissipation Principles

The seismic loading affects the reinforced concrete (RC) building with no masonry infill walls at the ground floor because of the discontinuity in the lateral stiffness and strength along with the building height. As a result, under the seismic loading, the ground story columns will be subjected to inelastic deformation and an excessive lateral load, consequently, the soft story of the building will collapse. (Sahoo & Rai, 2013) The seismic performance of the buildings can be enhanced either by decreasing the seismic demand or by local modifications i.e., strengthening columns of the ground floor through the implementation of energy dissipation systems.

2.7.3 Previous Research on Selective Seismic Control Techniques

Previous research on selective techniques for structural strengthening of reinforced concrete (RC) buildings has focused on evaluating the characteristics of the control system and showing their efficiency to achieve the performance objectives. The authors of such studies do not design their plans primarily to strengthen ductility, but rather to comprehensive strengthening to the entire system and reduce the inter-story drift. All the covered previous studies on strengthening techniques are based on the employment of various energy dissipation devices are discussed below.

2.7.3.1 Energy Dissipation Devices

2.7.3.1.1 Metallic Yielding Dampers

According to (Khampanit et al., 2014; Sahoo & Rai, 2010) studies, existing RC structures cannot be modified to increase longitudinal steel percentage or reduce the transverse stirrups size at the projected locations of plastic hinges. As a result, RC structures were modified using external intervention techniques. One of the efficient intervention techniques that takes advantage of passive energy dissipating devices is their ability to dissipate seismic energy, therefore decreasing the deformation and load on the existing RC members. Studies have shown that RC structures' seismic performance is enhanced with the use of metallic yielding dampers.

In the conducted study by Khampanit et al. buckling-restrained braces (BRBs) were applied to strengthened non-ductile Reinforced Concrete (RC) frame, the results showed that in the presence of the BRBs, stiffness, lateral force capacity, and energy dissipation were significantly increased. Further, the loops in the strengthened specimen Figure 10 were extremely stable and showed virtually no pinching, as the behavior of a system with a bilinear hysteretic response. Figure 11 showed the yielding of the RC frame that has been assumed at 1% drift, and 0.25% yielding of the BRBs is calculated based on the configuration of the BRBs.

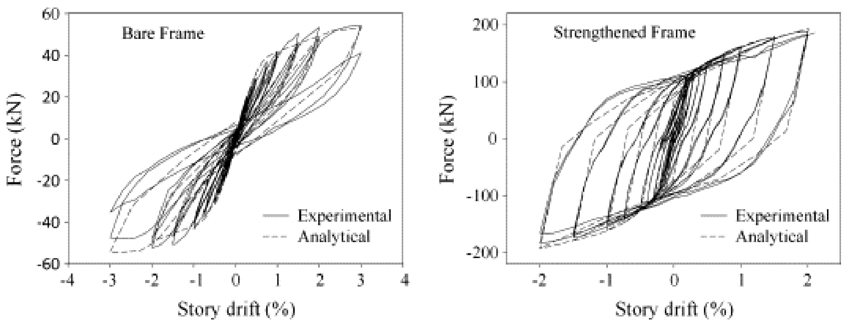

Figure 10. Comparison of loops in the strengthened specimen and the bare frame (Khampanit et al., 2014)

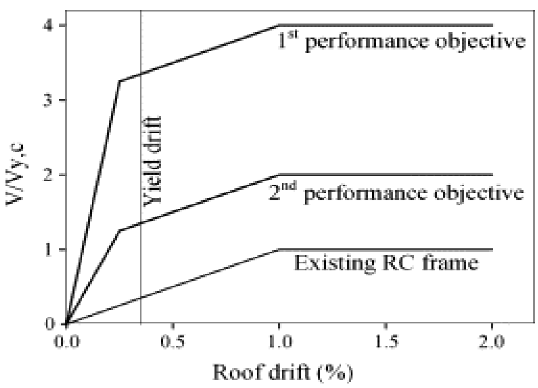

Figure 11. Yielding of the BRBs (Khampanit et al., 2014)

2.7.3.1.2 Energy Dissipative Bracing (EDB)

A conventional braced system failed to withstand earthquakes due to a weak connection between frame and bracing, and a limited capacity for ductility, low energy dissipation (Sabelli et al., 2003). Therefore, several retrofitting strategies are suggested by various codes such as FEMA and ASCE to evaluate excessive casualties or collapses of the damaged RC buildings (Agency, 2006; NEHRP, 2006; Pekelnicky et al., 2012). Energy Dissipative Bracing (EDB) systems are incorporated into a structure's frame. The system is distinguished by the capability to dissipate seismic energy and significantly minimize the braced structure inter-story drifts (Constantinou et al., 1998; Tsai et al., 1993).

According to (Rabi et al., 2021) study proposed a retrofit technique for existing reinforced concrete (RC) buildings by using an energy-based passive Energy Dissipative Bracing (EDB) system design. Pushover and non-linear dynamic analyses have been conducted to compare their performance. According to the results, the proposed technique is effective in avoiding the concentration of damage at a single story and providing a proportional distribution of the added strength provided by EDBs along with the height of the structure.

2.7.3.1.3 Hysteretic Energy Dissipative Bracing (HEDB)

Based on statistical analyses of nonlinear dynamics performed by (Di Cesare & Ponzo, 2017) on approximately a thousand case studies have shown the effectiveness of supporting at least one design approach to retrofit RC frame building through a hysteretic bracing system. The study aimed to achieve a maximum top displacement in response to seismic demand, furthermore, the proposed procedure imposes a maximum inter-story drift limit based on the size of the drifts between floors.

Moreover, this research recommended a simplified process for configuring a dissipation system according to linear analysis plus the employment of an appropriate behavior factor, to facilitate the common implementation of passive control methods. According to (Di Cesare et al., 2014) the mechanical characteristics of the dissipating system were evaluated experimentally and numerically using a displacement-focused design procedure to limit inter-story drifts after the yielding of the frame. Experimentally two design solutions for chevron braces with a Hysteretic Dissipation system have been tested, using similar stiffness but with different yield strength and ductility requirements. Furthermore, the nonlinear time-history analysis, results showed that the design procedure provides a lower limit of yield-load variation over which Maximum acceleration and Maximum Inter-story Drift Ratio become constant. With the yield-load variation of about 50%, the devices will dissipate the maximum amount of energy corresponding to an appropriate maximum required ductility.

2.7.3.1.4 Dissipative Energy Device Based on The Plasticity of Metals

According to (Franco et al., 2010), tests and analyses have been conducted to validate the utilized device which was designed based on the metal's plasticity when applied tangential stress through torsion. The results showed that a uniform hysteretic behavior was observed on the device, with loops that demonstrated regular and symmetrical shapes. Further, low-cycle fatigue strength is high in this device. The presence of early plasticity behavior leads to an early dissipation of energy.

2.7.3.1.5 Seismic Strengthening for RC Frames with Soft Ground Story

Sahoo and Rai worked on the improvement in seismic performance of non-ductile RC framing with a soft story at ground floor level which can be accomplished through two different strengthening techniques. Column retrofit is the first technique to increase the strength, stiffness, and rotational capability of the deteriorated columns of the ground-story only by adding partial steel caging. The second technique, referred to as a full retrofit, utilizes aluminum shear links considered as additional means of dissipating energy, along with strengthened columns of ground stories as shown in Figure 12. The RC frame transfers its lateral load to these dissipating devices using steel collector beams and chevron braces. For assessing the structural performance of the existing and strengthened frames, nonlinear static and dynamic analyses are performed. The investigated parameters are (i) inter-story drift, (ii) residual drift, (iii) energy dissipation (iv) yield mechanism, and (v) lateral strength. Because of the large energy dissipation in the shear links, the fully retrofitted frame controlled the drift response effectively by avoiding the collapse of the soft story In addition, the fully retrofitted frame achieved the required yield mechanism without exceeding the design target drift. (Sahoo & Rai, 2013).

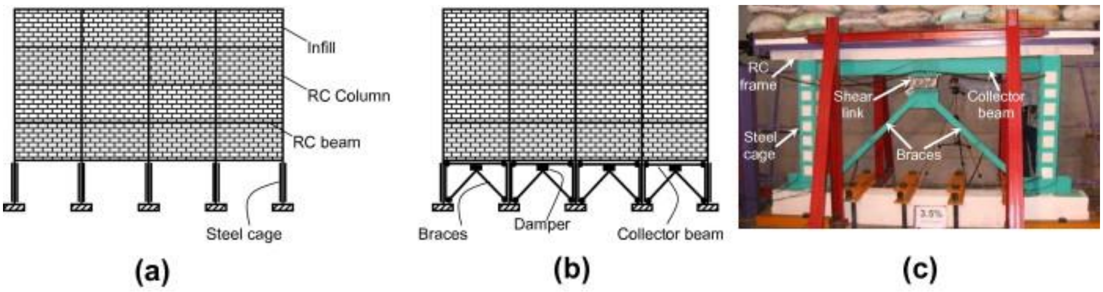

Figure 12. (a) Diagram of the column retrofitted frame, (b) diagram of the fully retrofitted frame, and (c) fully retrofitted frame with different elements depicted in detail (Sahoo & Rai, 2013).

2.7.3.1.6 Seismic Design of RC Braced Frames with Metallic Fuses

According to (Tena-Colunga & Nangullasmú-Hernández, 2015) parametric study focused on evaluating the seismic design for various reinforced concrete moment-resisting braced frames (RC-MRBFs) by the implementation of hysteretic energy dissipating device braced with a chevron of steel through the application of static nonlinear analyses. According to the results, the suitable mechanism is achieved based on the defined stiffness balances in which initially, the hysteretic devices system yield and enhance the maximum local displacement ductility, however in the moment frame initiation of yielding is only observed at the ends of the beam.

2.7.3.1.7 Saw Type Seismic Energy Dissipaters

(Demir & Husem, 2018) researchers conducted experimental, numerical, and theoretical studies such as nonlinear finite element (FE) analysis of Seismic Saw Type Dissipaters (STSED) which have high dissipation capacity to protect buildings from earthquake damage during strong seismic activity. STSED consists of a set of specially shaped metallic yielding components that dissipate energy through yielding in flexure. Static and symmetric hysteretic behavior of the STSED has been demonstrated under cyclic loads with fast energy dissipation and no abrupt strength degradation. STSED reached up to 3.33 times the design displacement before losing its load-bearing capacity and demonstrated impressive ductility (13.98 experimentally, 14.43 numerically). Further, because of the test, the equivalent viscous damping ratio ranged between 21.87 and 45.16 percent.

2.7.3.1.8 Recentering Energy Dissipative Brace

Since strong earthquakes will cause large residual drifts in steel frames, (Zhang & Ye, 2019) researchers developed a re-centering energy dissipative (RCED) brace that could pull steel frames with a friction damper back to their original positioning after the occurrence of an earthquake. The results indicate that the RCED- braced frame dissipated almost all the energy.

2.7.3.1.9 Adaptive Hysteretic Damper

According to (Gandelli et al., 2021) study investigates the force-displacement response of the Adaptive Hysteretic Damper AHD and proposes and validates a simple linear equivalent design method for braced buildings implemented with AHD. After developing the seismic-retrofit intervention, it is applied to the design of a real-life hospital case-study. In buildings that contain high-technological components, such as hospitals and emergency centers, high peak floor accelerations would be detrimental to sensitive non-structural features. These components include electric network, elevators, false ceilings, and computers whose integrity is essential. Therefore, Adaptive Hysteretic Damper AHD has been developed which can modulate their damping and stiffness based on the intensity of the quake (e.g., peak ground acceleration) so that: (i) the peak ground acceleration is reduced, and the nonstructural elements protection is enhanced when the quake is a minor earthquake; and (ii) there is no adverse impact on structural safety when a major earthquake occurs.

2.7.4 The Present Research Seismic Control Technique

In this research MAURER SHARK (Short-Stroke Hysteretic Damper) energy dissipation system is incorporated into an existing reinforced concrete building located in Turkiye, this seismic system is developed to enhance the seismic performance of the building by, limit inter-story drift, while preventing the damages of the structure caused by a seismic event. Nonlinear Time History Analysis is conducted to investigate the system performance to decrease the input energy, drift, displacement, and acceleration. A description in detail of the system and the analysis are presented in chapter 3.

Chapter 3

METHODOLOGY

3.1 Introduction

The procedure used to conduct this study is outlined in this chapter and associated numerous steps such as model details and modeling method, earthquake record selection, scaling, and evaluation of earthquake data, building seismic assessment, performance-based earthquake engineering, and finally, proposing a method for building strengthening by using diagonal energy dissipation. Also, this chapter contains some specific details of methods and major terminologies.

3.2 Research Methodology

A three-stage process is followed in this research methodology. The first stage consists of designing two different buildings with different configurations, materials, and numbers of stories, etc. The second stage consists of the implementation of MAURER SHARK energy dissipation device in the braced frame of the designed buildings in different installation placements. Finally, the third stage consists of evaluating the performance of the original and the strengthened building and comparing them based on the results obtained from nonlinear time-history analyses by applying 11 pairs of earthquakes to the buildings.

3.3 Introducing Buildings Bracing System

3.3.1 MAURER SHARK Energy Dissipation Device

3.3.1.1 Implementation in The Bracing Systems of The Building

SHARK Damper is an inventive energy dissipation device that can provide absolute structural safety and reduce the risk of potential damage caused by earthquakes. The design, testing, and quality management of the bracing system comply according to EN15129. The SHARK device shown in Figure 13 is made of steel, its innovative design, represents a simple but extremely efficient energy absorber. When the structure be subjected to loads, the damper operates within its elastic system and acts as a rigid spring to provide structural support. When an earthquake occurs, the SHARK's specially shaped hysteretic lamellas experience plastic deformation to dissipate seismic energy.

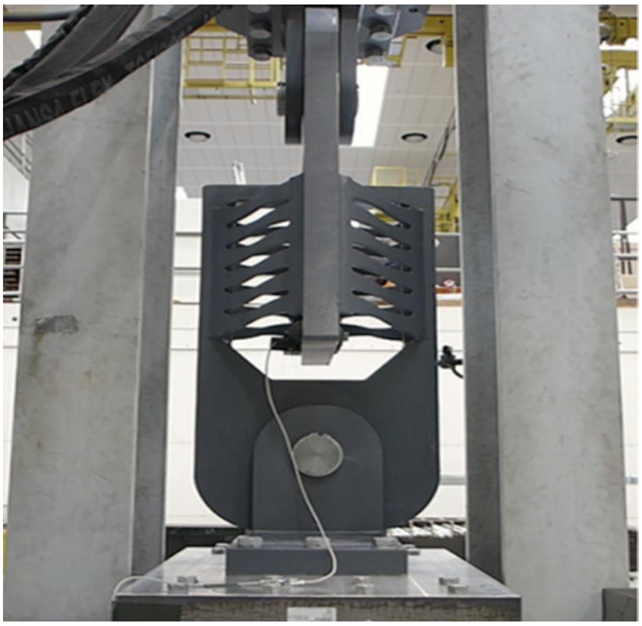

Figure 13. SHARK performance at max tension

On the four faces of the hollow section of the dissipative core shown in Figure 14 below, there are a series of hysteretic lamellas which dissipate the energy. For severe ultimate limit state (ULS) earthquakes, the damper provides stable and reliable performance. The damper can endure up to 4-5 MCE events without any failure due to the special shape of the lamellas. It is important to note that the parallel redundant configuration of lamellas assures high safety even after multiple earthquake excitations since, after an unavoidable failure of one lamella, the rest offer proportional resistance and damping functions. This seismic system is developed to limit inter-story drift, while prevention the damages of the structure caused by a seismic event, by incorporating MAURER SHARK into the building's reinforced concrete or steel frame bracing system. The configuration of SHARK is shown in Figures 15. Table 3 provides the sizes and performance data of SHARK. Furthermore, there is second form known as SHARK-Adaptive which minimizes the accelerations at each level to ensure better protection of sensitive non-structural components. The SHARK-Adaptive damper features a unique “two stage” hysteretic loop that allows for adjustment of effective stiffness and damping based on the intensity of the earthquake. In this study SHARK have been applied to Deniz building.

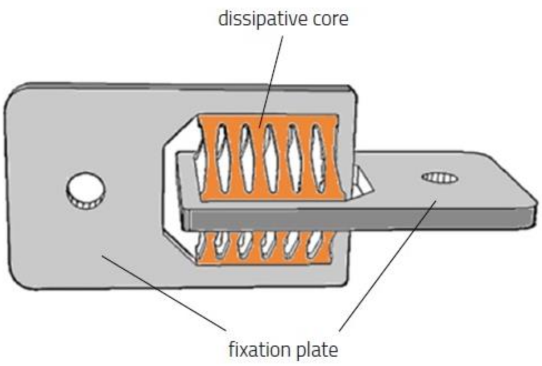

Figure 14. SHARK damper dissipation core and fixation plate

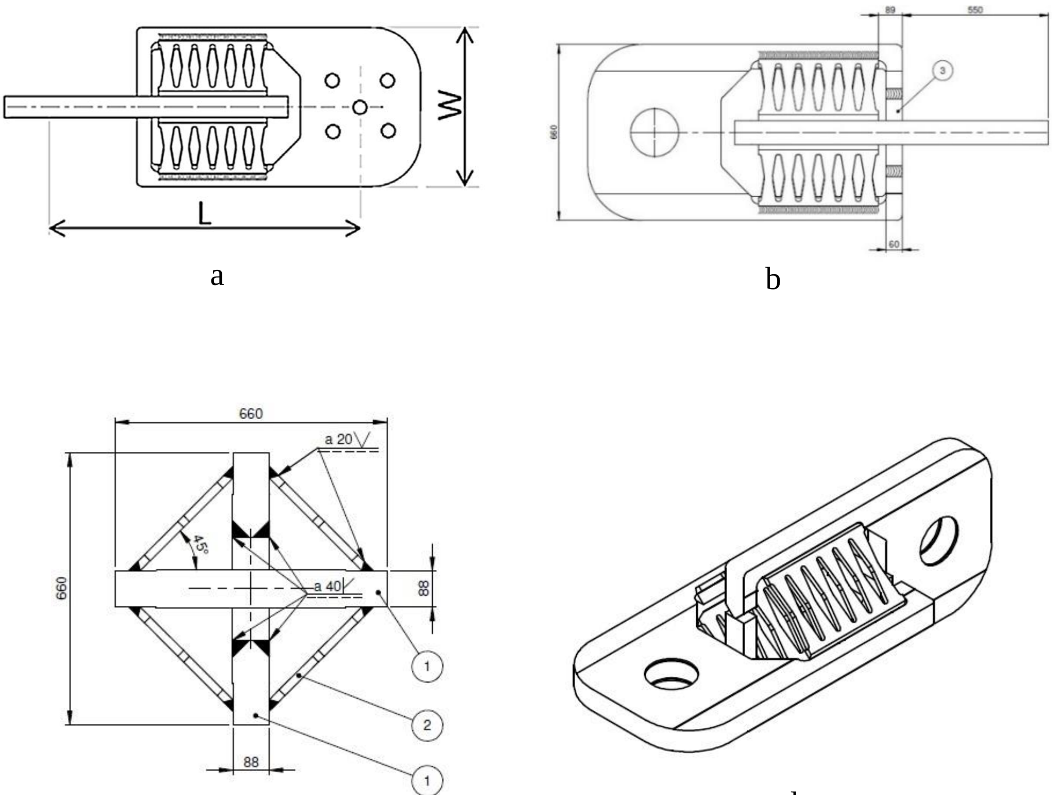

Figure 15. MAURER SHARK (a) damper configuration, (b) side view, (c) front view and (d) 3D view

Table 3. Sizes and performance data of SHARK

FMCE [KN] MASS	FY [KN]	K_{el} [KN/mm]	K_{pl} [KN/mm]	dSLS [±mm]	dMCE [±mm]	d_{cd} [±mm]	L [mm]	W [mm]	d_y [mm]	F_{pl} (KN)
350	220	100	4	≤ 1	35	50	700	560	2.2	411.2
700	410	165	6	≤ 1	50	70	800	580	2.484	815.1
1000	615	245	9	≤ 1	50	70	900	600	2.510	1222.4
1400	820	325	12	≤ 1	50	70	1000	620	2.523	1629.7
1700	1020	410	15	≤ 1	50	70	1100	640	2.487	2032.7
2100	1230	490	18	≤ 1	50	70	1200	660	2.510	2444.8
2400	1430	570	21	≤ 1	50	70	1300	680	2.508	2847.3

3.3.1.2 Advantages of SHARK Implementation

The utilizing of SHARK energy dissipation device has the following advantages:

- There is no need for regular maintenance and the use of only one material provides high reliability.
- The building structural systems have a similar service life.
- Provide stable response up to 3-4 MCE earthquake events without any failure.
- High level of safety due to the parallel configuration of hysteretic lamellas.
- Uncomplicated bilinear model appropriate for analysis.
- Having a compact size.
- A convenient visual inspection and replacement process if needed after a fire or other unforeseen event.
- Exceptional fatigue strength in case of wind, as well as service loads
- Design following European Standard EN15129 or according to other Standards upon request.

3.3.1.3 Possible Installation Layout

A typical installation layout is illustrated by two examples Figure 16 below. Additionally, MAURER provides the steel components of the brace system upon request. In general, the connection to the construction can be screwed or welded, as appropriate for the project, it also can be connected directly to the original frame of the building by connections to the middle of the beam and ends of the columns (Massumi & Absalan, 2013). However, as there is additional shear force in the beam particularly because of this force and this shear force should be transferred to the element by the device by applying steel jacketing around the beams to show the effectiveness of the connections to transfer the loads. For this study installation layout 1 is applied to the buildings and, according to the first data provided in Table 3.

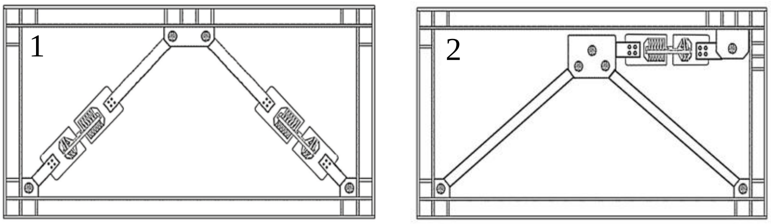

Figure 16. Installation layout 1 and 2 (MAURER, 2020)

3.3.1.4 Maurer SHARK Performance

The performance of the SHARK has been successfully tested as shown in Figure 17 showed a perfect hysteretic loop according to the European Standard EN 15129 at EUCENTRE Laboratory in Pavia (Italy) and Bundeswehr University of Munich.

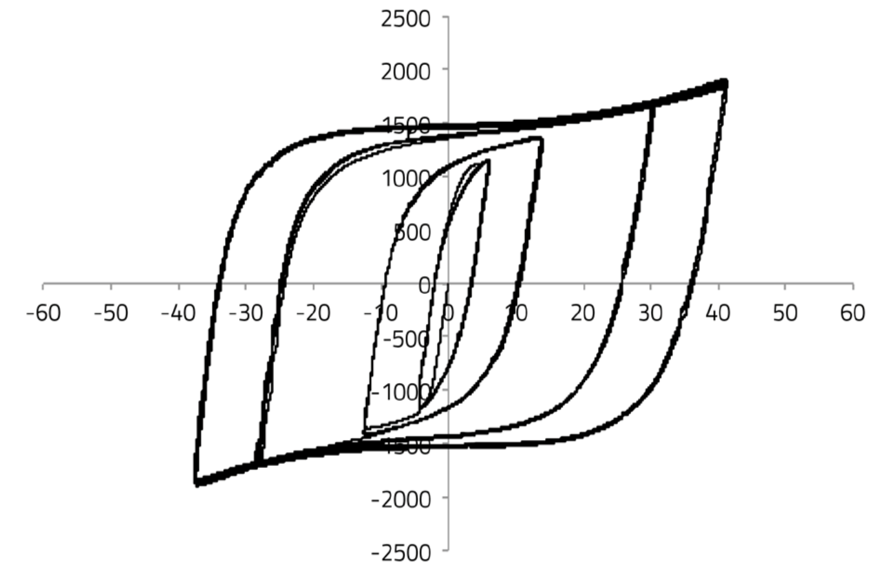

Figure 17. Experimental bilinear hysteretic loop of SHARK (MAURER, 2020)

3.3.1.5 MAURER SHARK Device optimization

As part of a nonlinear finite element FEM analysis, both SHARK and SHARK-Adaptive have been designed and optimized. Whenever necessary, they can also be customized to meet customer-specific requirements. Table 4 provides a comparison between MAURER SHARK and other types of seismic control systems such as Buckling Restrained Braces BRB and Fluid Viscous Dampers FVD.

Table 4. Device's optimization comparison (MAURER, 2020)

	MAURER SHARK		Other types	
	SHARK	SHARK-Adaptive	BRB	FVD
Protection of the structure (During severe ULS earthquake)	very good	very good	very good	very good
Protection of non-structural components (during minor SLS earthquake)	poor	very good	very poor	very good
Long-term reliability (against wear and fatigue problems)	very good	very good	very good	poor
Redundant safety level	very good	very good	very poor	poor
Easy visual inspection	very good	very good	very poor	poor
Easy to replace	very good	very good	very poor	very good
Low cost	very good	proper	very good	very poor

3.4 Deniz Building Modeling

3.4.1. Description of the Building

Deniz Building (DB) residence was built in 1973, It has characteristic features that can represent approximately 71 of the reinforced concrete buildings in Antakya Turkiye. There are 2 apartments on each floor of the building (Figure 18). Therefore, it is not symmetrical concerning the x-axis.

Figure 18. Deniz apartment

The cross-section dimensions of the column element used while modeling was taken as 20x70 and 20x80 given in the project. The size of a few columns is 25x100. The building is an 8-story RC frame, with a height of 2.9 meters for each story, the total structure height above the base is 23.2 meters. There is no earthquake resisting shear wall or reinforced concrete core around the elevator in the building. There are 17 columns in the building, and the sections and reinforcement ratios of these columns vary between floors. C16 concrete and St-I reinforcing steel properties were used in the modeling of this building. The performance level of the building was determined. According to the area where the Deniz building is located on the coordinated of Latitude: 36.210103° Longitude 36.159782°, the coordinates the ground condition of this area is very tight layers of sand, gravel and hard clay or weathered, very cracked weak rocks.

3.4.2 Building Properties

ETABS software has been used to create a three-dimensional model design and analysis of the multi-story building. ETABS follows ACI 318-11 to employ the performance-based design the lateral load-bearing systems. According to AFAD and TBEC the site class "C" is considered for Deniz building and the spectrum curve is calculated based on this site class. Therefore, Figure 19 presents the target response spectrum curve corresponding to this region.

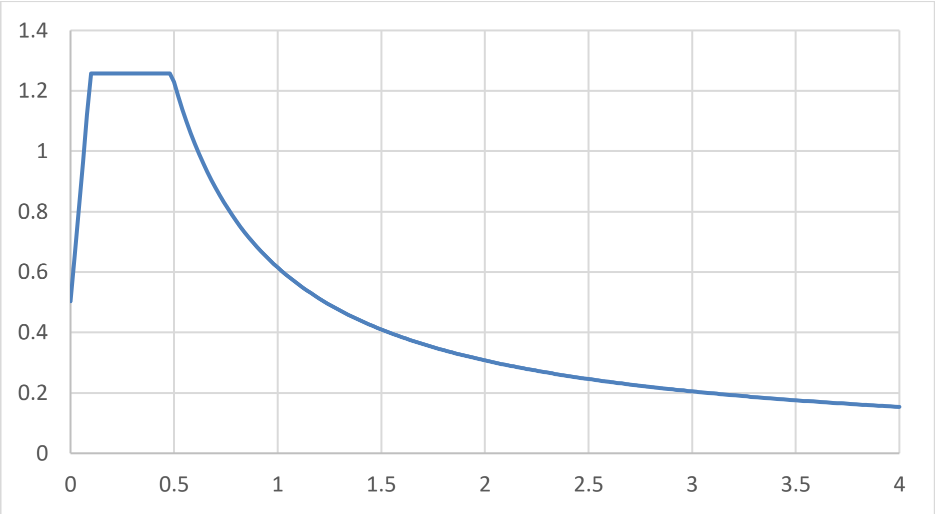

Figure 19. Target response spectrum of site class C

The ACI 318-11 and ASCE 41-17 design codes have been utilized in the design of the reinforced concrete building, and all details have been observed and considered according to these standards. Hinges were assigned according to ASCE 41-17. Flexible behavior assumptions were used to model diaphragms. Table 5 and Figure 20 illustrates the size of members used in the analysis for 8-Story buildings.

Table 5. Frame section property definitions - concrete rectangular

Name	Material	Depth (mm)	Width (mm)	Design Type
BEAM 30X70	C16	700	300	Beam
BEAM20X60	C16	600	200	Beam
S10-1	C16	200	600	Column
S10-2	C16	200	400	Column
S10-BASEMENT	C16	200	700	Column
S10-GROUNDFLOOR	C16	200	600	Column
S1-1	C16	200	500	Column
S11-1	C16	200	600	Column
S11-2	C16	200	500	Column
S11-BASEMENT	C16	200	800	Column
S11-GROUNDFLOOR	C16	200	700	Column
S1-2	C16	200	400	Column
S12-1	C16	900	200	Column
S12-2	C16	400	200	Column
S12-BASEMENT	C16	1000	300	Column
S12-GROUNDFLOOR	C16	1000	200	Column
S13-1	C16	600	200	Column
S13-2	C16	400	200	Column
S13-BASEMENT	C16	700	200	Column
S13-GROUNDFLOOR	C16	600	200	Column
S14-1	C16	200	600	Column
S14-2	C16	200	400	Column
S14-BASEMENT	C16	200	700	Column
S14-GROUNDFLOOR	C16	200	600	Column
S15-1	C16	200	600	Column
S15-2	C16	200	400	Column
S15-BASEMENT	C16	200	700	Column
S15-GROUNDFLOOR	C16	200	600	Column
S16-1	C16	200	900	Column
S16-2	C16	200	700	Column
S16-BASEMENT	C16	300	1000	Column
S16-GROUNDFLOOR	C16	250	1000	Column
S17-1	C16	200	800	Column
S17-2	C16	200	700	Column
S17-BASEMENT	C16	250	1000	Column
S17-GROUNDFLOOR	C16	200	1000	Column
S1-BASEMENT	C16	200	700	Column
S1-GROUNDFLOOR	C16	200	600	Column
S2-1	C16	200	800	Column
S2-2	C16	200	700	Column
S2-BASEMENT	C16	250	1000	Column
S2-GROUNDFLOOR	C16	200	1000	Column
S3-1	C16	200	800	Column
S3-2	C16	200	600	Column
S3-BASEMENT	C16	250	1000	Column
S3-GROUNDFLOOR	C16	200	900	Column

S4-1	C16	600	200	Column
S4-2	C16	500	200	Column
S4-BASEMENT	C16	800	200	Column
S4-GROUNDFLOOR	C16	700	200	Column
S5-1	C16	200	600	Column
S5-2	C16	200	500	Column
S5-BASEMENT	C16	200	800	Column
S5-GROUNDFLOOR	C16	200	700	Column
S6-1	C16	800	200	Column
S6-2	C16	700	200	Column
S6-BASEMENT	C16	1000	250	Column
S6-GROUNDFLOOR	C16	1000	200	Column
S7-1	C16	500	200	Column
S7-2	C16	400	200	Column
S7-BASEMENT	C16	700	200	Column
S7-GROUNDFLOOR	C16	500	200	Column
S8-1	C16	600	200	Column
S8-2	C16	500	200	Column
S8-BASEMENT	C16	800	200	Column
S8-GROUNDFLOOR	C16	700	200	Column
S9-1	C16	200	800	Column
S9-2	C16	200	700	Column
S9-BASEMENT	C16	250	1000	Column
S9-GROUNDFLOOR	C16	200	1000	Column

Table 6. Frame section property definitions - concrete column reinforcing

Name	Clear Cover to Ties (mm)	Bars 3-Dir	Bars 2-Dir	Longitudinal Bar Size	Corner Bar Size
S10-1	16.6	3	2	14d	14d
S10-2	16.6	2	2	14d	14d
S10-BASEMENT	15.6	3	2	16d	16d
S10-GROUNDFLOOR	16.6	3	2	14d	14d
S1-1	16.6	3	2	14d	14d
S11-1	16.6	3	2	14d	14d
S11-2	16.6	3	2	14d	14d
S11-BASEMENT	15.6	3	2	16d	16d
S11-GROUNDFLOOR	15.6	3	2	16d	16d
S1-2	16.6	2	2	14d	14d
S12-1	15.6	2	3	16d	16d
S12-2	15.6	2	3	16d	16d
S12-BASEMENT	15.6	2	4	16d	16d

S12-GROUNDFLOOR	15.6	2	3	16d	16d
S13-1	16.6	3	2	14d	14d
S13-2	16.6	3	2	14d	14d
S13-BASEMENT	15.6	3	2	16d	16d
S13-GROUNDFLOOR	16.6	3	2	14d	14d
S14-1	16.6	3	2	14d	14d
S14-2	16.6	3	2	14d	14d
S14-BASEMENT	15.6	3	2	16d	16d
S14-GROUNDFLOOR	16.6	3	2	14d	14d
S15-1	16.6	3	2	14d	14d
S15-2	16.6	3	2	14d	14d
S15-BASEMENT	15.6	3	2	16d	16d
S15-GROUNDFLOOR	16.6	3	2	14d	14d
S16-1	15.6	3	2	16d	16d
S16-2	15.6	3	2	16d	16d
S16-BASEMENT	15.6	4	2	16d	16d
S16-GROUNDFLOOR	16.6	3	2	14d	14d
S17-1	15.6	3	2	16d	16d
S17-2	15.6	3	2	16d	16d
S17-BASEMENT	15.6	4	2	16d	16d
S17-GROUNDFLOOR	15.6	3	2	16d	16d
S1-BASEMENT	15.6	3	2	16d	16d
S1-GROUNDFLOOR	16.6	3	2	14d	14d
S2-1	15.6	3	2	16d	16d
S2-2	15.6	3	2	16d	16d
S2-BASEMENT	15.6	4	2	16d	16d
S2-GROUNDFLOOR	15.6	3	2	16d	16d
S3-1	15.6	3	2	16d	16d
S3-2	16.6	3	2	14d	14d
S3-BASEMENT	15.6	4	2	16d	16d

S3-GROUNDFLOOR	15.6	3	2	16d	16d
S4-1	16.6	2	3	14d	14d
S4-2	16.6	2	3	14d	14d
S4-BASEMENT	15.6	2	3	16d	16d
S4-GROUNDFLOOR	15.6	2	3	16d	16d
S5-1	16.6	3	2	14d	14d
S5-2	16.6	3	2	14d	14d
S5-BASEMENT	15.6	3	2	16d	16d
S5-GROUNDFLOOR	15.6	3	2	16d	16d
S6-1	15.6	2	3	16d	16d
S6-2	15.6	2	3	16d	16d
S6-BASEMENT	16.6	2	3	14d	14d
S6-GROUNDFLOOR	15.6	2	3	16d	16d
S7-1	16.6	2	2	14d	14d
S7-2	16.6	2	2	14d	14d
S7-BASEMENT	15.6	2	3	16d	16d
S7-GROUNDFLOOR	16.6	2	3	14d	14d
S8-1	16.6	3	2	14d	14d
S8-2	16.6	3	2	14d	14d
S8-BASEMENT	15.6	3	2	16d	16d
S8-GROUNDFLOOR	15.6	3	2	16d	16d
S9-1	15.6	3	2	16d	16d
S9-2	15.6	3	2	16d	16d
S9-BASEMENT	15.6	3	2	16d	16d
S9-GROUNDFLOOR	15.6	3	2	16d	16d

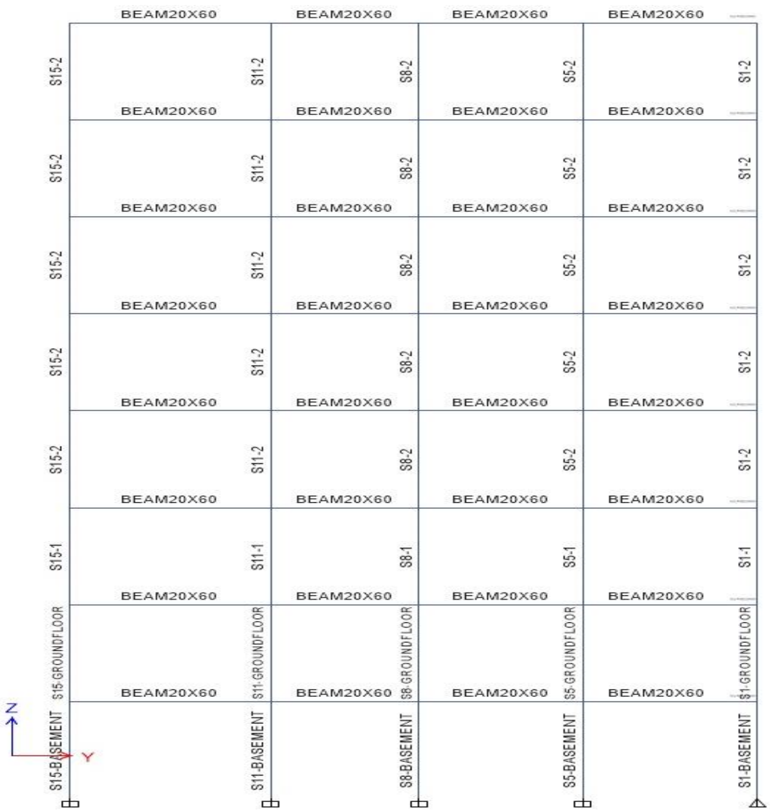

Figure 20. Frame sections on Y-Z plane

3.4.2.1 Load Combinations Applied to the Structure

The following combinations of loads that have been considered to analyze the building is in accordance with TBEC-2018 regulations:

1.4DL + 1.6LL

0.9DL ± EQX ± 0.3EQY

0.9DL ± EQY ± 0.3EQX

DL + LL ± EQX ± 0.3EQY

DL + LL ± EQY ± 0.3EQX

3.4.2.2 Gravity Loads

The dead and live loads based on the residential use of the building are used as specified below.

- Floor Dead Load: 4.2 KN/m² - Floor Live Load: 2 KN/m²

3.4.3 Modal Design and Analysis

The design of the 8-story building is conducted according to the specified plan and sections without considering the infill walls, however according to the original plan there is balconies along all the X-axis which prevent the possibility of energy absorber implementation. Therefore, the balconies on the edges of the X-axis are removed and, on the X-axis of the strengthened building the energy absorber is applied on edges. Further, an analysis was conducted to comprehend the structure's dynamic behavior and to determine and evaluate the behavior of the strengthened structure with MAURER energy dissipators. The obtained vibration periods and frequencies are presented in Table 7, the 8-story model and plan layout are presented in Figures 21 and 22 respectively.

Table 7. Vibration periods and frequencies

	DB 8-Story	
Mode	Period (sec)	Frequency (cyc/sec)
1	1.232	0.812
2	1.058	0.945
3	1.011	0.99
4	0.41	2.44
5	0.355	2.819
6	0.336	2.981
7	0.243	4.111
8	0.21	4.752
9	0.195	5.127
10	0.17	5.884
11	0.146	6.854
12	0.133	7.537

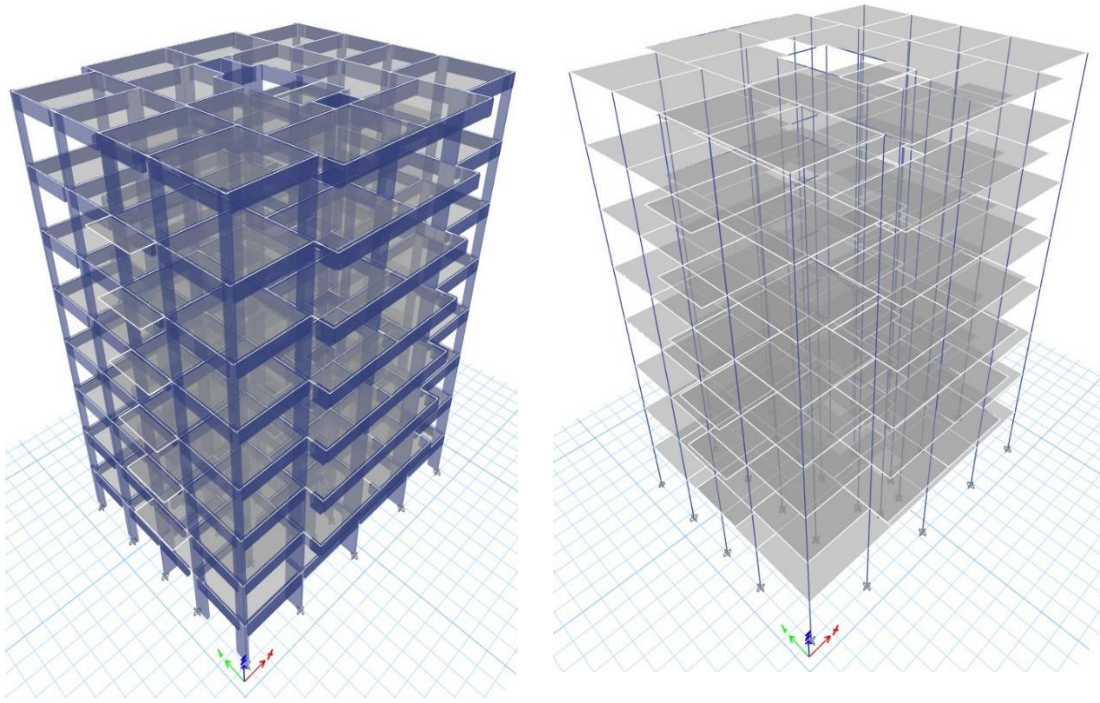

Figure 21. 8-Story building model layout in ETABS

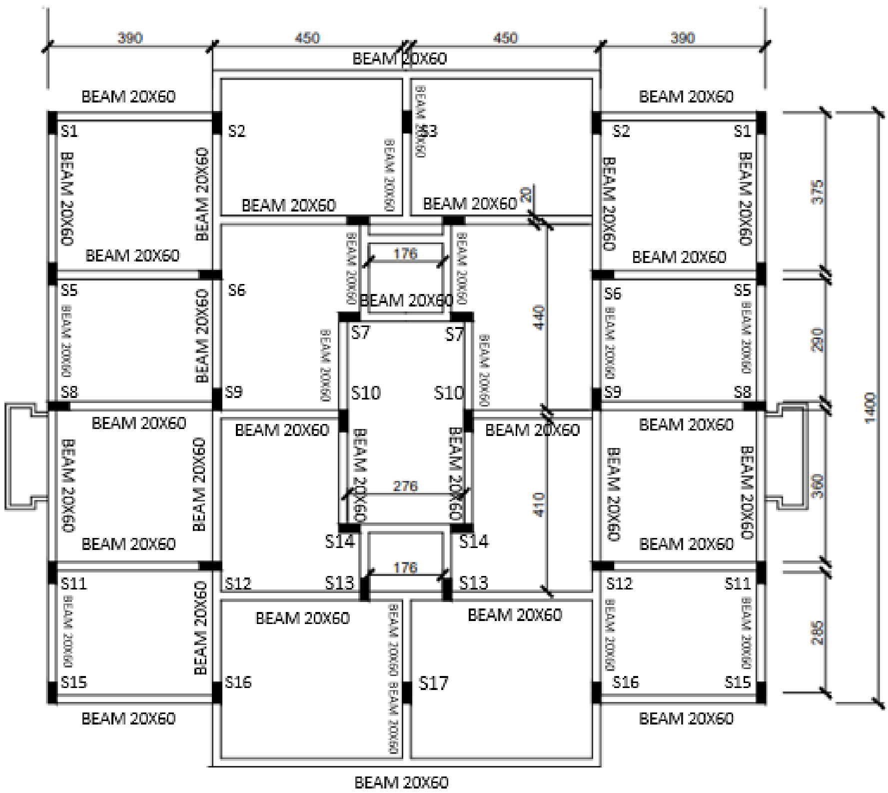

Figure 22. Deniz building plan layout

3.4.4 Performance Analysis for Deniz Building

The building does not have any earthquake resistance system. The performance of the building of the structure is given in Table 8 and Figure 23. According to results the 4th floor of the Deniz building has a performance level of failure, as severely damaged columns are formed and all the shear forces on this floor are carried by the damaged columns.

Table 8. Joint properties of load-bearing elements on the 4th floor of the building

	A-B	B-IO (minimum)	IO-LS (pronounced)	LS-CP (advanced)	Total
Beam	0	79	0	0	79
Column	0	0	0	32	32

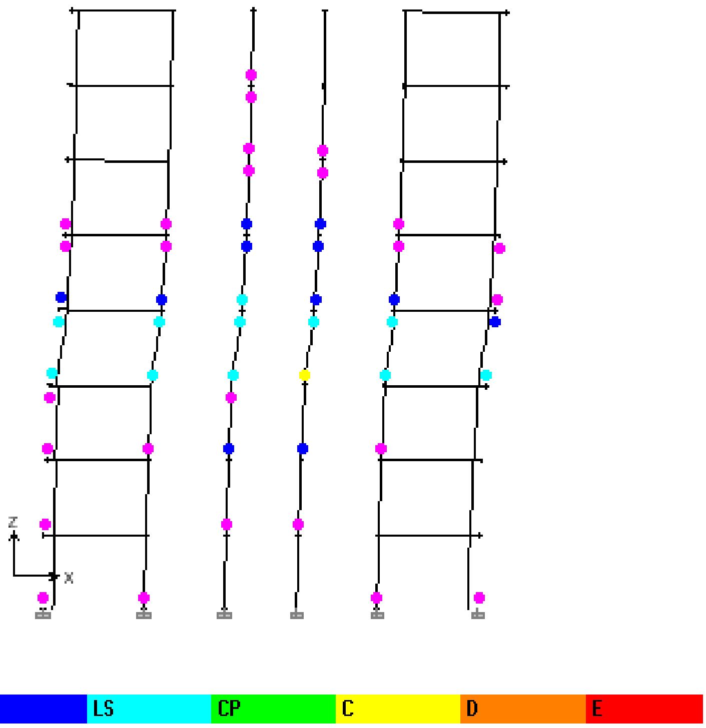

Figure 23. Plastic hinges of the building side view subjected to earthquake event

3.4.5 Design for Seismic Loads

According to Turkish Building Earthquake Code (TBEC-2018) and Turkiye Earthquake Hazard Maps Interactive Web Application (AFAD), Deniz Building Earthquake Ground Motion level have earthquake location with 10% probability of exceedance in 50 years (recurrence period of 475 years) movement level. Further Local Soil Class ZC Very tight layers of sand, gravel and hard clay or weathered, very cracked weak rocks. The building importance factor I is for the residential Deniz building. The response modification coefficient R, which reduces the seismic design force for the structures that responds inelastically it's considered between Intermediate reinforced concrete moment frames and ordinary reinforced concrete moment frames. The following factors and coefficients have been applied to analyze the building behavior when subjected to earthquakes.

Applied factors and coefficients according to TBEC-2018:

Response Modification Factor	R = 4
System Overstrength Factor	Ω_0 = 3
Importance Factor	I = 1
Short period map spectral acceleration coefficient	S_S = 1.048
Map spectral acceleration coefficient for a 1.0 second period	S_1= 0.273
Maximum ground acceleration [g]	PGA = 0.445
Maximum ground speed [cm/sec]	PGV = 27.550

Design spectral acceleration coefficients:

$$S_{DS} = S_S\ F_S \tag{1}$$

$$S_{D1} = S_1\ F_1 \tag{2}$$

where,

SDS = Short period design spectral acceleration coefficient

SD1 = Design spectral acceleration coefficient for a period of 1.0 second

F_S = 1.2 (Site Coefficient)

F_1 = 1.5 (Site Coefficient)

$$T_a = C_T \, h_n^{3/4} \quad (3)$$

where,

T_a = The empirical dominant natural vibration period

Ct = 0.1 (Coefficient for reinforced concrete frames)

h_n = Height of the building

3.4.6 Nonlinear Time-History Analysis

A nonlinear time history analysis (NLTHA) can be performed to simulate a structure's behavior and seismic response under dynamic loading of a severe earthquake as stated by (Wilkinson & Hiley, 2006). NLTHA requires a mathematical model that can incorporate the nonlinear characteristics of loads and deformations of the components.

Plastic hinges have been applied to the beams and columns, uncoupled hinges as M3 to the beams which correspond to each degree of freedom and coupled hinges as P-M2-M3 to the columns in which more than one degree of freedom is considered at a time since the earthquake is applied in the x and y directions. According to the TBEC-2018, a set of 11 earthquake records is required to evaluate the adequacy of the analyzed seismic design. Due to the explicit modeling of the nonlinear response, so no modification is required to the resulting internal forces.

3.4.6.1 Earthquake Records Selection and Scaling

Records of earthquakes should be selected and scaled appropriately so that the analysis can be completed with results that are approximate the actual behavior. A description of the situations to be considered in the selection and scaling of a set of earthquake records is provided below:

- The earthquake records will be selected based on their compatibility with the design earthquake ground motion. The records will be chosen based on the distance from the fault, the ground conditions, and the source of the fault mechanism. The priority will be given to records of previous earthquakes that have occurred in the region.
- It may be difficult to determine earthquakes according to the above conditions, therefore simulated ground motion records in the time domain can be utilized. The simulated produced earthquake record matched the actual earthquake in the region.
- A matched to target response the average spectra should not be smaller than the target design spectrum. Spectrum method can also be used to scale earthquake records. Matching earthquake records can be accomplished using programs such as SAP2000, SEISMOMATCH, and ETABS.

For this research, seismic records shown in Table 6 were obtained from the PEER database (Center, 2013). For nonlinear dynamic analyses of structures, seismic input is typically defined in terms of time series of acceleration whose response spectrums are applicable with a specific target response spectrum. An earthquake-resistant structure's seismic design depends largely on the seismic response spectrum obtained from an earthquake-hazard analysis. Furthermore, an algorithm for generating realistic design acceleration time series is based on spectral matching in the time domain. Disaggregating the hazards leads to the determination of the controlling scenario for an earthquake in terms of distance and magnitude. Analyses of this kind require input in the form of time series with a response spectrum that corresponds to the target spectrum. Initial time series consisting of empirical recordings from past earthquakes or numerical simulations of the ground motion for the design event is modified to develop design time series.

Scaling and spectral matching are the two methods that can be utilized to modify the time series to be consistent with the target spectrum, Scaling method involves multiplying a constant factor by the time series to ensure that the spectrum over a specified period range is either the same as or exceeds the design spectrum. While in the spectral matching method, the frequency content of a time series is adjusted at all spectral periods to match the design spectrum. (Al Atik & Abrahamson, 2010) For this study, the spectral matching method is applied by using SeismoMatch and ETABS programs to match the earthquake records to the target response spectrum, the match is done according to the time domain and based on the ASCE 7 -16.

Table 9. Selected earthquake records

No.	Earthquake	Year	Magnitude	Rjb (km)	Rrup (km)	Peer No.
1	"Duzce_ Turkiye"	1999	7.14	12.02	12.04	1602
2	"Friuli_ Italy-01"	1976	6.5	33.32	33.4	122
3	"Imperial Valley-06"	1979	6.53	15.19	15.19	164
4	"Kern County"	1952	7.36	38.42	38.89	15
5	"Kobe_ Japan"	1995	6.9	24.85	24.85	1100
6	"Kocaeli_ Turkiye"	1999	7.51	10.56	13.49	1148
7	"Landers"	1992	7.28	34.86	34.86	838
8	"Loma Prieta"	1989	6.93	39.32	39.51	762
9	"Manjil_ Iran"	1990	7.37	12.55	12.55	1633
10	"Morgan Hill"	1984	6.19	23.23	23.24	450
11	"Northridge-01"	1994	6.69	35.66	36.77	942

3.4.6.2 Ground Motions for Determining Design Displacements

Nonlinear time-history analyses were performed to estimate and evaluate the performance of the strengthened structure in compliance with TBEC-2018 code specifications. The obtained results are used to determine whether the strengthened structure will survive and sustain earthquakes more than the normal structure. The analyses were conducted by utilizing eleven pairs of ground motions chosen from various recorded events.

These ground motions are shown in Table 9. Figures 24 and 25 illustrate the response spectrum curves created for selected H1 which is the recorded ground motion in the first direction scaled and unscaled earthquake records, respectively. Further Figures 26 and 27 illustrate response spectrum curves created for selected H2 which is the other ground motion 90 degrees from the other recorded scaled and unscaled earthquake records, respectively. The earthquake scaling operation is performed in the time domain by applying spectral matching operation with 5% damping using ETABS software and it has been checked also by using SeismoMatch software.

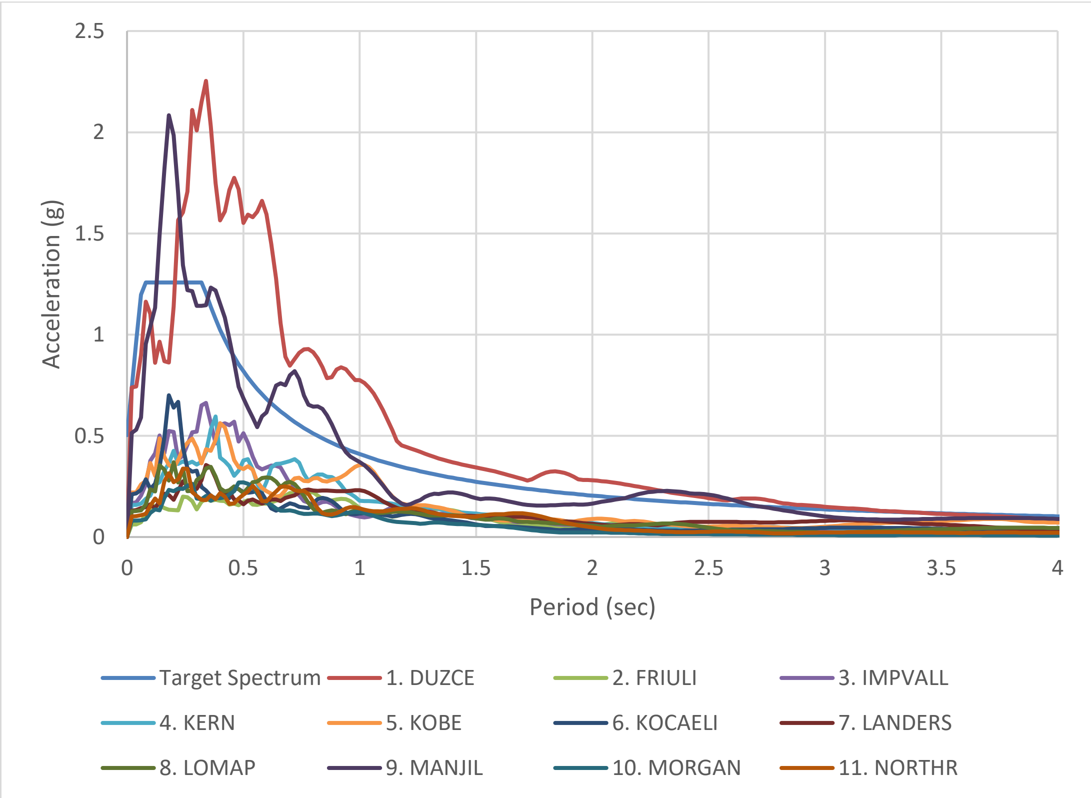

Figure 24. Unscaled H1 response spectrum of all earthquakes

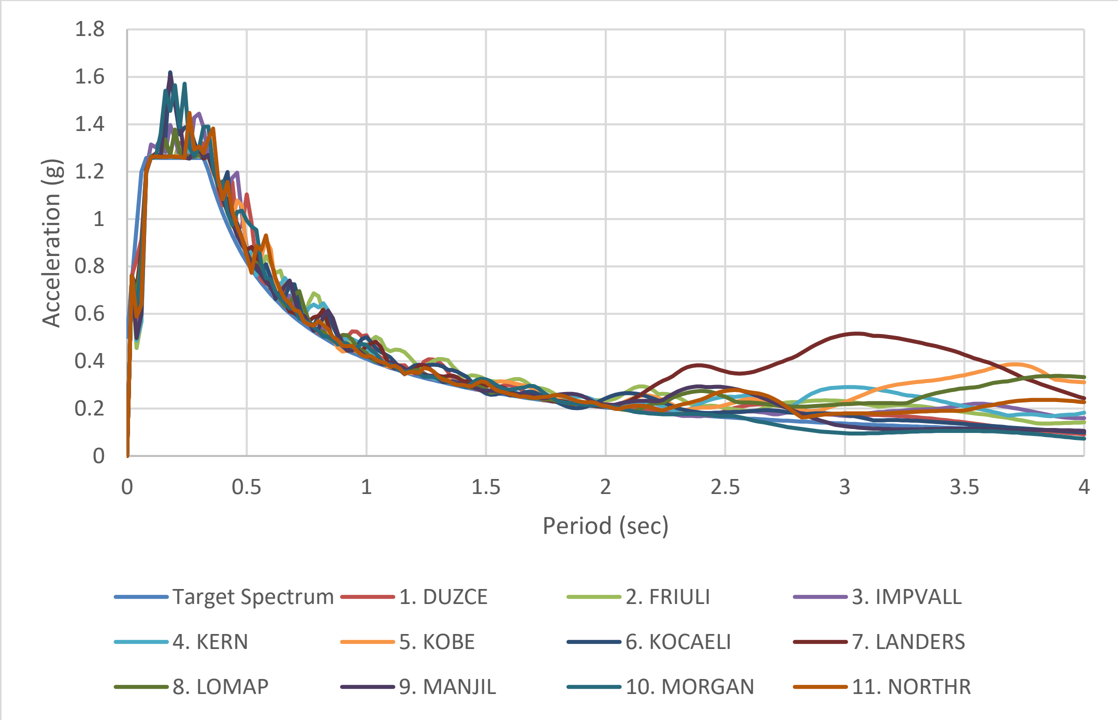

Figure 25. Scaled H1 response spectrum of all earthquakes

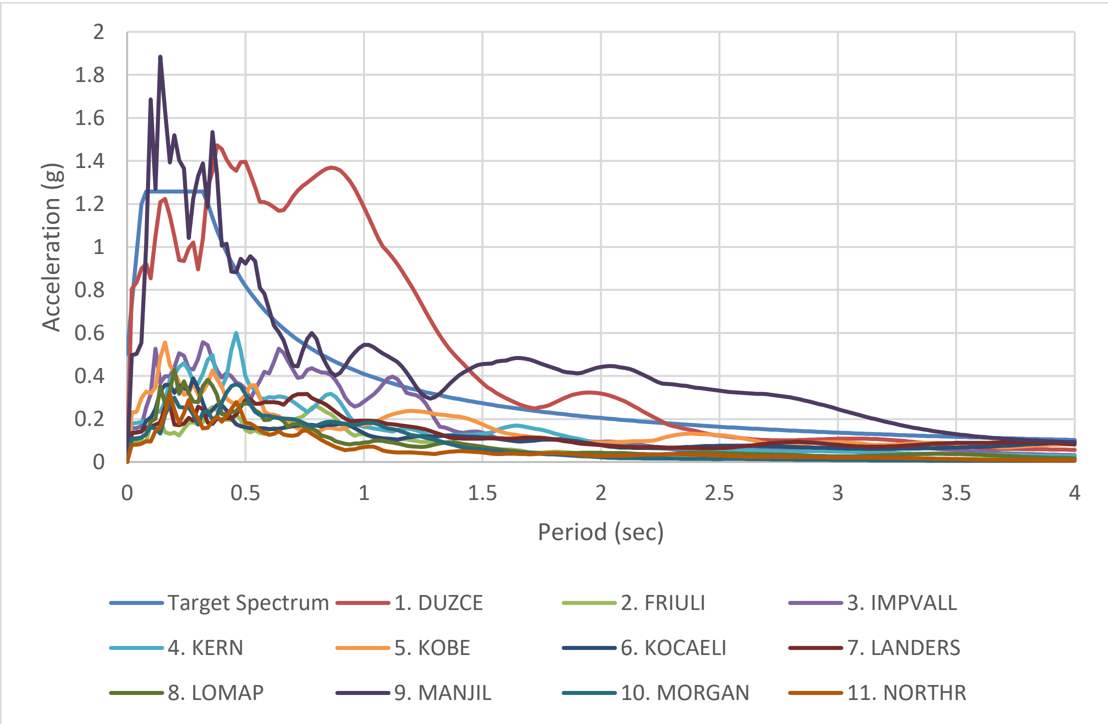

Figure 26. Unscaled H2 response spectrum of all earthquakes

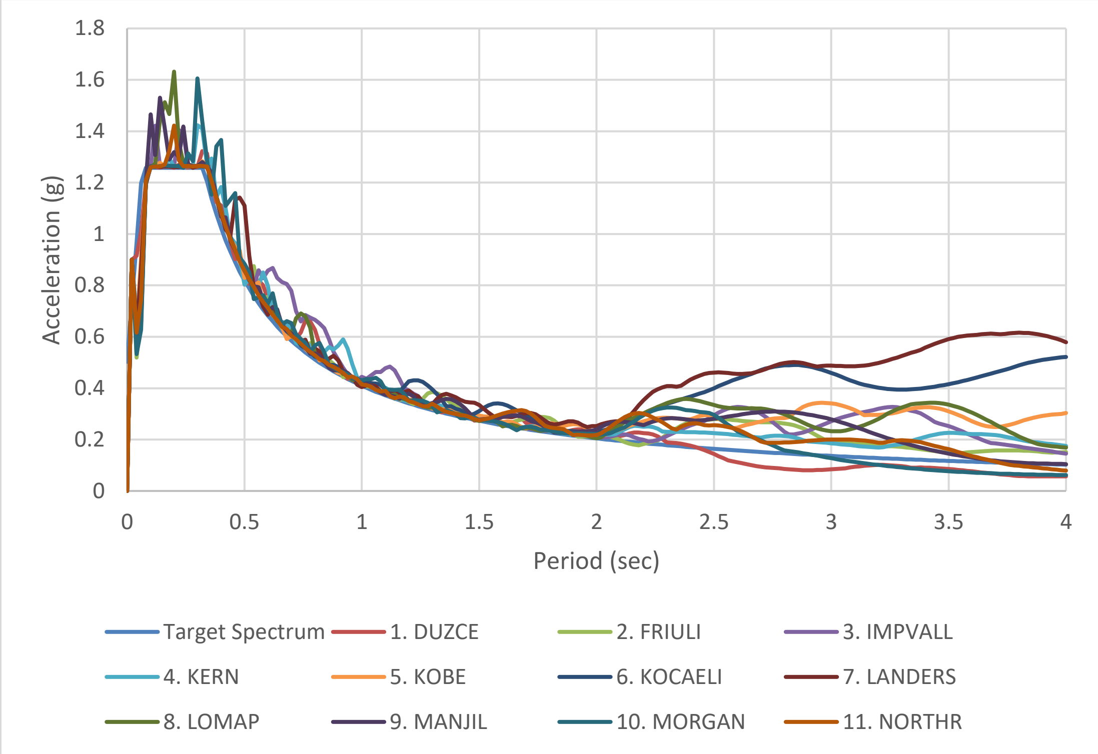

Figure 27. Scaled H2 response spectrum of all earthquakes

Figures 28 to 38 illustrates scaled and unscaled H1 time series selected earthquake records by using SeismoMatch. According to observations, there was a significant increase in earthquake accelerations, except for DUZCE earthquake.

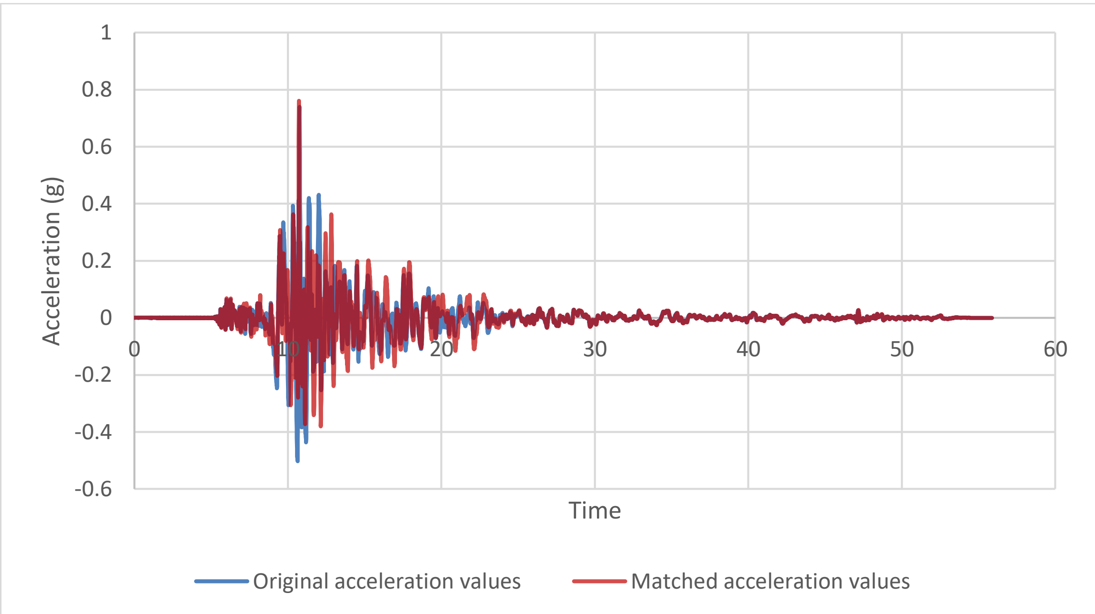

Figure 28. Scaled and unscaled H1 time series of Duzce earthquake

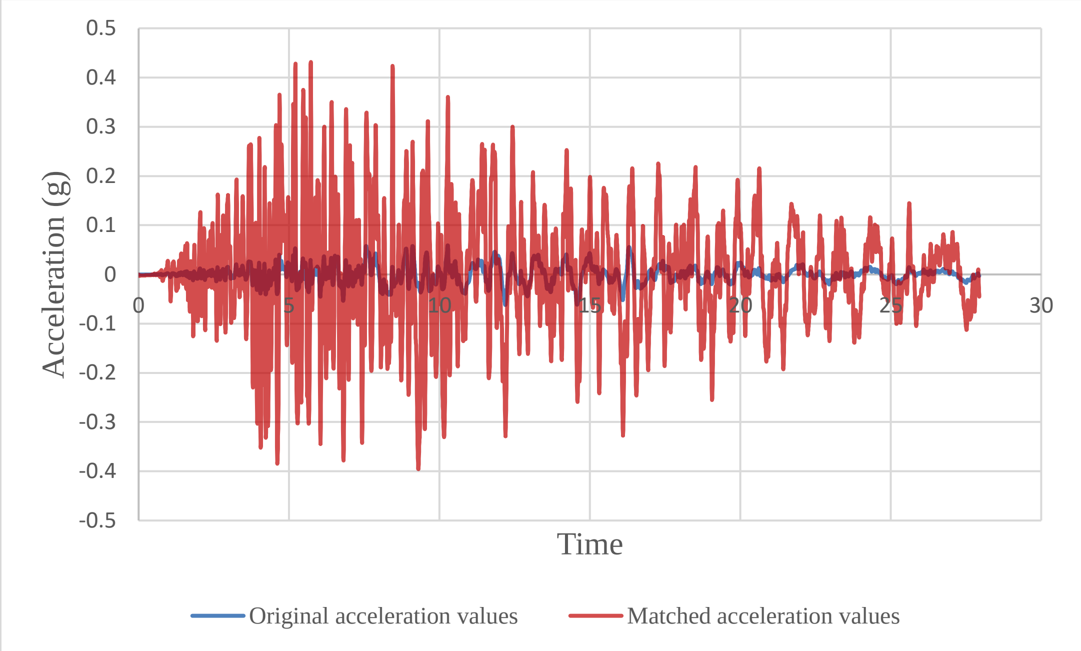

Figure 29. Scaled and unscaled H1 time series of Friuli earthquake

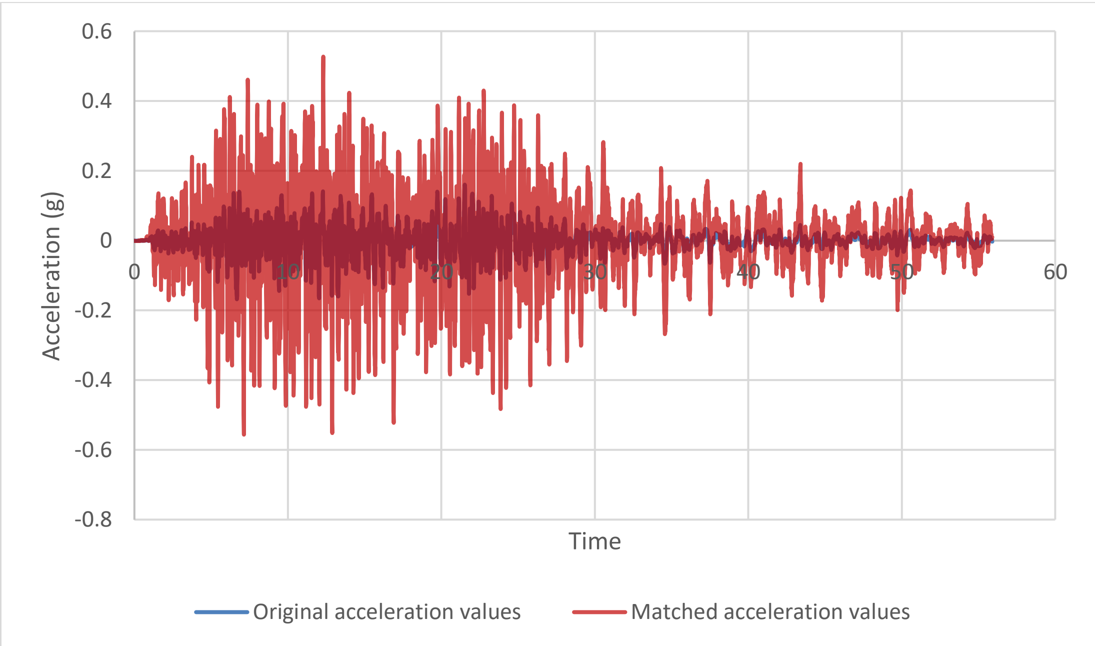

Figure 30. Scaled and unscaled H1 time series of Impvall earthquake

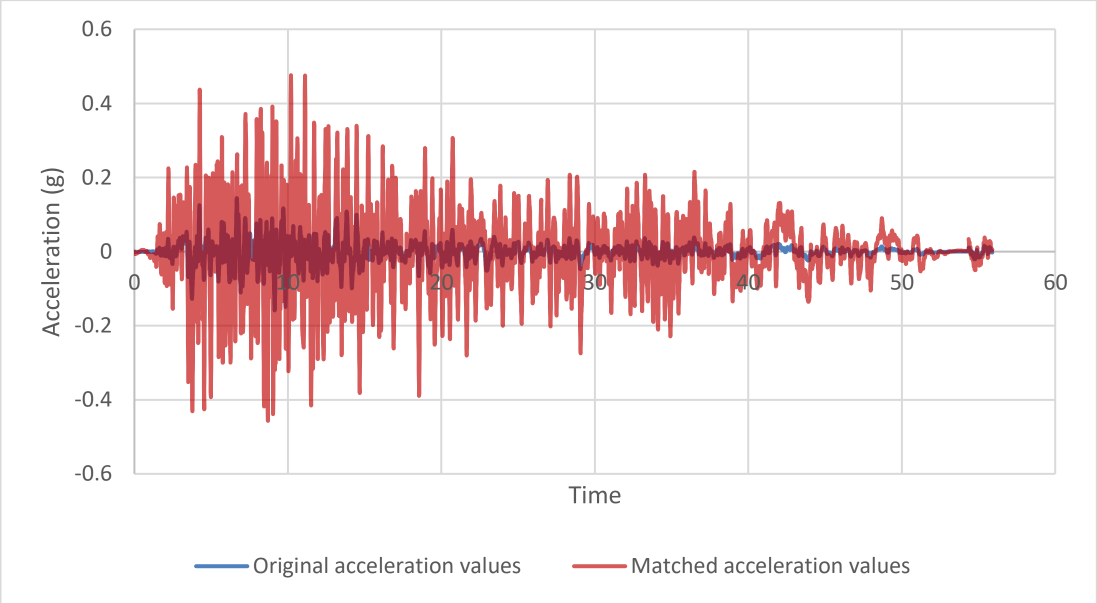

Figure 31. Scaled and unscaled H1 time series of Kern earthquake

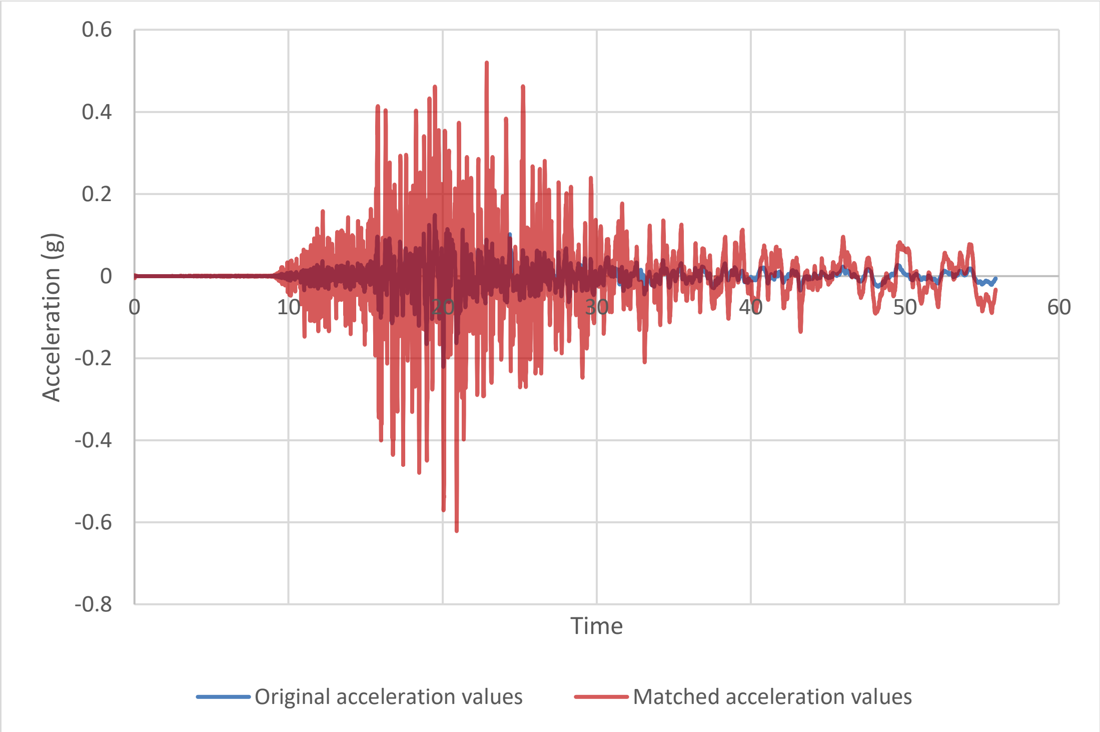

Figure 32. Scaled and unscaled H1 time series of Kobe earthquake

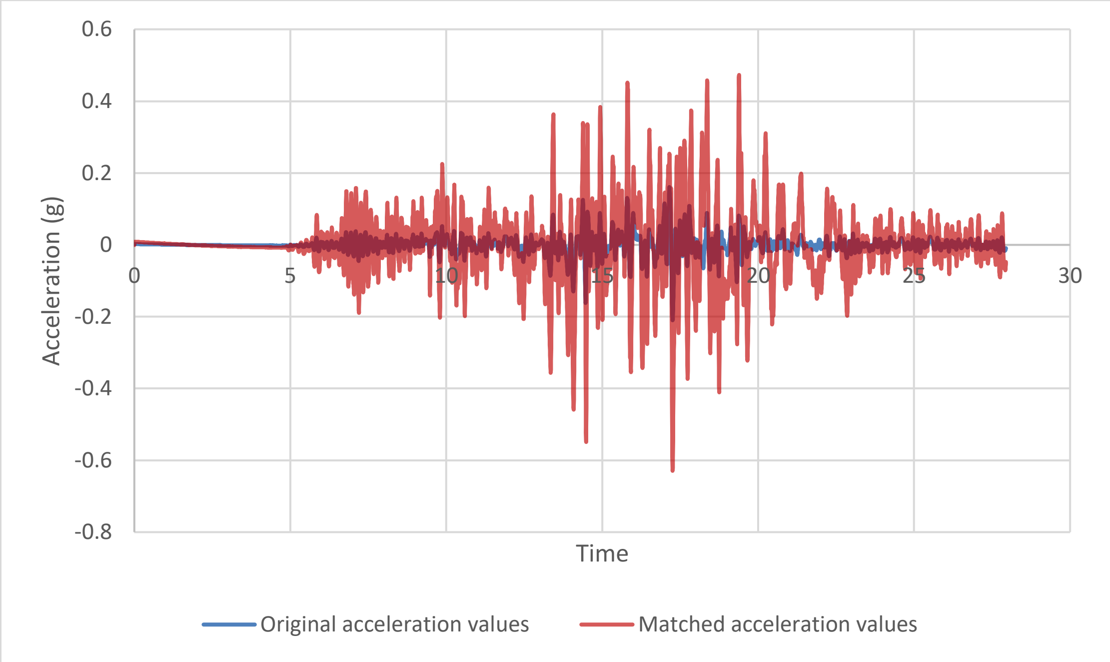

Figure 33. Scaled and unscaled H1 time series of Kocaeli earthquake

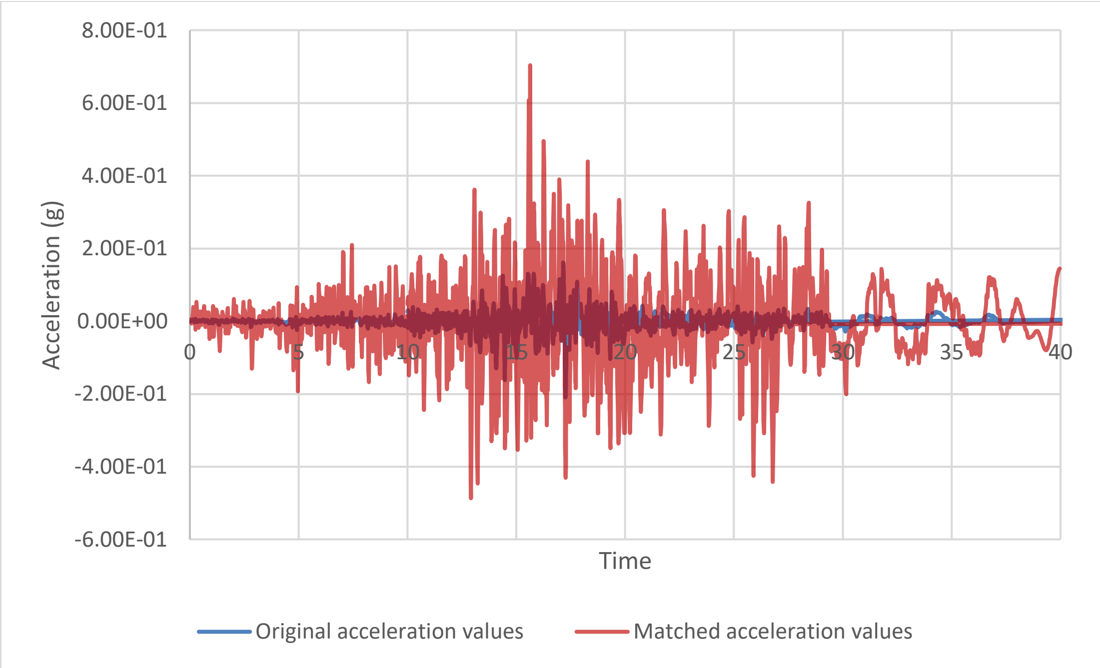

Figure 34. Scaled and unscaled H1 time series of Landers earthquake

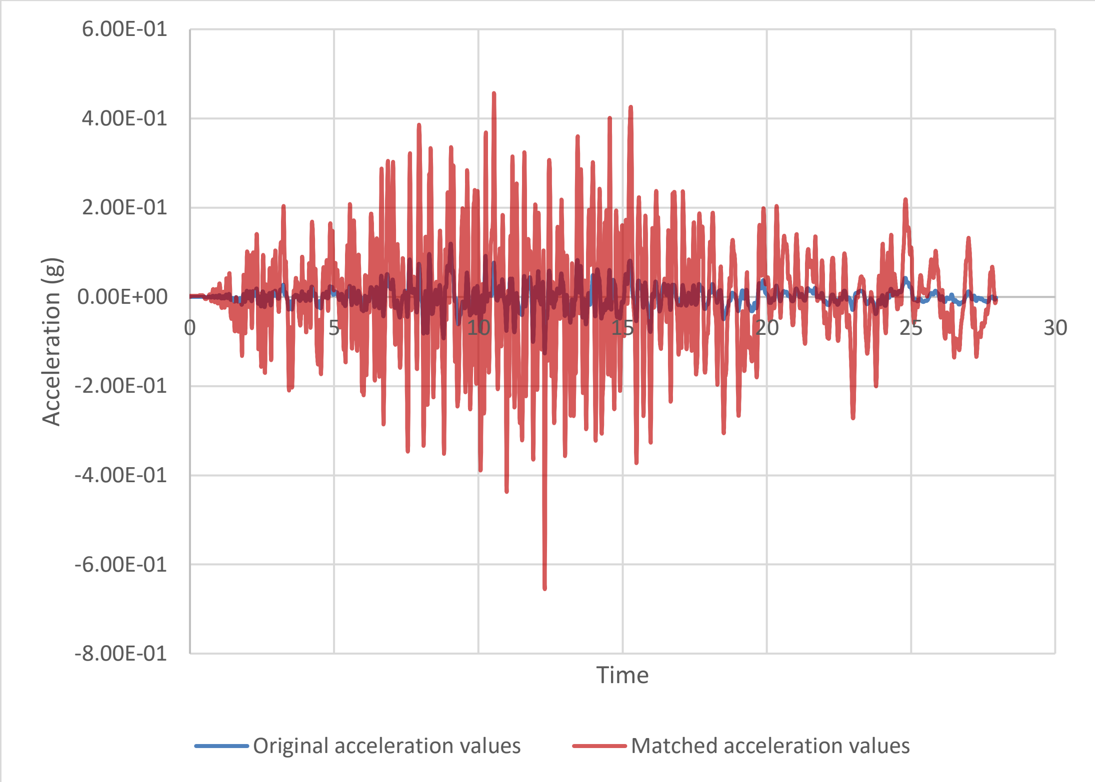

Figure 35. Scaled and unscaled H1 time series of Lomap earthquake

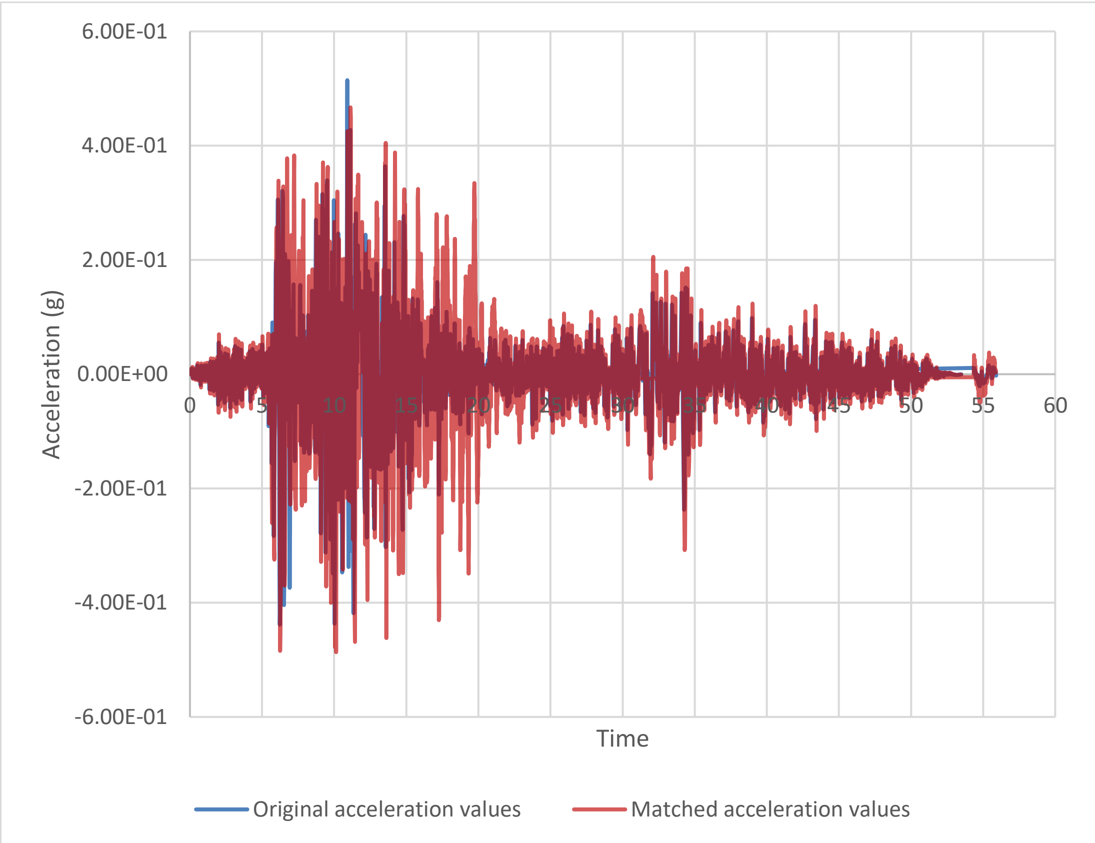

Figure 36. Scaled and unscaled H1 time series of Manjil earthquake

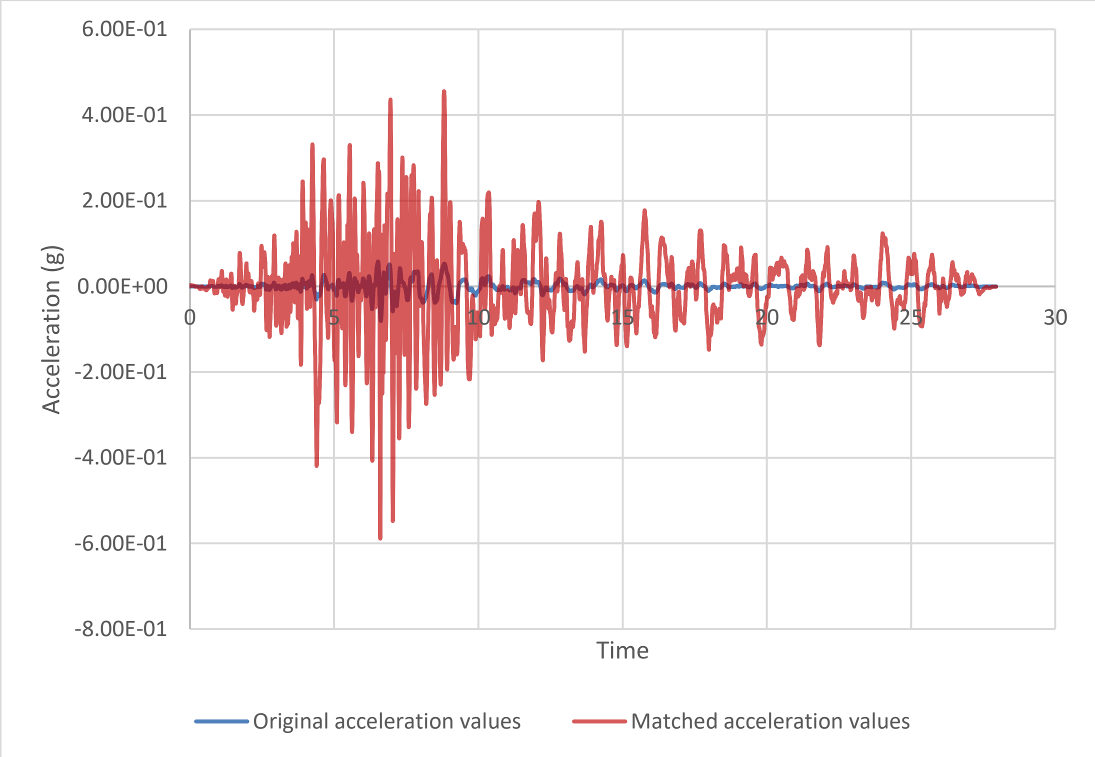

Figure 37. Scaled and unscaled H1 time series of Morgan earthquake

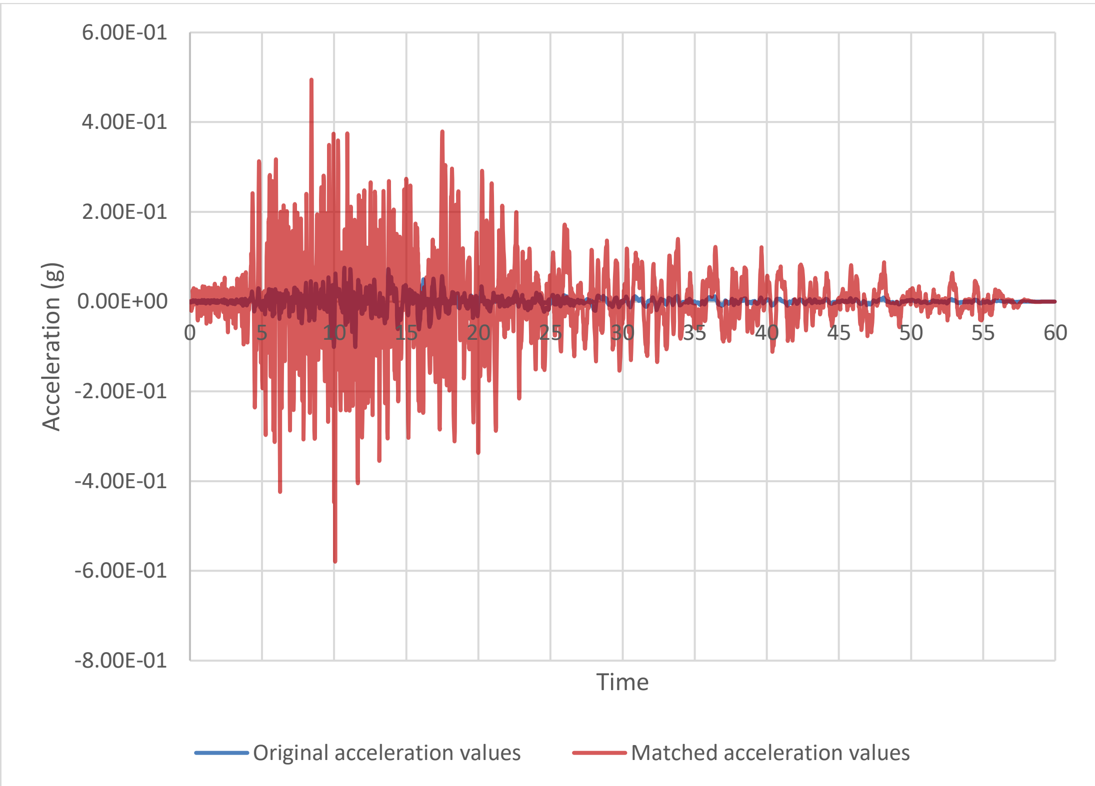

Figure 38. Scaled and unscaled H1 time series of Northr earthquake

Figures 39 to 49 illustrates scaled and unscaled H2 time series selected earthquake records by using SeismoMatch. According to observations, there was a significant increase in earthquake accelerations, except for DUZCE earthquake.

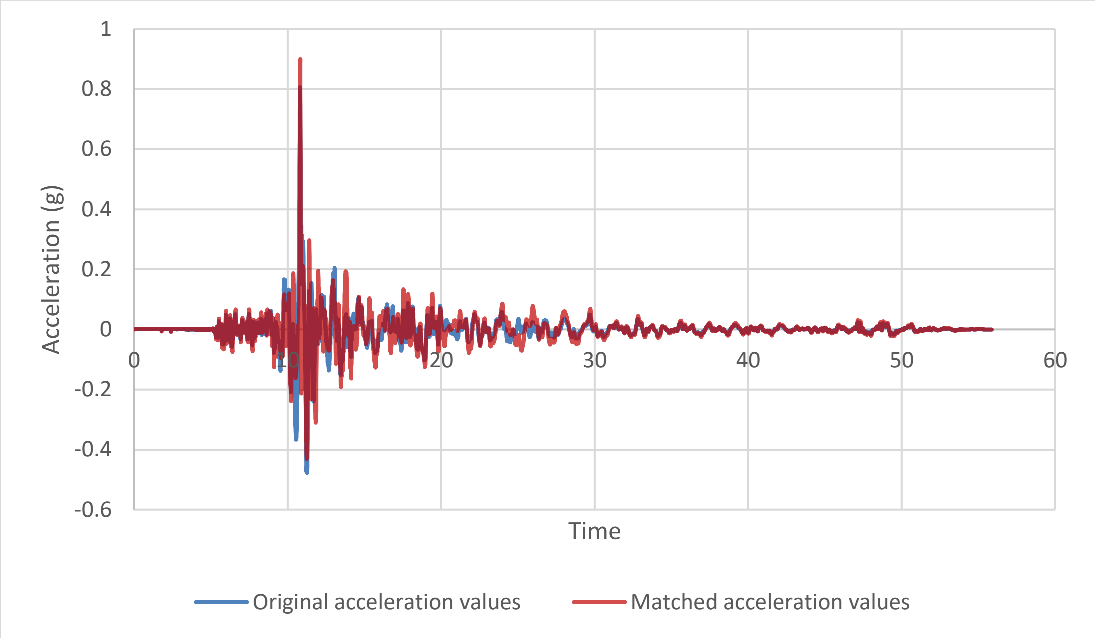

Figure 39. Scaled and unscaled H2 time series of Duzce earthquake

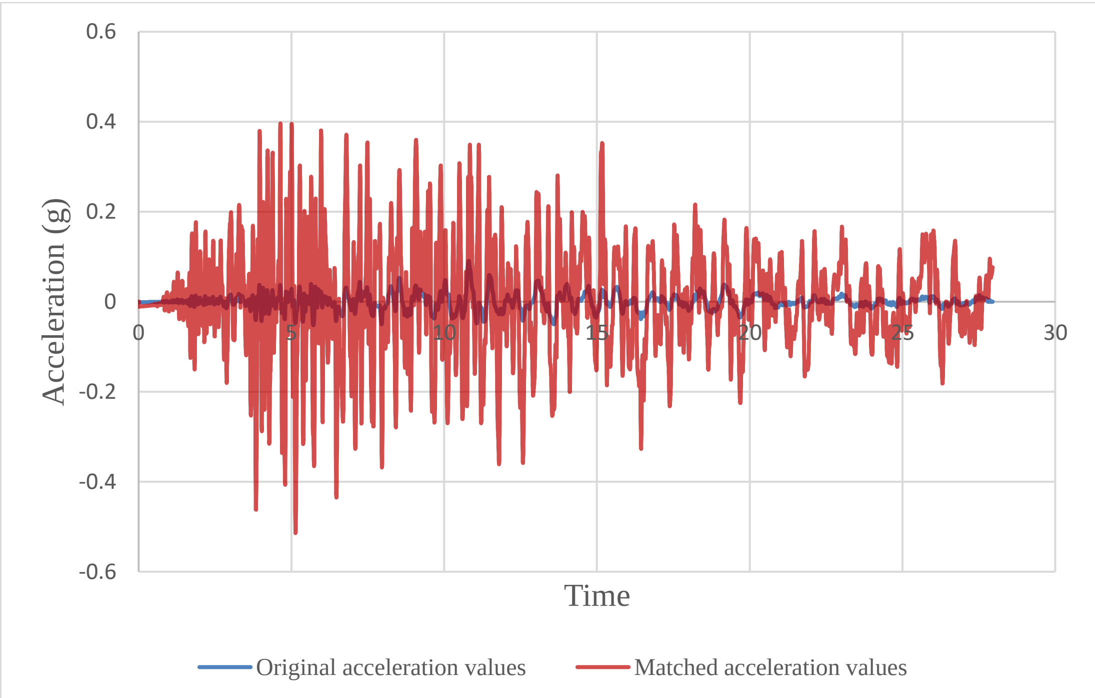

Figure 40. Scaled and unscaled H2 time series of Friuli earthquake

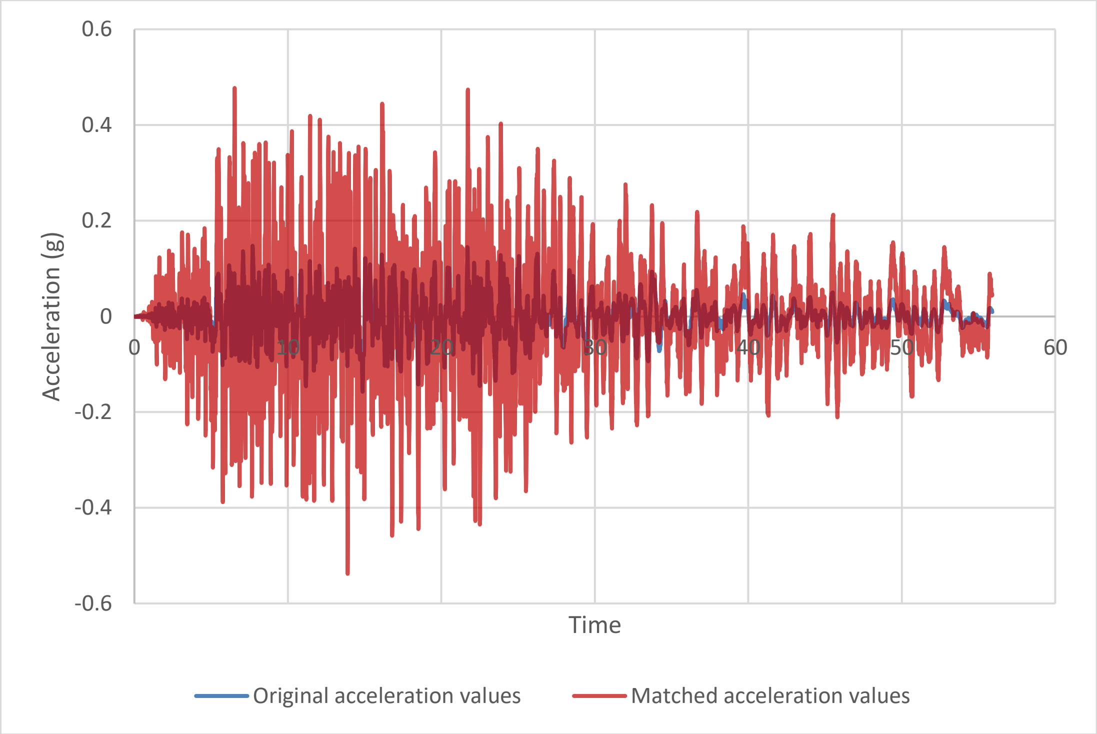

Figure 41. Scaled and unscaled H2 time series of Impvall earthquake

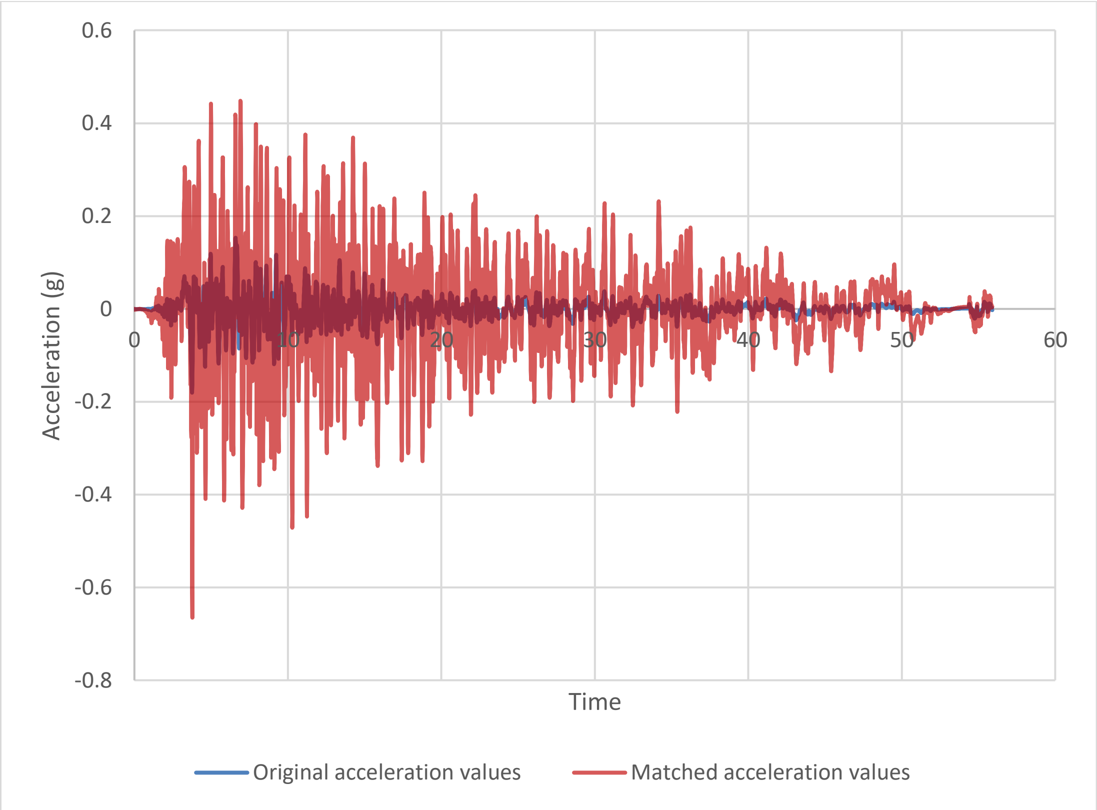

Figure 42. Scaled and unscaled H2 time series of Kern earthquake

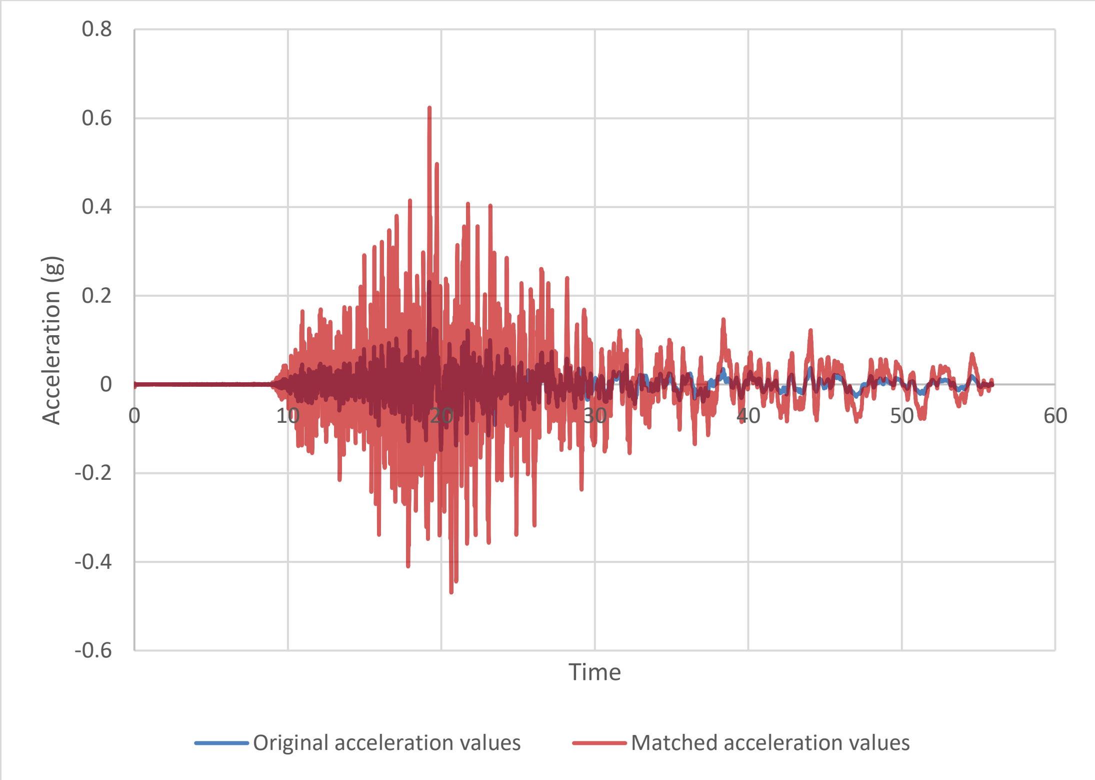

Figure 43. Scaled and unscaled H2 time series of Kobe earthquake

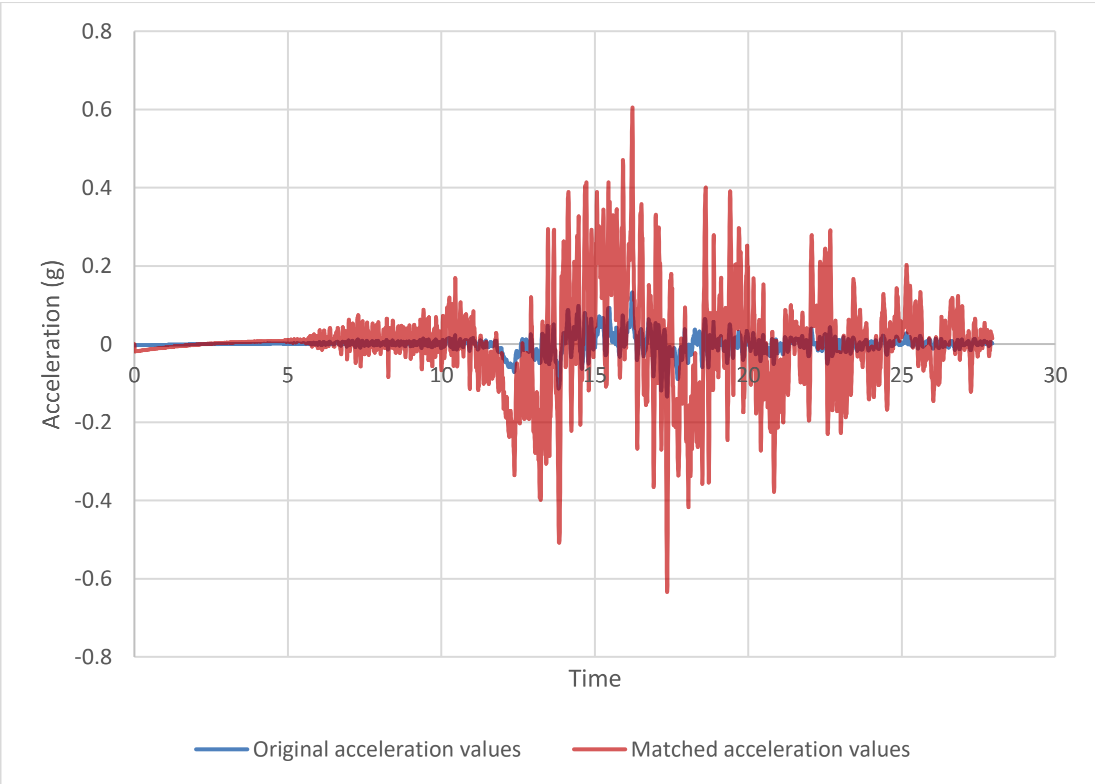

Figure 44. Scaled and unscaled H2 time series of Kocaeli earthquake

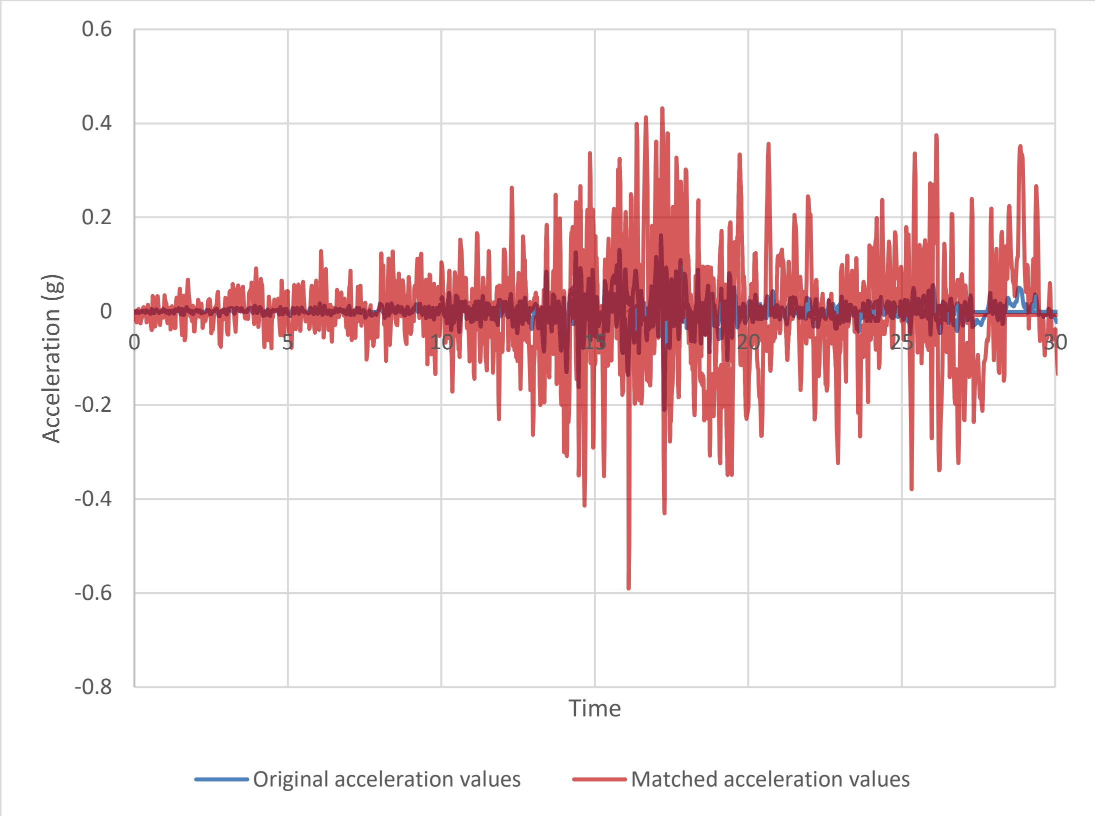

Figure 45. Scaled and unscaled H2 time series of Landers earthquake

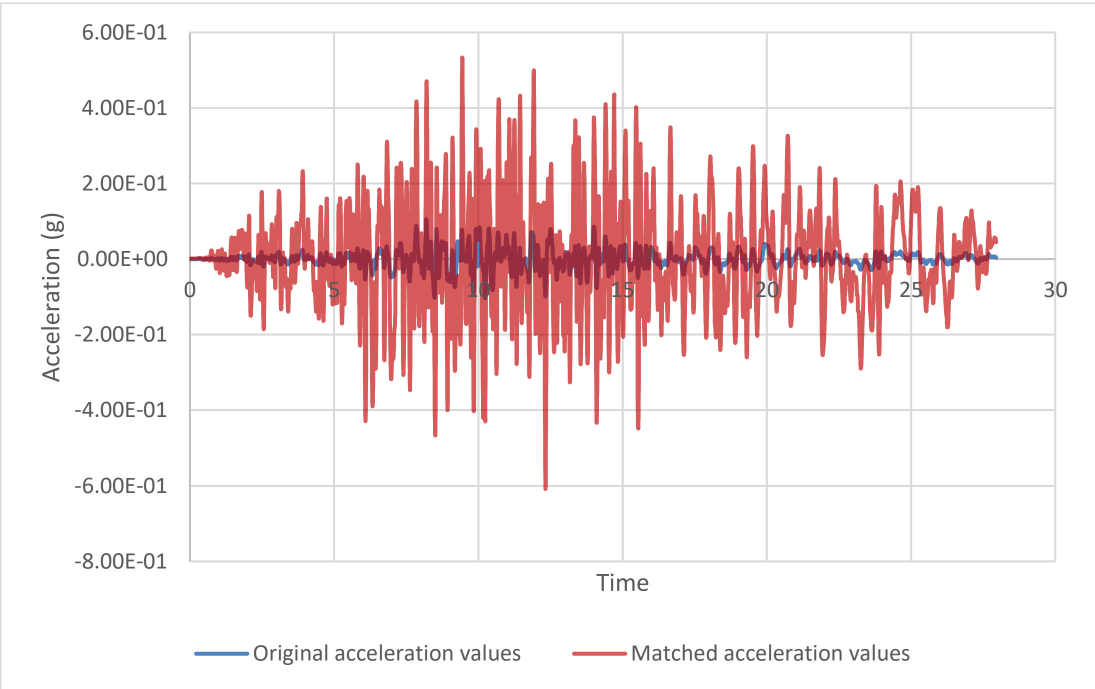

Figure 46. Scaled and unscaled H2 time series of Lomap earthquake

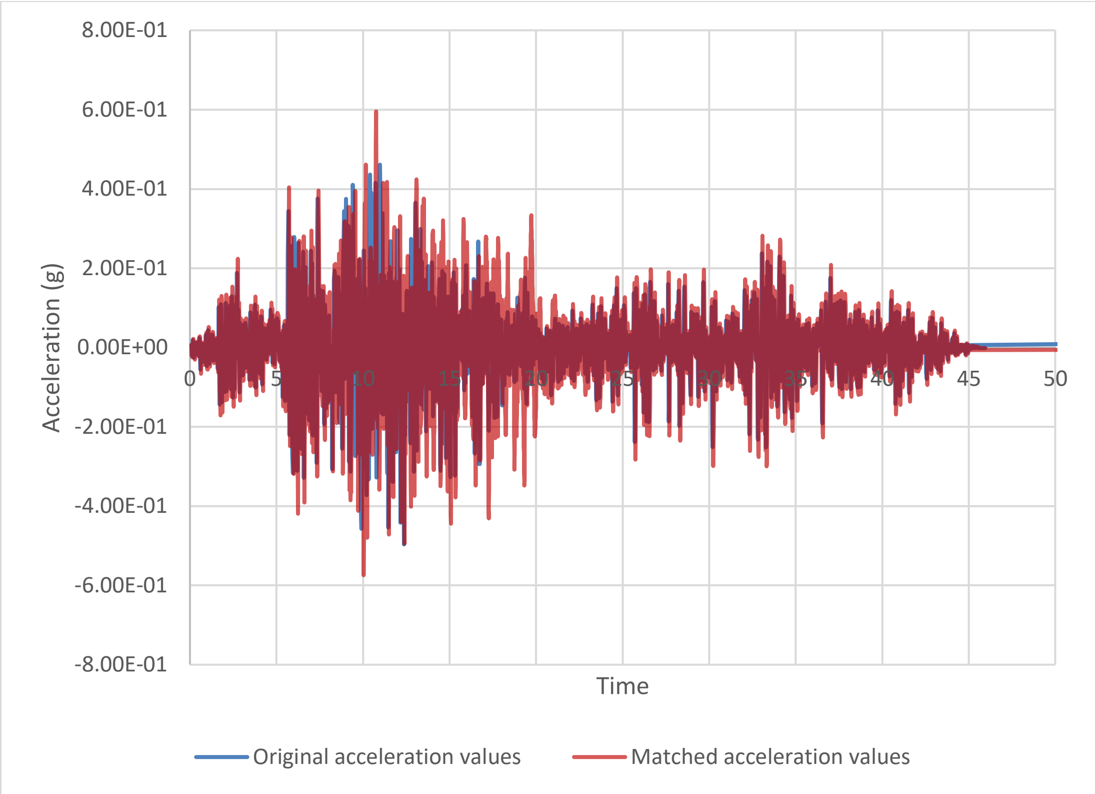

Figure 47. Scaled and unscaled H2 time series of Manjil earthquake

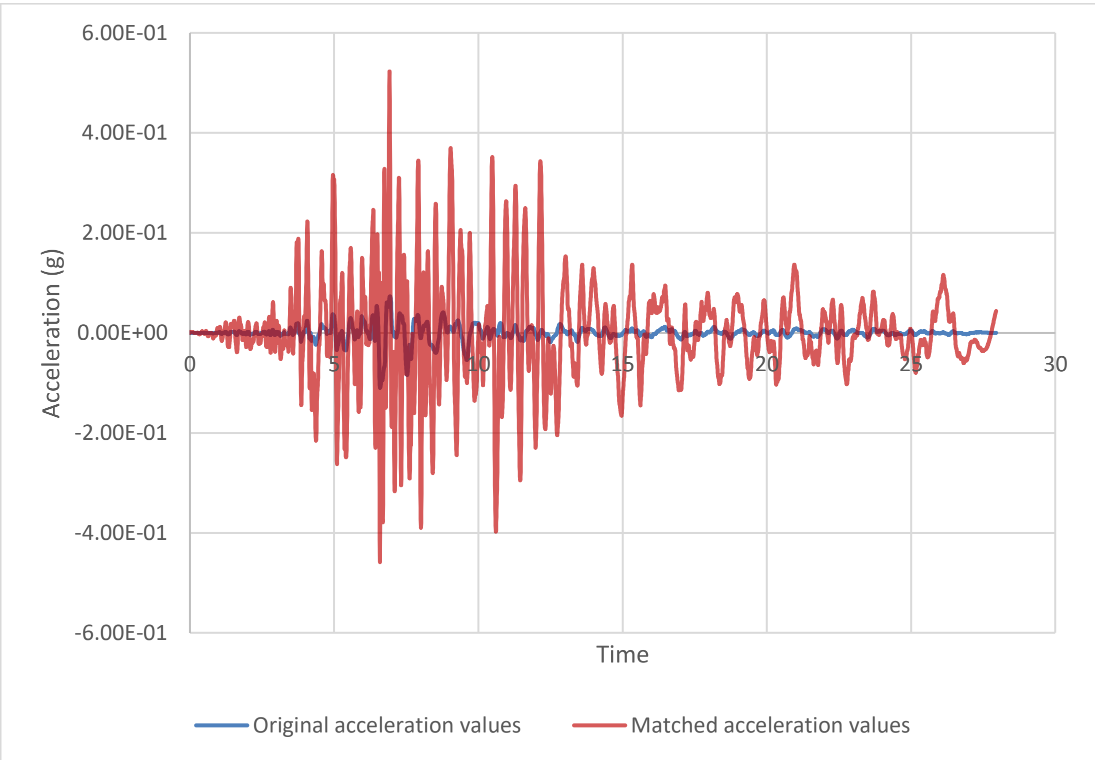

Figure 48. Scaled and unscaled H2 time series of Morgan earthquake

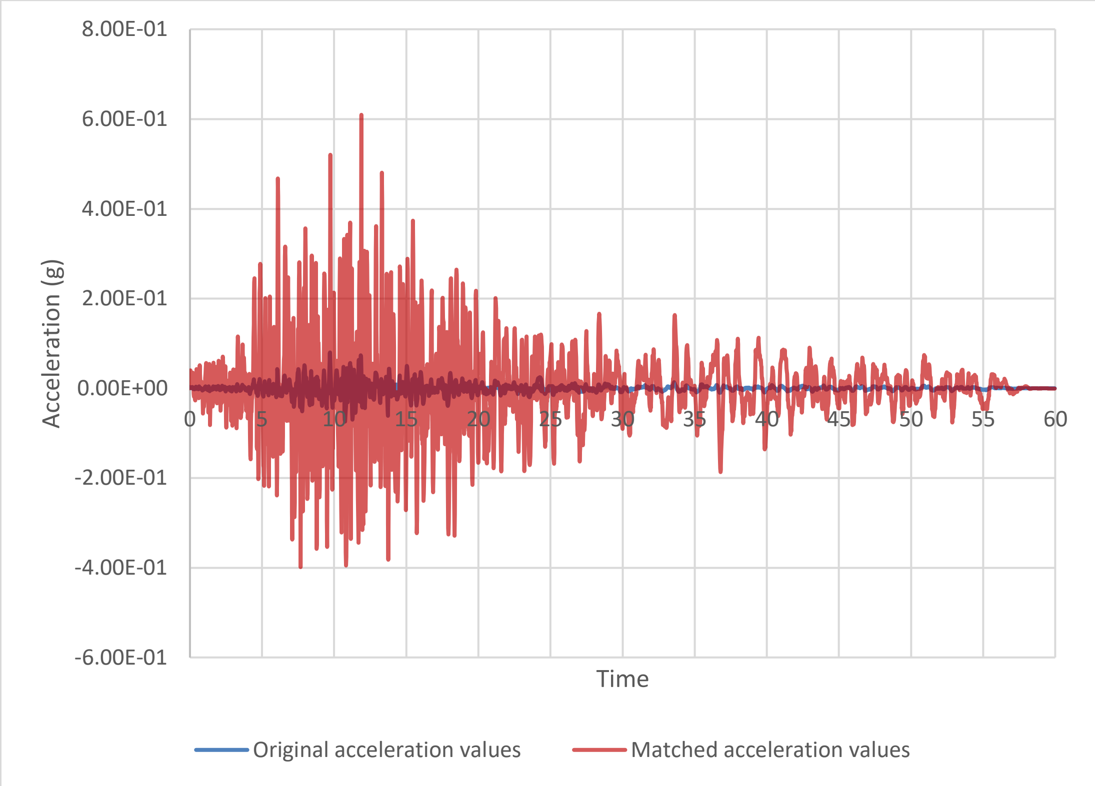

Figure 49. Scaled and unscaled H2 time series of Northr earthquake

Chapter 4

ANALYSIS RESULTS AND DISCUSSION

4.1 Introduction

In this chapter, a variety of results of NLTHA have been carried out considering a set of 11 accelerograms matching on both original and strengthened buildings, are discussed, and compared to demonstrate the effectiveness of employing the proposed MAURER SHARK energy absorber in seismic strengthening.

4.2 A Description of Modelling and Seismic Response

The seismic responses, considered for investigation and comparison, includes story displacement, drift, and acceleration as well as input energy to the building moreover, Inter-story drift check according to TBEC-2018. All the selected earthquake records have been subjected to the buildings as X-X Y-Y which is the X-Direction of the building and X-direction of the earthquake and Y-direction of the building and Y-direction of the earthquake. Furthermore, X-Y Y-X is the X-Direction of the building and Y-direction of the earthquake and Y-direction of the building and X-direction of the earthquake. As stated by TBEC-2018 which indicate that at least eleven earthquake ground motion sets will be used in nonlinear calculations to be made in the time history. Acceleration records in two perpendicular horizontal directions will be affected simultaneously in the direction of the (X) and (Y) principal axes of the system. Then the axes of the acceleration records will be rotated 90^{o} and the calculation will be repeated.

4.3 Results of the Considered Buildings by NLTHA

As a representative of the numerical results of NLTHA, Figures 50 to 74 demonstrate the time histories and response of the seismic effects of the designed buildings subjected to the DUZCE X-X Y-Y earthquake. Furthermore, Tables 10 to 18 demonstrate the maximum response of stories in X and Y directions respectively for the designed 8-Story buildings. The 8- Story building have been strengthened by the implementation of MAURER SHARK in two configurations as shown in Figures 50 and 60 The connection of the SHARK device is applied to the beams and the bottom ends of the columns.

4.3.1 Comparing Results of 8-Story Deniz Building

4.3.1.1 MAURER SHARK Configuration 1 Subjected to DUZCE X-X Y-Y

The strengthening of the 8-Story Deniz building is accomplished by the implementation of MAURER SHARK (MS) in the configuration shown in Figure 50. For economical design, parameters of the smallest size of the energy absorber of MAURER SHARK (see Table 3) are used in the modelling.

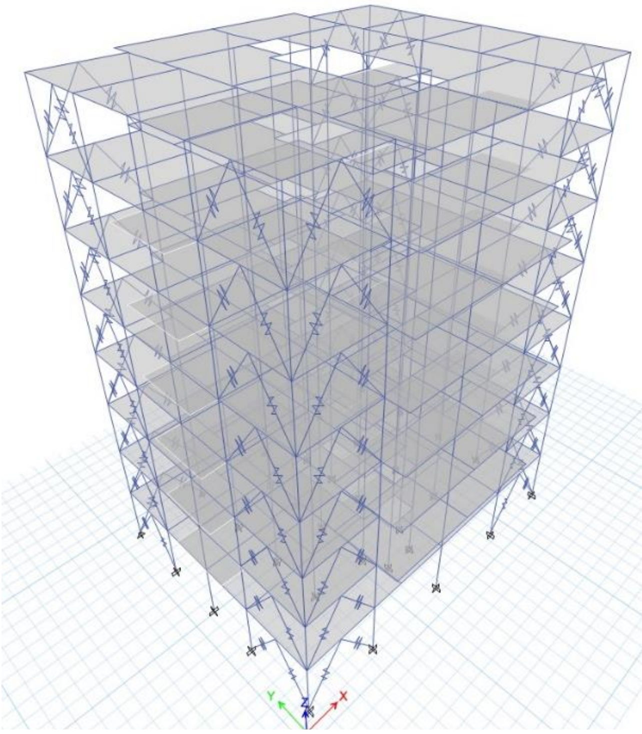

Figure 50. 8-Story building with MAURER SHARK configuration

4.3.1.1.1 Time History of 8-Story Deniz Building with Configuration 1 of MS Results Comparison

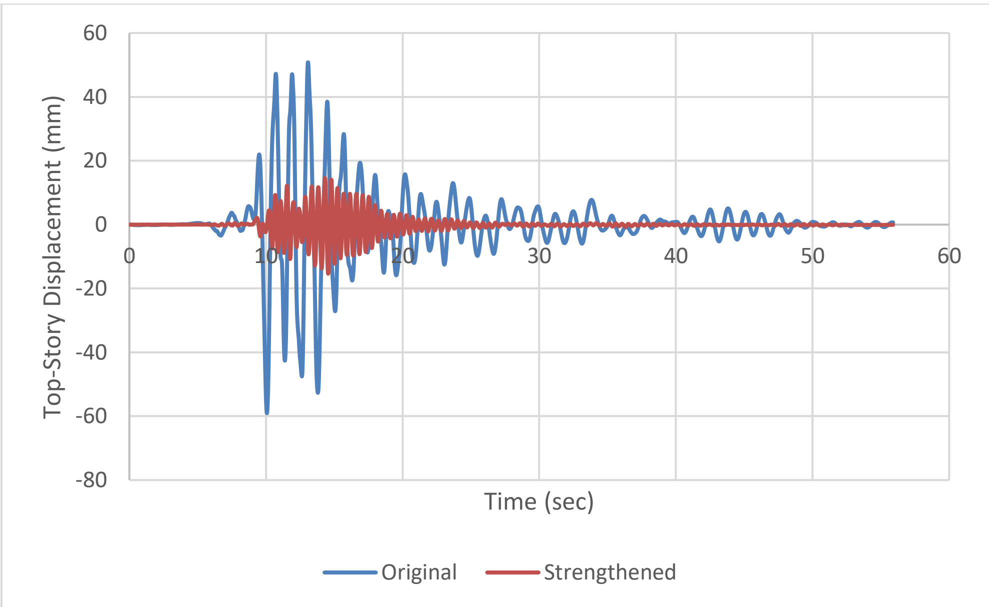

Figure 51. Top-story displacement in X-direction of 8-story building with configuration 1 of MS subjected to Duzce X-X Y-Y earthquake

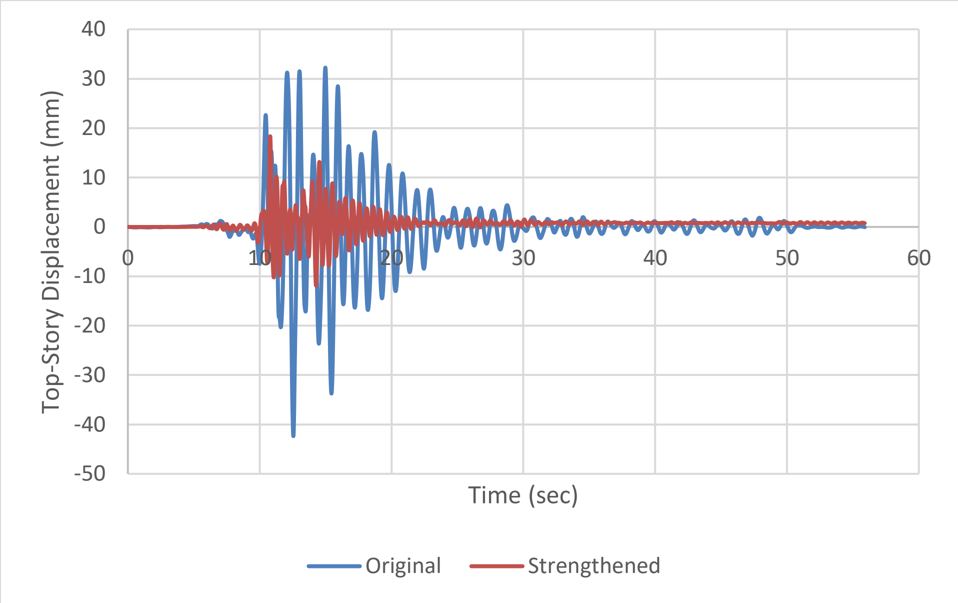

Figure 52. Top-story displacement in Y-direction of 8-story building with configuration 1 of MS subjected to Duzce X-X Y-Y earthquake

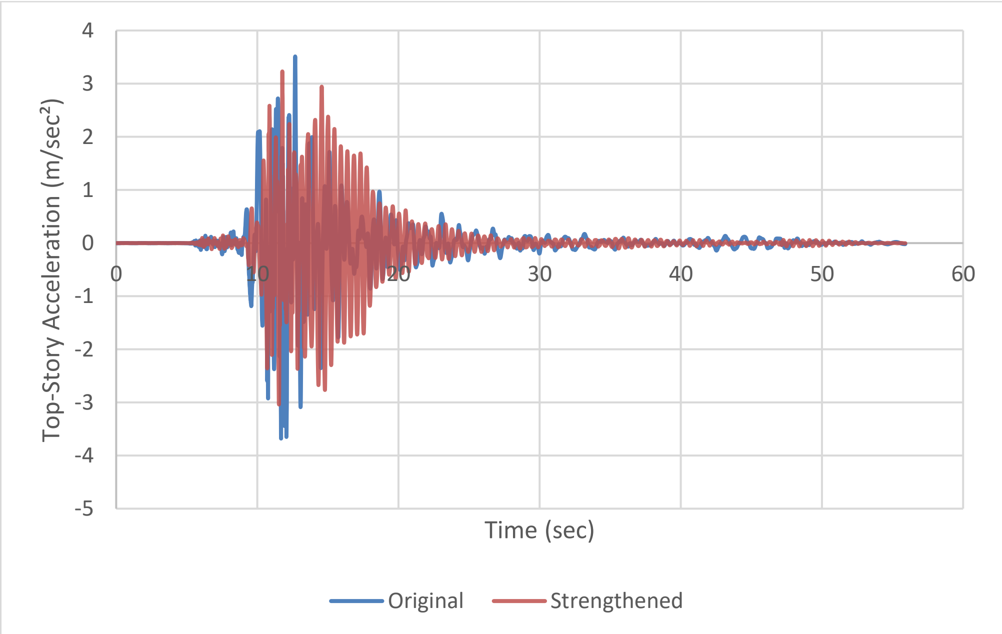

Figure 53. Top-story acceleration in X-direction of 8-story building with configuration 1 of MS subjected to Duzce X-X Y-Y earthquake

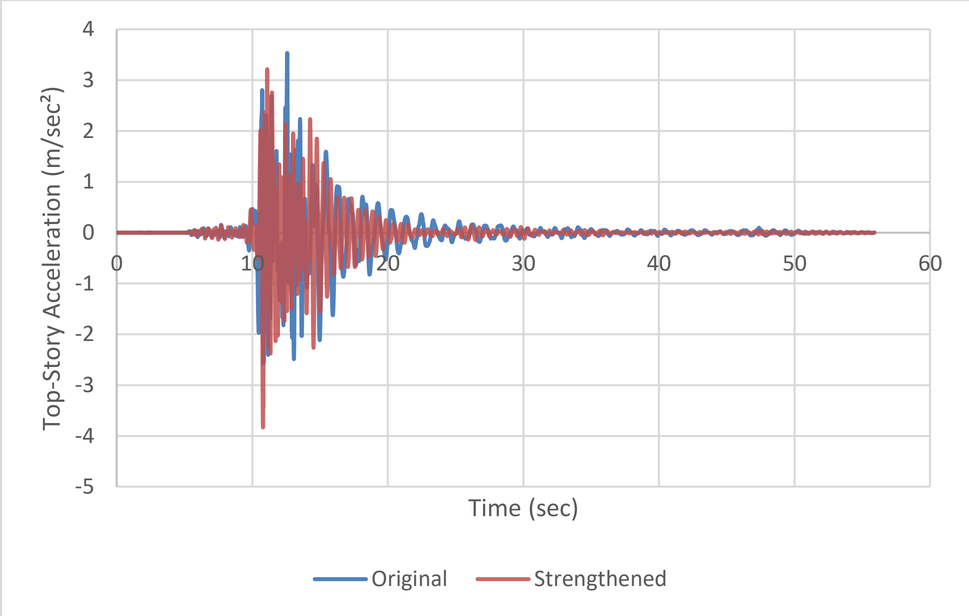

Figure 54. Top-story acceleration in Y-direction of 8-story building with configuration 1 of MS subjected to Duzce X-X Y-Y earthquake

4.3.1.1.2 Story Response of 8-Story Deniz Building with Configuration 1 of MS Results Comparison

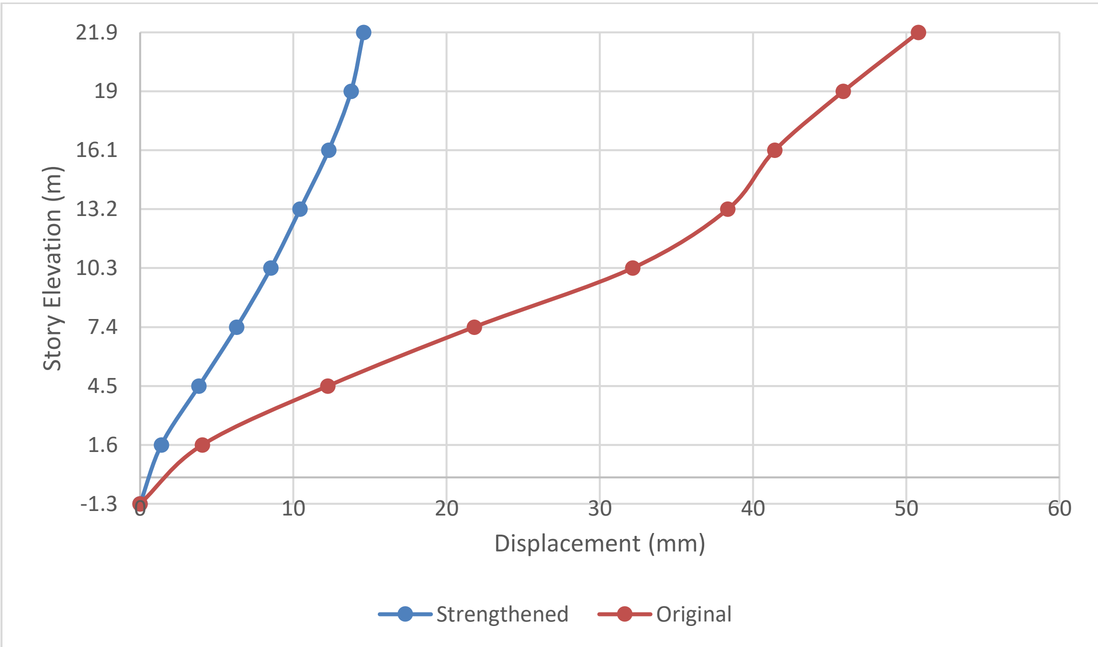

Figure 55. Stories displacement in X-direction of 8-story building with configuration 1 of MS subjected to Duzce X-X Y-Y earthquake

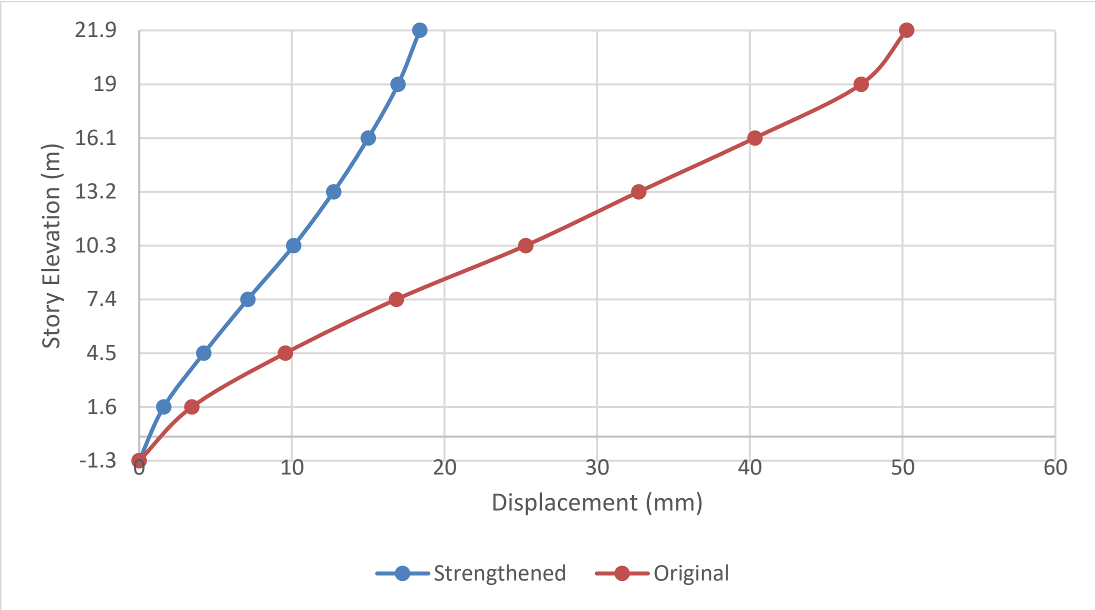

Figure 56. Stories displacement in Y-direction of 8-story building with configuration 1 of MS subjected to Duzce X-X Y-Y earthquake

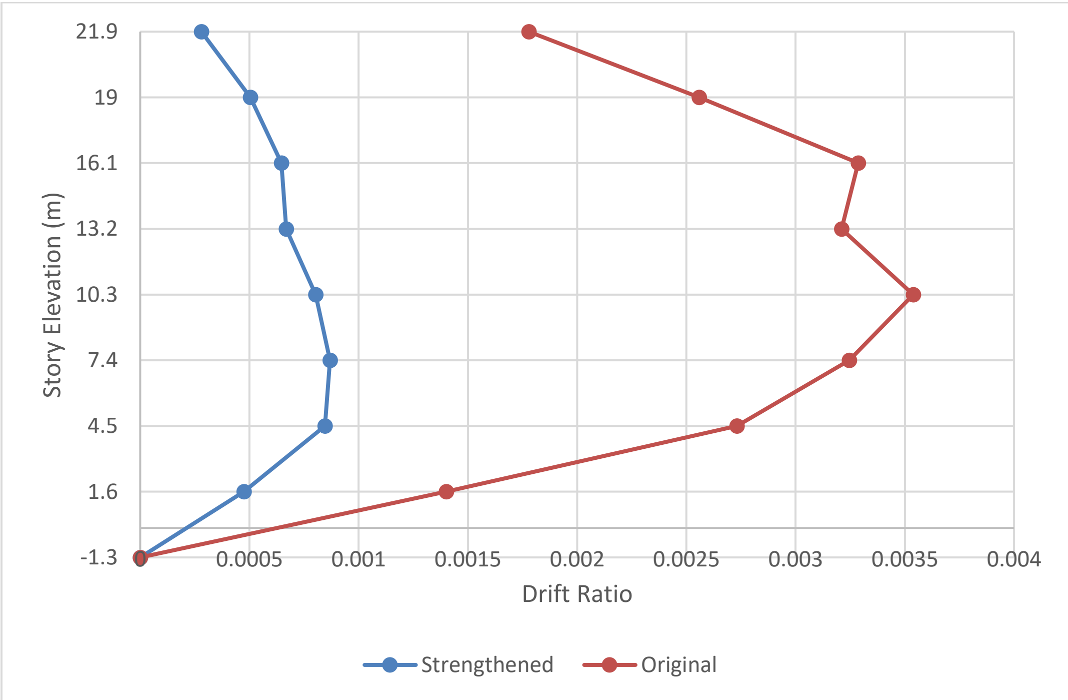

Figure 57. Stories drift in X-direction of 8-story building with configuration 1 of MS subjected to Duzce X-X Y-Y earthquake

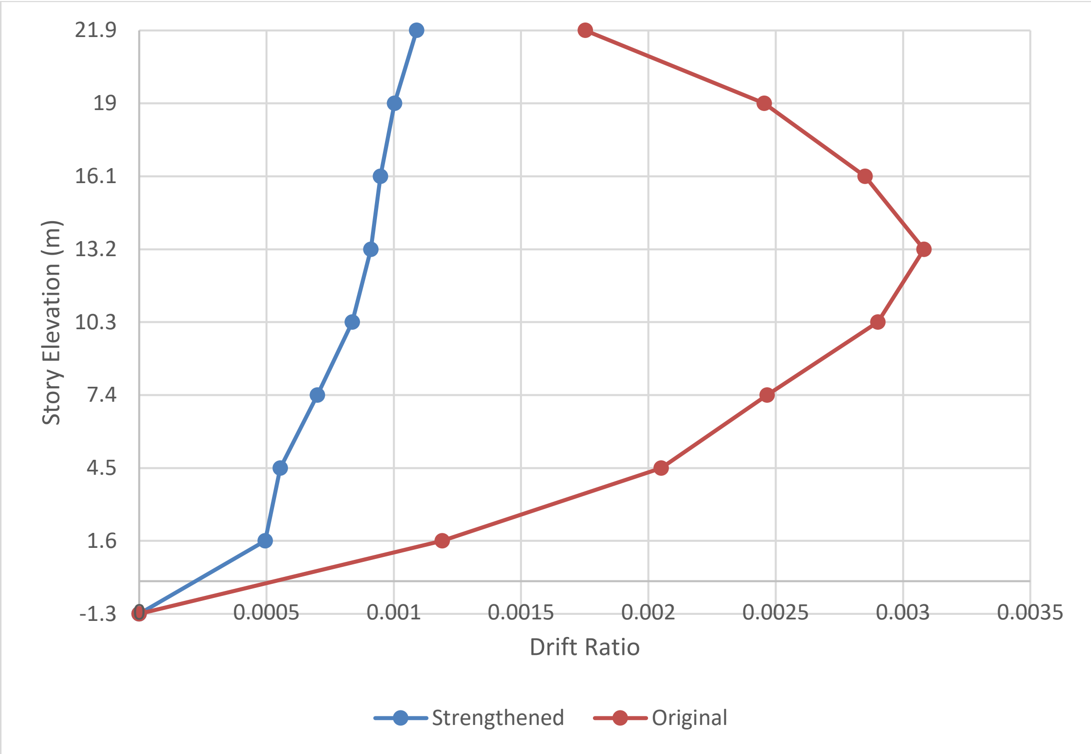

Figure 58. Stories drift in Y-direction of 8-story building with configuration 1 of MS subjected to Duzce X-X Y-Y earthquake

4.3.1.1.3 Input Energy of 8-Story Deniz Building with Configuration 1 of MS Results Comparison

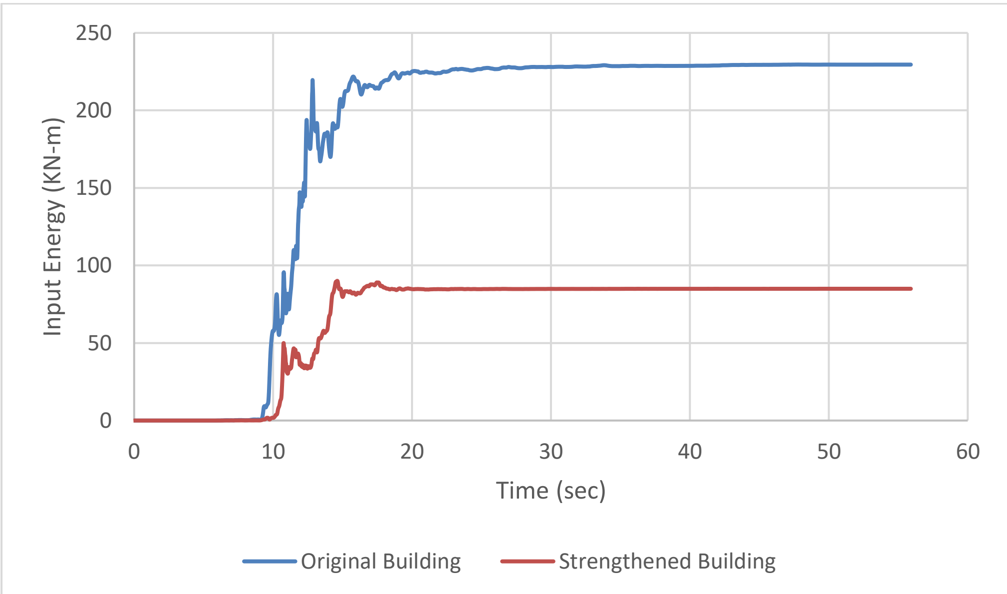

Figure 59. Input energy of 8-story building with configuration 1 of MS subjected to Duzce X-X Y-Y earthquake

Figures 51 to 59 demonstrated that the implementation of MAURER SHARK to the building resulted in a considerable response. As it can be seen in Figures 51 and 52 the time history response has resulted in a significant reduction of the Top Story Displacement for DUZCE X-X Y-Y in the X and Y directions of the building respectively.

Further, Figures 53 and 54 showed a minimal reduction of the Top Story Acceleration for DUZCE X-X Y-Y in the X and Y directions of the building respectively. However, in some cases during minor SLS events, the SHARK generally operates within its elastic range and behaves like a stiff restrainer without much reduction of the earthquake input. This performance characteristic can lead to an increment of the peak story acceleration, which can be prejudicial to the non-structural components and technological contents for buildings such as hospitals, fire stations, police stations, data centers, emergency centers, or substantial commercial structures. To address this issue, the SHARK-Adaptive configuration can be utilized at a higher cost when compared to MAURER SHARK.

Moreover, Figures 55 to 58 demonstrate all stories' responses to displacement and drift. Figures 55 and 56 showed that there was a significant displacement reduction of all stories in both the X and Y direction of the building. Figures 57 and 58 showed that there was a significant drift reduction of all stories in both X and Y directions of the building respectively. Lastly, Figure 59 demonstrated the considerable input energy reduction of the strengthened building when compared to the original building. The same results apply to section 4.3.1.2 the 8-Story building with configuration 2 as the shown responses in Figures 61 to 69.

4.3.1.1.4 Maximum Response of 8-Story Deniz Building with Configuration 1 of MS Results Comparison

In the interest of succinctness, this study does not present graphical results for all the considered earthquakes that were applied, Instead, the maximum response of the stories under the applied scaled earthquakes is presented in Tables 10 and 11 in the X and Y directions of the 8-Story Deniz building, respectively.

Table 10. Max story response in X-direction of 8-story Deniz building with configuration 1 of MS results

Output Case		Story Displacement (mm)	Story Drift (Ratio)	Story Acceleration (m/sec²)
1. DUZCE X-X Y-Y	Original	50.81	0.001778	3.27
	Strengthened	14.58	0.000281	2.9
Reduction %		71	84	11
1. DUZCE X-Y Y-X	Original	73.24	0.002688	4.38
	Strengthened	12.545	0.000243	2.64
Reduction %		83	91	40
2. FRIULI X-X Y-Y	Original	60.32	0.002108	2.88
	Strengthened	16.08	0.000347	3.51
Reduction %		73	83	-22
2. FRIULI X-Y Y-X	Original	67.65	0.002437	3.55
	Strengthened	15.46	0.000316	3.16
Reduction %		77	87	11
3. IMPVAL X-X Y-Y	Original	65.87	0.002333	3.52
	Strengthened	13.68	0.000293	2.62
Reduction %		79	87	26
3. IMPVAL X-Y Y-X	Original	64.1	0.002025	3.64
	Strengthened	14.51	0.000282	2.82
Reduction %		77	86	22
4. KERN X-X Y-Y	Original	72.1	0.002195	4.8
	Strengthened	15.98	0.000322	3.46
Reduction %		78	85	28
4.KERN	Original	56.05	0.001999	2.82

X-Y Y-X	Strengthened	13.67	0.000307	2.81
Reduction %		76	85	0.35
5.KOBE X-X Y-Y	Original	68.45	0.002648	4.7
	Strengthened	16.13	0.000349	3.6
Reduction %		76	87	23
5. KOBE X-Y Y-X	Original	63.7	0.002387	3.12
	Strengthened	12.4	0.00028	2.88
Reduction %		81	88	8
6.KOCAELI X-X Y-Y	Original	61.79	0.001786	4.35
	Strengthened	14.82	0.000303	3.02
Reduction %		76	83	31
6. KOCAELI X-Y Y-X	Original	50.077	0.002164	3.11
	Strengthened	11.91	0.000238	2.6
Reduction %		76	89	16
5. LANDERS X-X Y-Y	Original	63.73	0.002365	3.35
	Strengthened	15.54	0.000298	2.88
Reduction %		76	87	14
7. LANDERS X-Y Y-X	Original	52.25	0.001851	3.19
	Strengthened	14.94	0.000339	3.41
Reduction %		71	82	-7
8.LOMA X-X Y-Y	Original	75.64	0.002401	4.06
	Strengthened	13.77	0.000292	3.04
Reduction %		82	88	25
8. LOMA X-Y Y-X	Original	73.8	0.00278	4.13
	Strengthened	13.52	0.000315	2.71
Reduction %		82	87	34
9. MANJIL X-X Y-Y	Original	83.23	0.002287	3.73
	Strengthened	11.9	0.000266	2.5
Reduction %		86	88	33
9. MANJIL X-Y Y-X	Original	58.23	0.002207	3.25
	Strengthened	13.77	0.000301	2.8
Reduction %		76	86	14
10 MORGAN X-X Y-Y	Original	61.35	0.002433	4.11
	Strengthened	14.72	0.000281	2.48
Reduction %		76	88	40

10 MORGAN X-Y Y-X	Original	73.23	0.002769	2.41
	Strengthened	12.86	0.000256	2.77
Reduction %		82	91	-15
11. NORTHR X-X Y-Y	Original	66.27	0.00286	3.6
	Strengthened	12.18	0.000285	2.97
Reduction %		82	90	18
11. NORTHR X-Y Y-X	Original	60.63	0.001949	3.8
	Strengthened	13.37	0.0003	2.95
Reduction %		78	85	22

Table 11. Max story response in Y-direction of 8-story Deniz building with configuration 1 of MS results

Output Case		**Story Displacement (mm)**	**Story Drift (Ratio)**	**Story Acceleration (m/sec²)**
1. DUZCE X-X Y-Y	Original	50.26	0.001752	3.56
	Strengthened	18.37	0.000495	2.73
Reduction %		63	72	23
1. DUZCE X-Y Y-X	Original	46.97	0.001374	4.08
	Strengthened	17.89	0.000488	2.93
Reduction %		62	64	28
2. FRIULI X-X Y-Y	Original	49.9	0.001746	3.82
	Strengthened	18.27	0.000501	3.32
Reduction %		63	71	13
2. FRIULI X-Y Y-X	Original	42.23	0.001539	2.84
	Strengthened	18.25	0.000473	3.9
Reduction %		57	69	-37
3. IMPVAL X-X Y-Y	Original	49.87	0.001598	2.83
	Strengthened	16.94	0.000456	2.5
Reduction %		66	71	12
3. IMPVAL X-Y Y-X	Original	46.63	0.001381	2.83
	Strengthened	16.39	0.000467	2.98
Reduction %		65	66	-5
4. KERN X-X Y-Y	Original	44.21	0.001355	2.62
	Strengthened	17.33	0.000483	3.32

Reduction %		61	64	-27
4.KERN	Original	52.11	0.001464	3.55
X-Y Y-X	Strengthened	15.98	0.000463	2.74
Reduction %		69	68	23
5.KOBE	Original	48.96	0.001451	3.12
X-X Y-Y	Strengthened	14.77	0.000418	2.88
Reduction %		70	71	8
5. KOBE	Original	41.94	0.001392	3.48
X-Y Y-X	Strengthened	16.02	0.00041	3.17
Reduction %		62	70	9
6.KOCAELI	Original	41.23	0.001505	3.02
X-X Y-Y	Strengthened	12.06	0.000405	2.73
Reduction %		71	73	10
6. KOCAELI	Original	42.35	0.001306	3.36
X-Y Y-X	Strengthened	16.08	0.000424	2.45
Reduction %		62	68	27
7. LANDERS	Original	64.29	0.002458	3.66
X-X Y-Y	Strengthened	15.83	0.000441	2.96
Reduction %		75	82	19
7. LANDERS	Original	45.73	0.001413	3.23
X-Y Y-X	Strengthened	16.31	0.000509	3.52
Reduction %		64	64	-9
8.LOMA	Original	41.38	0.001696	3.28
X-X Y-Y	Strengthened	17.71	0.000547	3.29
Reduction %		57	68	-0.3
8. LOMA	Original	52.09	0.001554	3.5
X-Y Y-X	Strengthened	17.83	0.000525	3.37
Reduction %		66	66	4
9. MANJIL	Original	53.33	0.001725	2.65
X-X Y-Y	Strengthened	19.16	0.000577	3.22
Reduction %		64	67	-22
9. MANJIL	Original	51.4	0.001416	2.86
X-Y Y-X	Strengthened	16.81	0.000453	2.88
Reduction %		67	68	-0.7

10 MORGAN X-X Y-Y	Original	31.72	0.001296	2.92
	Strengthened	17.47	0.000586	3.37
Reduction %		45	55	-15
10 MORGAN X-Y Y-X	Original	54.83	0.001884	3.54
	Strengthened	18.07	0.000484	2.56
Reduction %		67	74	28
11. NORTHR X-X Y-Y	Original	49.65	0.001879	3.13
	Strengthened	14.39	0.000493	3.42
Reduction %		71	74	-9
11. NORTHR X-Y Y-X	Original	41.66	0.001832	3.75
	Strengthened	17.92	0.000476	3.49
Reduction %		57	74	6

Tables 10 and 11 demonstrated the maximum responses of 8-Story original and strengthened with configuration 1 buildings, story displacement, story drift, and story acceleration, all of which are significantly decreased compared to the original building. The reduction of the displacement in most of the cases are over 70% for X-direction, while, in Y-direction most of the cases are over 60%. The reduction of the drift in most of the cases are over 80% for X-direction, while, in Y-direction most of the cases are over 70%. Furthermore, the reduction of the acceleration in the X-direction most of the vary between 8% to 44% but some cases showed below 1% reduction, while in Y-direction vary between 4% to 28%. Further, 3 of the cases in X-direction resulted in acceleration increment varying between 7% up to 22%. While in Y-direction 9 of the cases resulted in acceleration increment of 0.3% and 27%. The acceleration increment can be due to the fact the SHARK performance characteristic may behave like a stiff restrainer in some earthquake events which led to an increment of the story acceleration, or it can be due to long-period earthquake, because of the close correlation between the period of the strengthened building and some of the selected earthquakes. Nevertheless, most of the strengthened buildings have shown significantly better seismic performance than the original ones, which approve of the effectiveness of SHARK as an energy dissipation device.

4.3.1.1.5 Input Energy of Original and Strengthened 8-Story Buildings with Configuration 1 of MS Results Comparison

The input energy caused by earthquakes subjected to original and strengthened buildings is shown in Table 12. According to the results, the strengthened building showed a significant decrease in the Input energy as compared to the original building.

Table 12. Input energy of 8-story Deniz building with configuration 1 of MS results

Output Case	Original kN-m	Strengthened kN-m	Reduction %
1. DUZCE X-X Y-Y	229.5858	90.0942	61
1. DUZCE X-Y Y-X	252.9478	113.9889	55
2. FRIULI X-X Y-Y	510.8472	153.1915	70
2. FRIULI X-Y Y-X	511.596	208.5827	59
3. IMPVAL X-X Y-Y	1034.5741	257.719	75
3. IMPVAL X-Y Y-X	829.4655	271.2382	67
4. KERN X-X Y-Y	483.8709	212.1759	56
4. KERN X-Y Y-X	555.8534	153.9982	72
5. KOBE X-X Y-Y	432.5402	109.6562	75
5. KOBE X-Y Y-X	469.9797	79.3143	83
6. KOCAELI X-X Y-Y	304.4265	86.4378	72
6. KOCAELI X-Y Y-X	221.4493	65.492	70
7. LANDERS X-X Y-Y	324.9492	104.8087	68

7. LANDERS X-Y Y-X	336.4976	117.8001	65
8. LOMA X-X Y-Y	592.2024	191.5439	68
8. LOMA X-Y Y-X	589.2366	163.445	72
9. MANJIL X-X Y-Y	343.3354	100.8728	71
9. MANJIL X-Y Y-X	357.7581	119.9789	66
10 MORGAN X-X Y-Y	271.8399	99.4532	63
10 MORGAN X-Y Y-X	273.9571	104.7164	62
11. NORTHR X-X Y-Y	340.3192	115.6935	66
11. NORTHR X-Y Y-X	415.5953	138.7465	67

4.3.1.1.6 Inter Story Drift Ratio (ISDR) limit according to TEC-2018

The variance of ISDR requirements along stories height of the 8-Story strengthened building is shown in Tables 13 and 14.

$$\Delta_i = u_i - u_{i-1} \quad (4)$$

$$\delta_i = \frac{R}{I}\Delta_i \quad (5)$$

$$\text{Max ISDR}\left(\frac{\delta_i}{h_i}\right) \le \frac{0.008\,k}{\lambda} \quad (6)$$

A building's drift demand is calculated by subtracting the consecutive story displacements, resulting from the analysis of the building under earthquake effects as specified by Eq. (4). By using Eq. (5), we can determine the effective story drift. The maximum ratio of story drift to story height is calculated as specified in Eq. (6) to determine the maximum ISDR of the building. The ISDR limit resulted to be 26%.

Table 13. ISDR in X-direction of 8-story building with configuration 1

Story No.	Original	Limit Check	Strengthened	Limit Check
8	0.013546	Within limit	0.00112	Within limit
7	0.012327	Within limit	0.002016	Within limit
6	0.008473	Within limit	0.002571	Within limit
5	0.017146	Within limit	0.002639	Within limit
4	**0.028507**	**More than limit**	0.003069	Within limit
3	**0.026357**	**More than limit**	0.003398	Within limit
2	0.022601	Within limit	0.00339	Within limit
1	0.011206	Within limit	0.001909	Within limit

Table 14. ISDR in Y-direction of 8-story building with configuration 1

Story No.	Original ISDR	Limit Check	Strengthened	Limit Check
8	0.008215	Within limit	0.001951	Within limit
7	0.019213	Within limit	0.002699	Within limit
6	0.020939	Within limit	0.00313	Within limit
5	0.02047	Within limit	0.0036	Within limit
4	0.023357	Within limit	0.004154	Within limit
3	0.020065	Within limit	0.003966	Within limit
2	0.016867	Within limit	0.003628	Within limit

1	0.009525	Within limit	0.002216	Within limit

According to the results, the ISDR in X-direction of the original building showed that stories 3 and 4 have more than the ISDR limit however, the strengthened building reduced the ISDR and performed within the limit. Furthermore, the ISDR for the strengthened building showed much less when compared to the original building.

4.3.1.2 MAURER SHARK Configuration 2 Subjected to DUZCE X-X Y-Y

The strengthening of the 8-Story Deniz building is accomplished by the implementation of the most economical size of MAURER SHARK in the configuration shown in Figure 60.

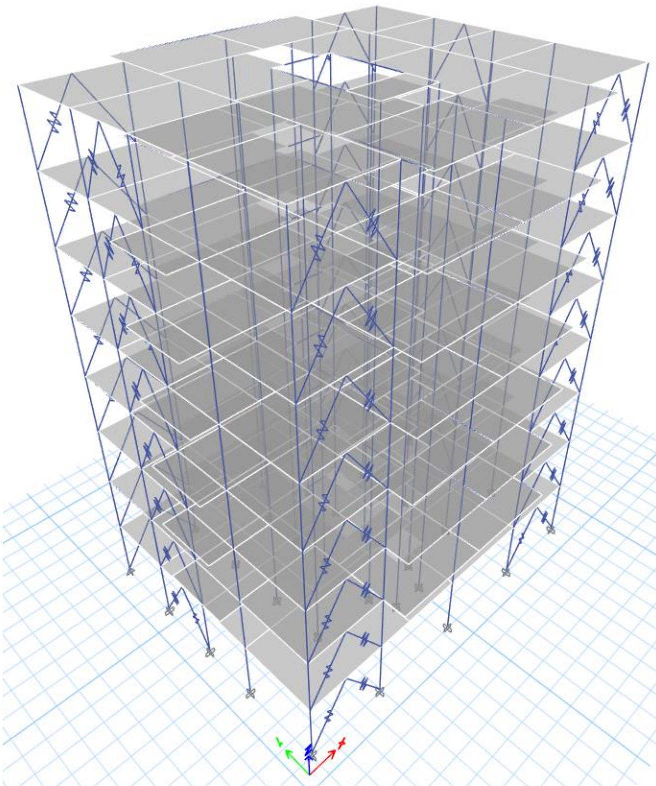

Figure 60. 8-Story building with MAURER SHARK on configuration 2

4.3.1.2.1 Time History of 8-Story Deniz Building with Configuration 2 of MS Results Comparison

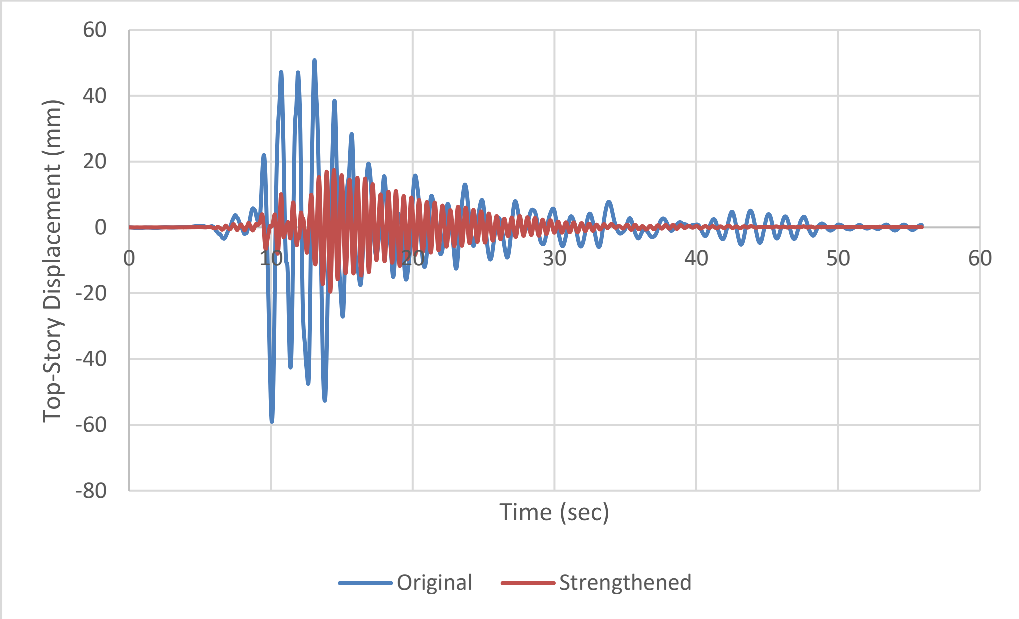

Figure 61. Top-story displacement in X-direction of 8-story building with configuration 2 of MS subjected to Duzce X-X Y-Y earthquake

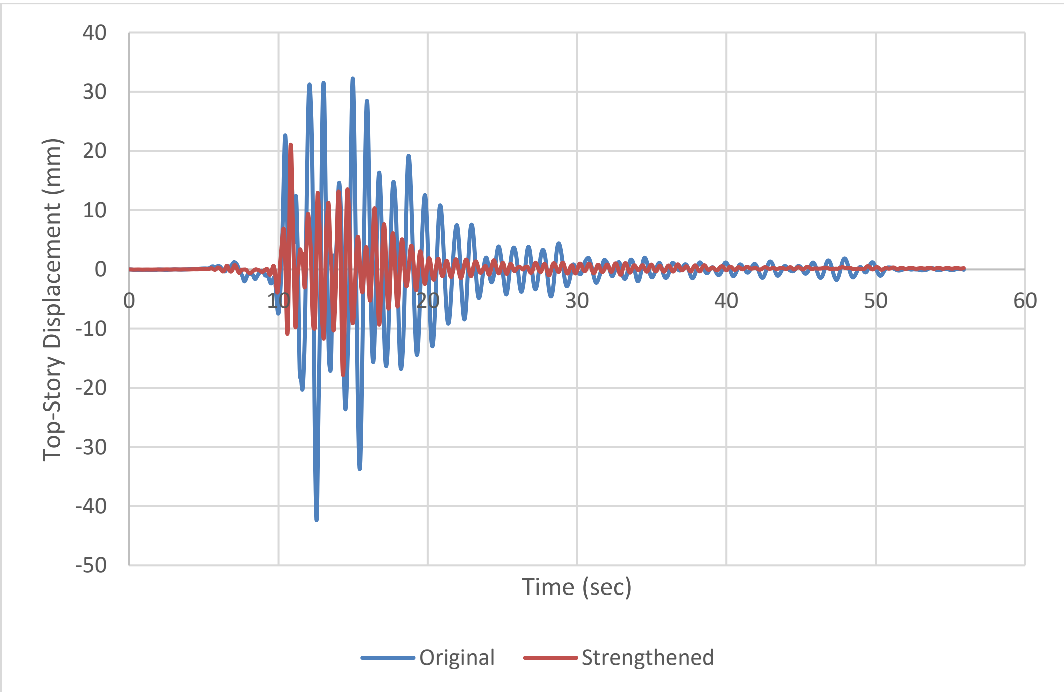

Figure 62. Top-story displacement in Y-direction of 8-story building with configuration 2 of MS subjected to Duzce X-X Y-Y earthquake

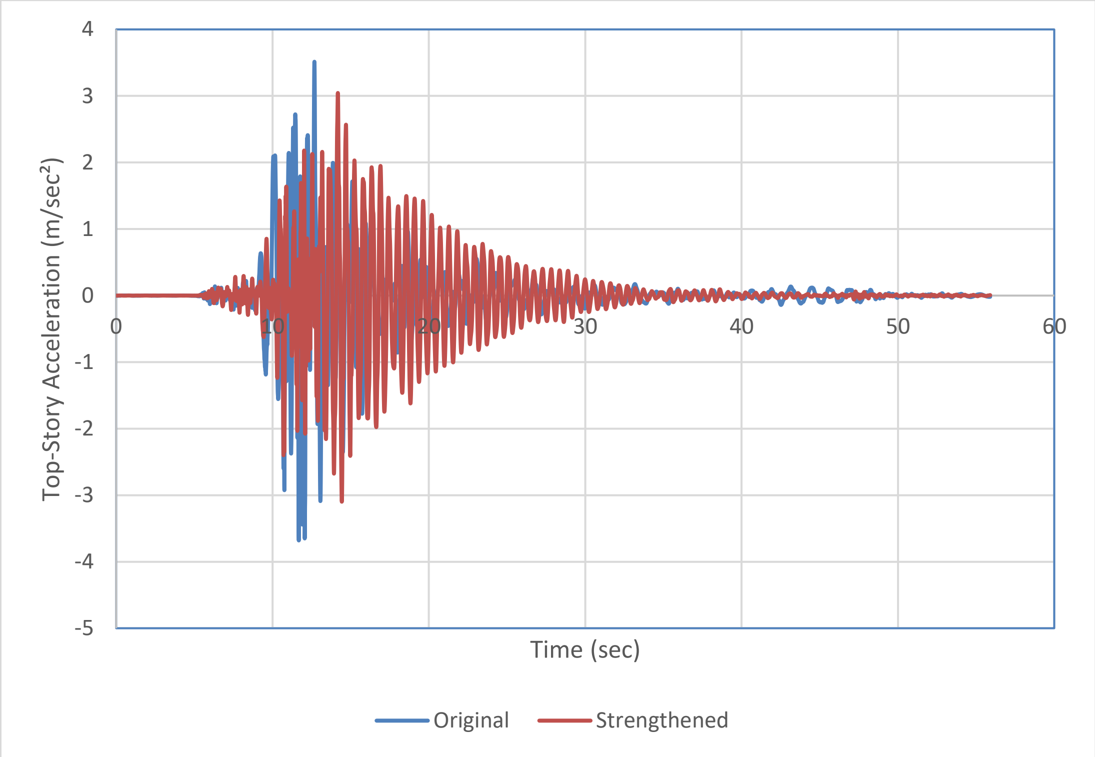

Figure 63. Top-story acceleration in X-direction of 8-story building with configuration 2 of MS subjected to Duzce X-X Y-Y earthquake

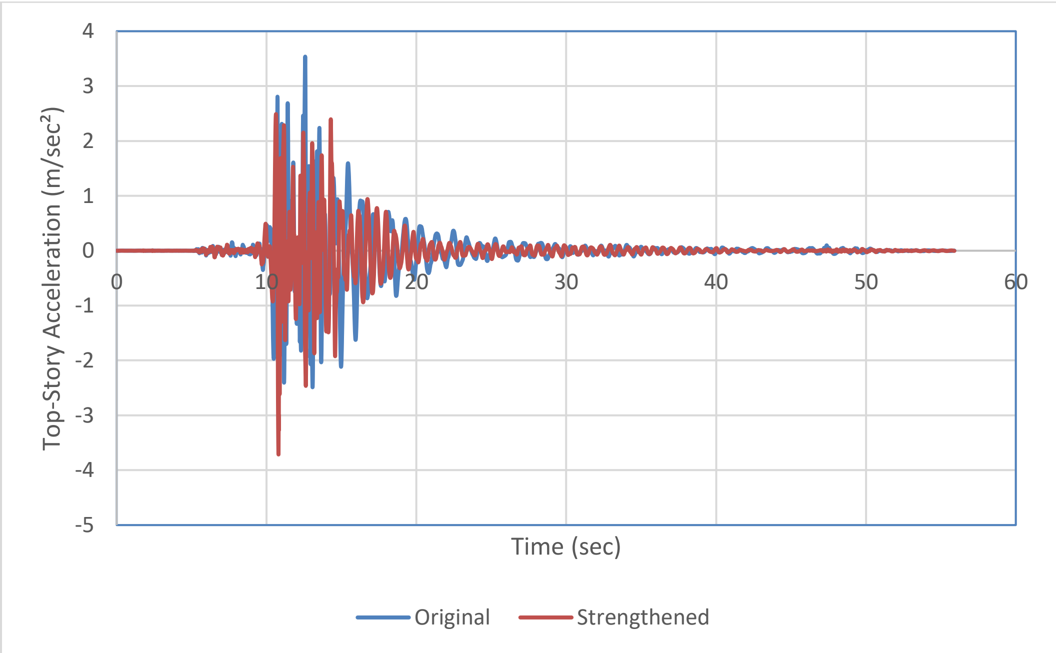

Figure 64. Top-story acceleration in Y-direction of 8-story building with configuration 2 of MS subjected to Duzce X-X Y-Y earthquake

4.3.1.2.2 Story Response of 8-Story Deniz Building with Configuration 2 of MS

Results Comparison

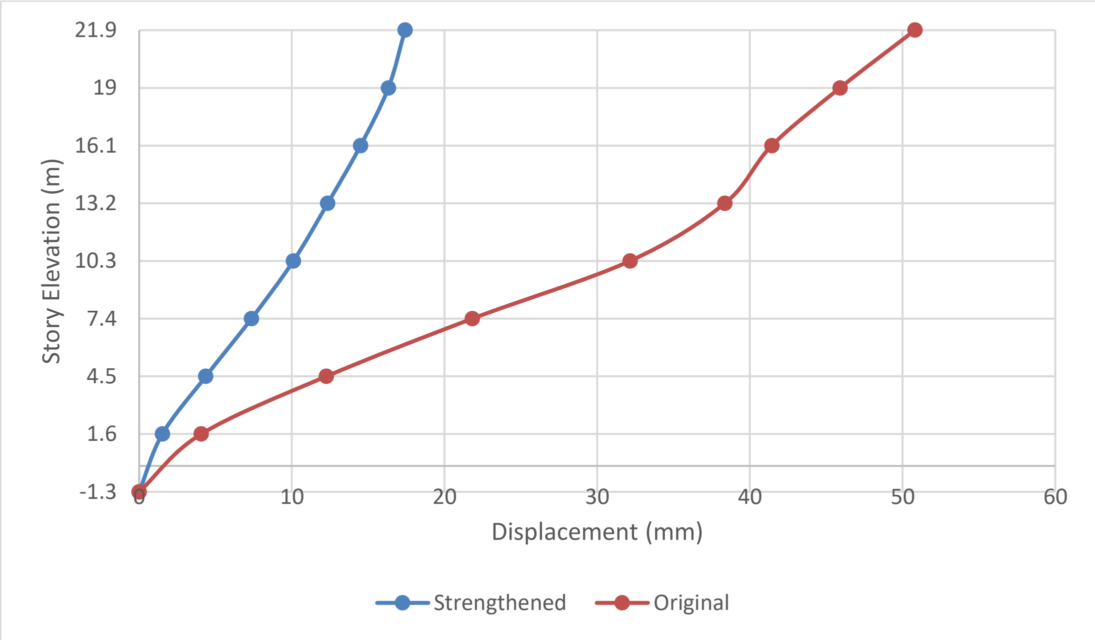

Figure 65. Stories displacement in X-direction of 8-story building with configuration 2 of MS subjected to Duzce X-X Y-Y earthquake

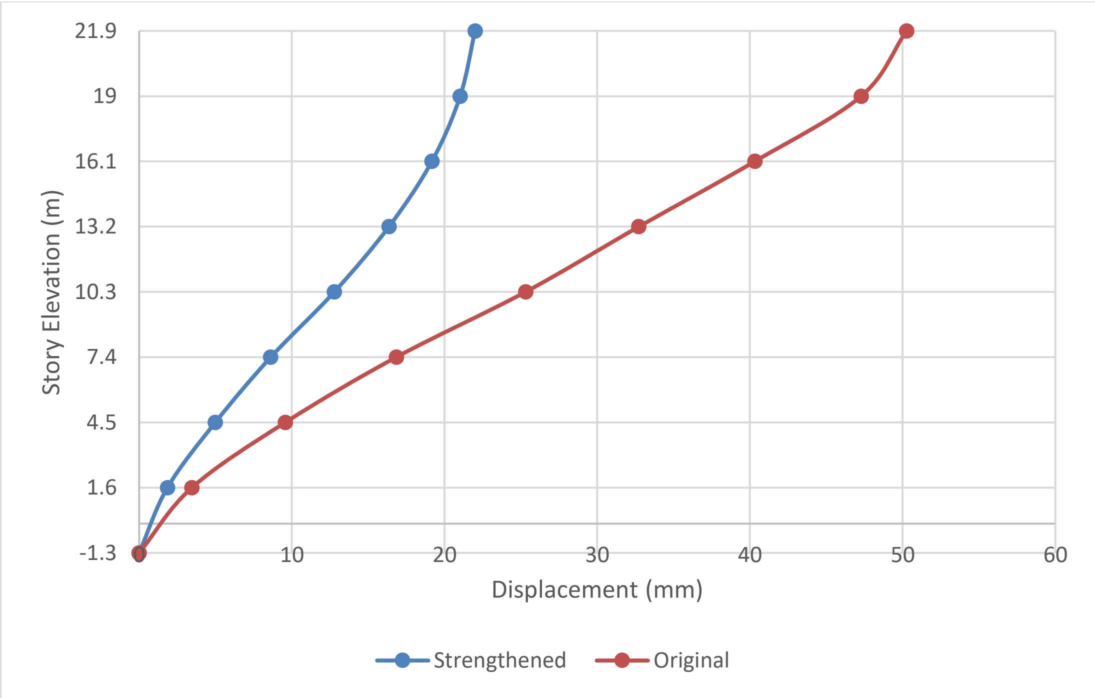

Figure 66. Stories displacement in Y-direction of 8-story building with configuration 2 of MS subjected to Duzce X-X Y-Y earthquake

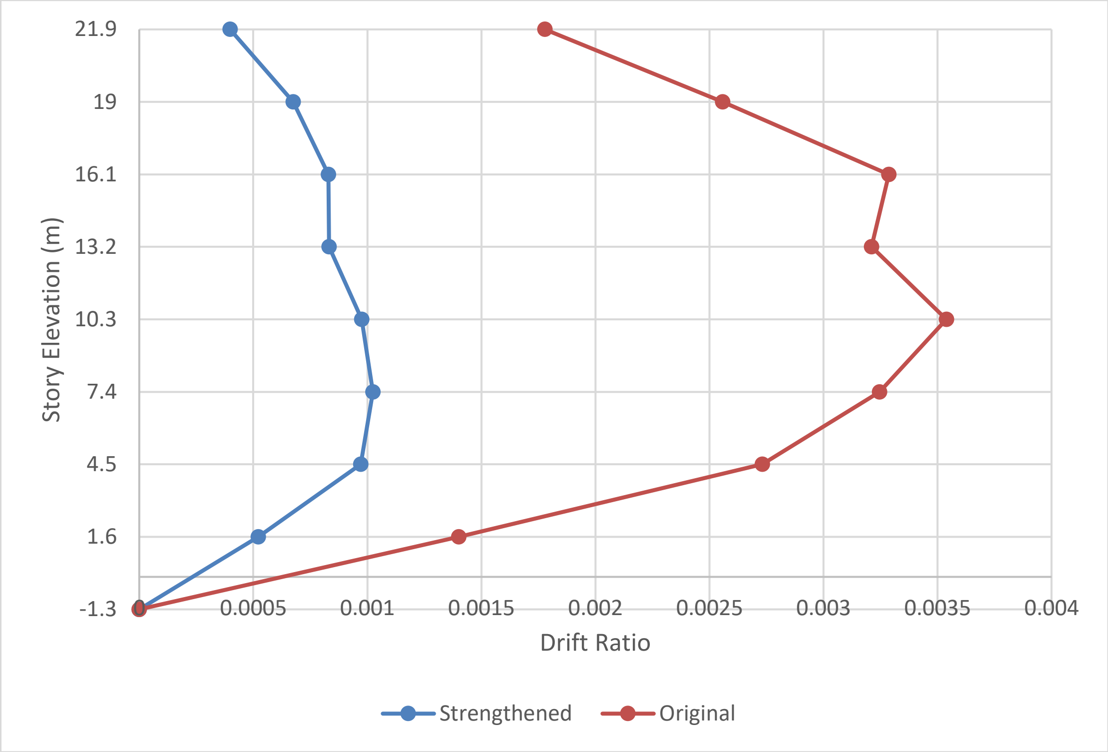

Figure 67. Stories drift in X-direction of 8-story building with configuration 2 of MS subjected to Duzce X-X Y-Y earthquake

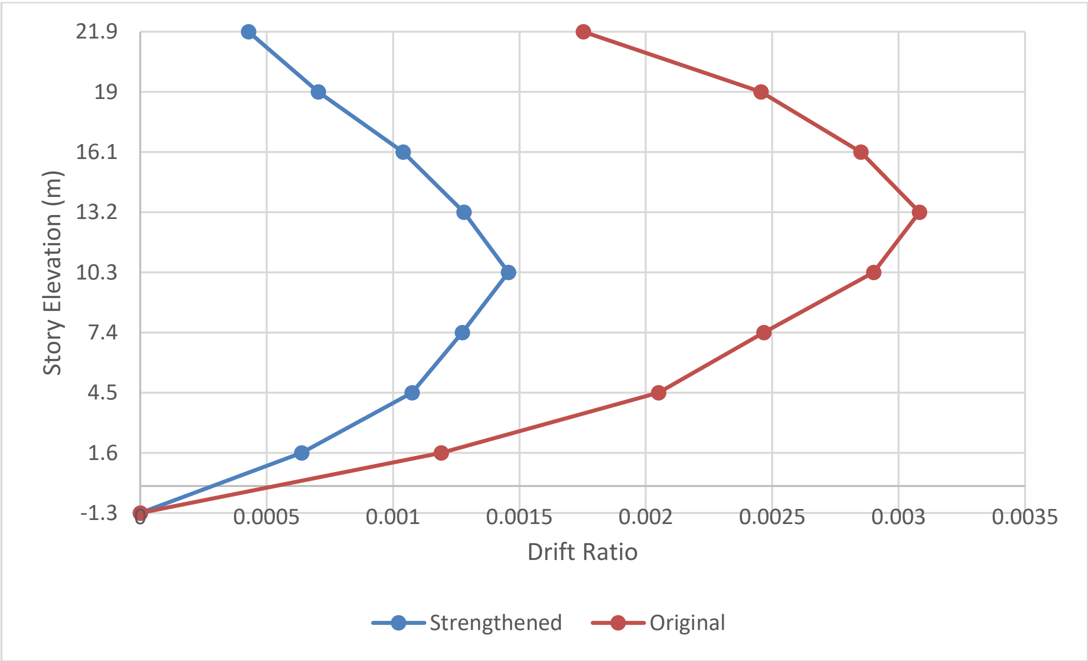

Figure 68. Stories drift in Y-direction of 8-story building with configuration 2 of MS subjected to Duzce X-X Y-Y earthquake

4.3.1.2.3 Input Energy of 8-Story Deniz Building with Configuration 2 of MS Results Comparison

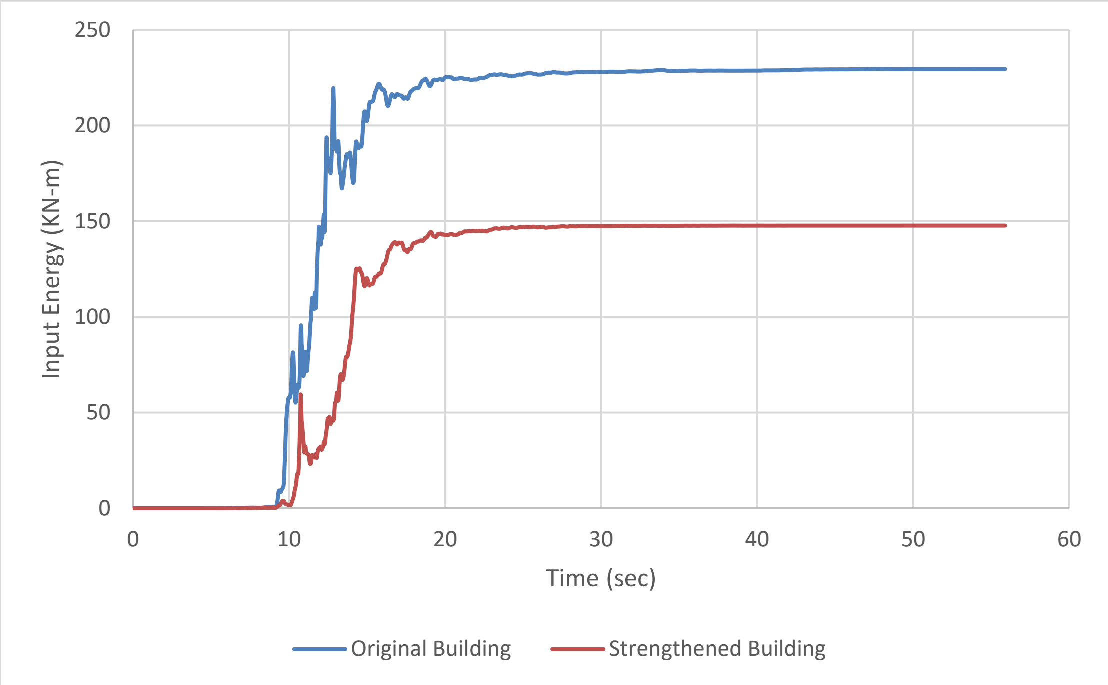

Figure 69. Input energy of 8-story building with configuration 2 of MS subjected to Duzce X-X Y-Y earthquake

Figures 61 to 69 demonstrated that the implementation of MAURER SHARK to the building resulted in a considerable response. As it can be seen in Figures 61 and 62 the time history response has resulted in a significant reduction of the Top Story Displacement for DUZCE X-X Y-Y in the X and Y directions of the building respectively.

Further, Figures 63 and 64 showed a minimal reduction of the Top Story Acceleration for DUZCE X-X Y-Y in the X and Y directions of the building respectively. Moreover, Figures 65 to 68 demonstrate all stories' responses to displacement and drift. Figures 65 and 66 showed that there was a significant displacement reduction of all stories in both the X and Y direction of the building. Figures 67 and 68 showed that there was a significant drift reduction of all stories in both X and Y directions of the building respectively. Lastly, Figure 69 demonstrated the considerable input energy reduction of the strengthened building when compared to the original building.

4.3.1.2.4 Maximum Response of 8-Story Deniz Building with Configuration 2 of MS Results Comparison

In the interest of succinctness, this study does not present graphical results for all the considered earthquakes that were applied, Instead, the maximum response of the stories is presented in Tables 15 to 16 in the X and Y directions of the 8-Story Deniz building, respectively.

Table 15. Max story response in X-direction of 8-story Deniz building with configuration 2 of MS

Output Case		Story Displacement (mm)	Story Drift (Ratio)	Story Acceleration (m/sec²)
1. DUZCE X-X Y-Y	Original	50.81	0.001778	3.27
	Strengthened	17.41	0.000398	2.9
Reduction %		66	78	11
1. DUZCE X-Y Y-X	Original	73.24	0.002688	4.38
	Strengthened	19.21	0.000403	3.03
Reduction %		74	85	31
2. FRIULI X-X Y-Y	Original	60.32	0.002108	2.88
	Strengthened	17.89	0.000349	3.21
Reduction %		70	83	-11
2. FRIULI X-Y Y-X	Original	67.65	0.002437	3.55
	Strengthened	19.67	0.000453	3.21
Reduction %		71	81	10
3. IMPVAL X-X Y-Y	Original	65.87	0.002333	3.52
	Strengthened	18.39	0.000437	2.99
Reduction %		72	81	15
3. IMPVAL X-Y Y-X	Original	64.1	0.002025	3.64
	Strengthened	17.4	0.000367	2.92
Reduction %		73	82	20

4. KERN X-X Y-Y	Original	72.1	0.002195	4.8
	Strengthened	16.53	0.000353	3.27
Reduction %		77	84	32
4.KERN X-Y Y-X	Original	56.05	0.001999	2.82
	Strengthened	19.65	0.00042	3.67
Reduction %		65	79	-30
5.KOBE X-X Y-Y	Original	68.45	0.002648	4.7
	Strengthened	17.5	0.000369	3.17
Reduction %		74	86	32
5. KOBE X-Y Y-X	Original	63.7	0.002387	3.12
	Strengthened	14.96	0.000358	2.49
Reduction %		76	85	20
6.KOCAELI X-X Y-Y	Original	61.79	0.001786	4.35
	Strengthened	18.36	0.000361	2.53
Reduction %		70	80	42
6. KOCAELI X-Y Y-X	Original	50.077	0.002164	3.11
	Strengthened	12.59	0.000262	2.79
Reduction %		75	88	10
5. LANDERS X-X Y-Y	Original	63.73	0.002365	3.35
	Strengthened	18.29	0.000482	4.44
Reduction %		71	80	-32
7. LANDERS X-Y Y-X	Original	52.25	0.001851	3.19
	Strengthened	17.04	0.000327	2.52
Reduction %		67	82	21
8.LOMA X-X Y-Y	Original	75.64	0.002401	4.06
	Strengthened	18.82	0.000424	2.96
Reduction %		75	82	27
8. LOMA X-Y Y-X	Original	73.8	0.00278	4.13
	Strengthened	19.01	0.000447	3.28
Reduction %		74	84	21
9. MANJIL X-X Y-Y	Original	83.23	0.002287	3.73
	Strengthened	18.65	0.000383	3.22
Reduction %		78	83	14
9. MANJIL X-Y Y-X	Original	58.23	0.002207	3.25
	Strengthened	19.34	0.000524	3.07

Reduction %		67	76	6
10 MORGAN X-X Y-Y	Original	61.35	0.002433	4.11
	Strengthened	19.43	0.000429	3.08
Reduction %		68	82	25
10 MORGAN X-Y Y-X	Original	73.23	0.002769	2.41
	Strengthened	21.03	0.000488	3.5
Reduction %		71	82	-45
11. NORTHR X-X Y-Y	Original	66.27	0.00286	3.6
	Strengthened	16.94	0.000473	3.5
Reduction %		74	83	3
11. NORTHR X-Y Y-X	Original	60.63	0.001949	3.8
	Strengthened	18.78	0.000464	3.53
Reduction %		69	76	7

Table 16. Max story response in Y-direction of 8-story Deniz building with configuration 2 of MS

Output Case		**Story Displacement (mm)**	**Story Drift (Ratio)**	**Story Acceleration (m/sec²)**
1. DUZCE X-X Y-Y	Original	50.26	0.001752	3.56
	Strengthened	21.08	0.000428	2.61
Reduction %		58	76	27
1. DUZCE X-Y Y-X	Original	46.97	0.001374	4.08
	Strengthened	15.22	0.000336	2.49
Reduction %		68	75	39
2. FRIULI X-X Y-Y	Original	49.9	0.001746	3.82
	Strengthened	15.74	0.00034	2.37
Reduction %		68	80	38
2. FRIULI X-Y Y-X	Original	42.23	0.001539	2.84
	Strengthened	17.4	0.000367	2.66
Reduction %		59	76	6
3. IMPVAL X-X Y-Y	Original	49.87	0.001598	2.83
	Strengthened	18.44	0.000431	2.93
Reduction %		63	73	-3
3. IMPVAL	Original	46.63	0.001381	2.83

X-Y Y-X	Strengthened	15.59	0.000339	2.5
Reduction %		67	75	12
4. KERN	Original	44.21	0.001355	2.62
X-X Y-Y	Strengthened	20.1	0.000435	2.93
Reduction %		55	68	-12
4.KERN	Original	52.11	0.001464	3.55
X-Y Y-X	Strengthened	19.52	0.000366	2.91
Reduction %		62	75	18
5.KOBE	Original	48.96	0.001451	3.12
X-X Y-Y	Strengthened	17.2	0.000291	2.38
Reduction %		65	80	24
5. KOBE	Original	41.94	0.001392	3.48
X-Y Y-X	Strengthened	19.6	0.00041	2.85
Reduction %		53	71	18
6.KOCAELI	Original	41.23	0.001505	3.02
X-X Y-Y	Strengthened	15.39	0.000357	3.06
Reduction %		63	76	-1.3
6. KOCAELI	Original	42.35	0.001306	3.36
X-Y Y-X	Strengthened	19.77	0.000369	2.97
Reduction %		53	72	12
7. LANDERS	Original	64.29	0.002458	3.66
X-X Y-Y	Strengthened	17.22	0.000318	2.24
Reduction %		73	87	39
7. LANDERS	Original	45.73	0.001413	3.23
X-Y Y-X	Strengthened	16.76	0.000341	2.36
Reduction %		63	76	27
8.LOMA	Original	41.38	0.001696	3.28
X-X Y-Y	Strengthened	17.32	0.000427	2.79
Reduction %		58	75	15
8. LOMA	Original	52.09	0.001554	3.5
X-Y Y-X	Strengthened	15.94	0.000402	2.32
Reduction %		69	74	34
9. MANJIL	Original	53.33	0.001725	2.65
X-X Y-Y	Strengthened	18.38	0.000413	2.74
Reduction %		65	76	-3.4

9. MANJIL	Original	51.4	0.001416	2.86
X-Y Y-X	Strengthened	16.24	0.000419	2.79
Reduction %		68	70	2
10 MORGAN	Original	31.72	0.001296	2.92
X-X Y-Y	Strengthened	18.95	0.000353	2.87
Reduction %		40	73	2
10 MORGAN	Original	54.83	0.001884	3.54
X-Y Y-X	Strengthened	15.27	0.000325	2.44
Reduction %		72	83	31
11. NORTHR	Original	49.65	0.001879	3.13
X-X Y-Y	Strengthened	17.05	0.00031	2.89
Reduction %		66	83	8
11. NORTHR	Original	41.66	0.001832	3.75
X-Y Y-X	Strengthened	18.25	0.000343	3.79
Reduction %		56	81	-1

Tables 15 and 16 demonstrated the maximum responses of 8-Story original and strengthened with configuration 2 building, story displacement, story drift, and story acceleration, all of which are significantly decreased compared to the original building. The reduction of the displacement in most of the cases are over 65% for X-direction, while, in Y-direction most of the cases are over 55%. The reduction of the drift in most of the cases are over 80% for X-direction, while, in Y-direction most of the cases are over 70%, which is the same as for configuration 1. Furthermore, the reduction of the acceleration in the X-direction in most of the cases varies between 3% to 42% while in Y-direction most of the cases vary between 2% to 39%. Further, 4 of the cases in X-direction resulted in acceleration increment varying between 11% up to 45%. 5 of the cases in Y-direction resulted in acceleration increment varying between 1% up to 12%.

By comparing the results of configuration 1 and configuration 2 it showed that displacement and drift results are very close. However, the acceleration results in the X-direction showed that there is a slight difference with the acceleration reduction percentage but there is more acceleration increment percentage for configuration 2. While the Y-direction showed that configuration 1 has better performance in the acceleration reduction when compared to configuration 2.

Further, as mentioned earlier this can be due to SHARK performance may behave like a stiff restrainer in some earthquake events, in which this issue can be addressed by the usage of SHARK-Adaptive which can provide effective protection of non-structural components and technological content of the building because of the flexible damper response (minimization of peak floor accelerations) under weak but frequent SLS earthquakes.

Further, due to long-period earthquakes, because of the close correlation between the period of the strengthened building and some of the selected earthquakes. Nevertheless, both configurations have shown significantly better seismic performance than the original ones, which approve of the effectiveness of SHARK as an energy dissipation device in both configurations.

4.3.1.2.5 Input Energy of 8-Story Deniz Building with Configuration 2 of MS Results Comparison

The input energy caused by earthquakes subjected to original and strengthened buildings is shown in Table 17. According to the results, the strengthened building showed a significant decrease in the Input energy as compared to the original building.

Table 17. Input energy of 8-story Deniz building with configuration 2 of MS results

Output Case	Original kN-m	Strengthened kN-m	Reduction %
1. DUZCE X-X Y-Y	**229.5858**	147.7328	36
1. DUZCE X-Y Y-X	**252.9478**	96.6466	62
2. FRIULI X-X Y-Y	**510.8472**	183.0025	64
2. FRIULI X-Y Y-X	**511.596**	200.9595	61
3. IMPVAL X-X Y-Y	**1034.5741**	531.0618	49
3. IMPVAL X-Y Y-X	**829.4655**	378.2784	54
4. KERN X-X Y-Y	**483.8709**	293.0583	39
4. KERN X-Y Y-X	**555.8534**	305.6324	45
5. KOBE X-X Y-Y	**432.5402**	128.5034	70
5. KOBE X-Y Y-X	**469.9797**	145.0765	69
6. KOCAELI X-X Y-Y	**304.4265**	106.6303	65
6. KOCAELI X-Y Y-X	**221.4493**	108.9572	51
7. LANDERS X-X Y-Y	**324.9492**	111.8569	66
7. LANDERS X-Y Y-X	**336.4976**	101.8414	70
8. LOMA X-X Y-Y	**592.2024**	257.867	56
8. LOMA X-Y Y-X	**589.2366**	204.2867	65
9. MANJIL X-X Y-Y	**343.3354**	178.379	48
9. MANJIL X-Y Y-X	**357.7581**	170.0593	52
10 MORGAN X-X Y-Y	**271.8399**	151.0671	44
10 MORGAN X-Y Y-X	**273.9571**	123.1499	55
11. NORTHR X-X Y-Y	**340.3192**	199.1478	41
11. NORTHR X-Y Y-X	**415.5953**	215.1773	48

4.3.1.2.6 ISDR limit according to TBEC-2018

The variance of ISDR requirements along stories height of the 8-Story strengthened building is shown in Tables 18 and 19.

A building's drift demand is calculated by subtracting the consecutive story displacements, resulting from the analysis of the building under earthquake effects as specified by Eq. (4) By using Eq. (5), we can determine the effective story drift. the maximum ratio of story drift to story height is calculated as specified in Eq. (6) to determine the maximum ISDR of the building. According to the results, the ISDR requirements should be less than 26 percent, which is a limit according to TBEC-2018.

Table 18. ISDR in X-direction of 8-story building with configuration 2

Story No.	Original ISDR	Limit Check	Strengthened	Limit Check
8	0.013546	Within limit	0.001506	Within limit
7	0.012327	Within limit	0.002509	Within limit
6	0.008473	Within limit	0.002965	Within limit
5	0.017146	Within limit	0.003104	Within limit
4	**0.028507**	**More than limit**	0.003789	Within limit
3	**0.026357**	**More than limit**	0.004122	Within limit
2	0.022601	Within limit	0.003928	Within limit
1	0.011206	Within limit	0.00209	Within limit

Table 19. ISDR in Y-direction of 8-story building with configuration 2

Story No.	Original ISDR	Limit Check	Strengthened	Limit Check
8	0.008215	Within limit	0.001346	Within limit
7	0.019213	Within limit	0.002556	Within limit
6	0.020939	Within limit	0.003874	Within limit
5	0.02047	Within limit	0.004936	Within limit
4	0.023357	Within limit	0.005742	Within limit
3	0.020065	Within limit	0.005008	Within limit
2	0.016867	Within limit	0.004327	Within limit
1	0.009525	Within limit	0.002551	Within limit

According to the results, the ISDR in X-direction of the original building showed that stories 3 and 4 have more than the ISDR limit however, the strengthened building reduced the ISDR and performed within the limit. Furthermore, the ISDR for the strengthened building showed much less when compared to the original building.

4.3.1.3 Comparing Configuration 1 and 2 Results

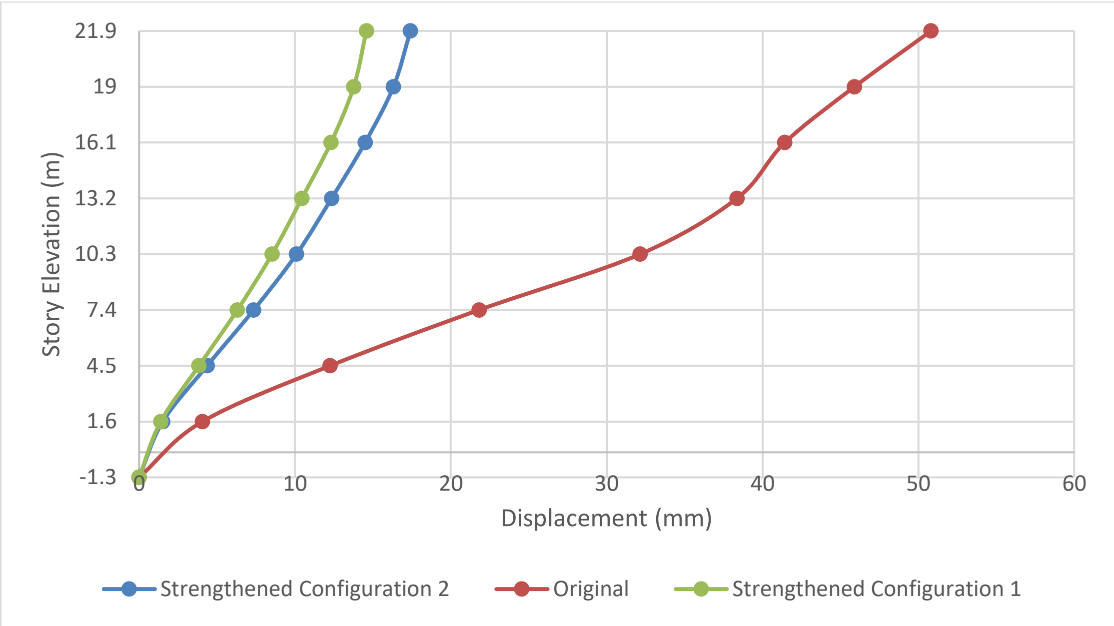

Figure 70. Comparison of stories displacement in X-direction of 8-story building with configuration 1 and 2 of MS subjected to Duzce X-X Y-Y earthquake

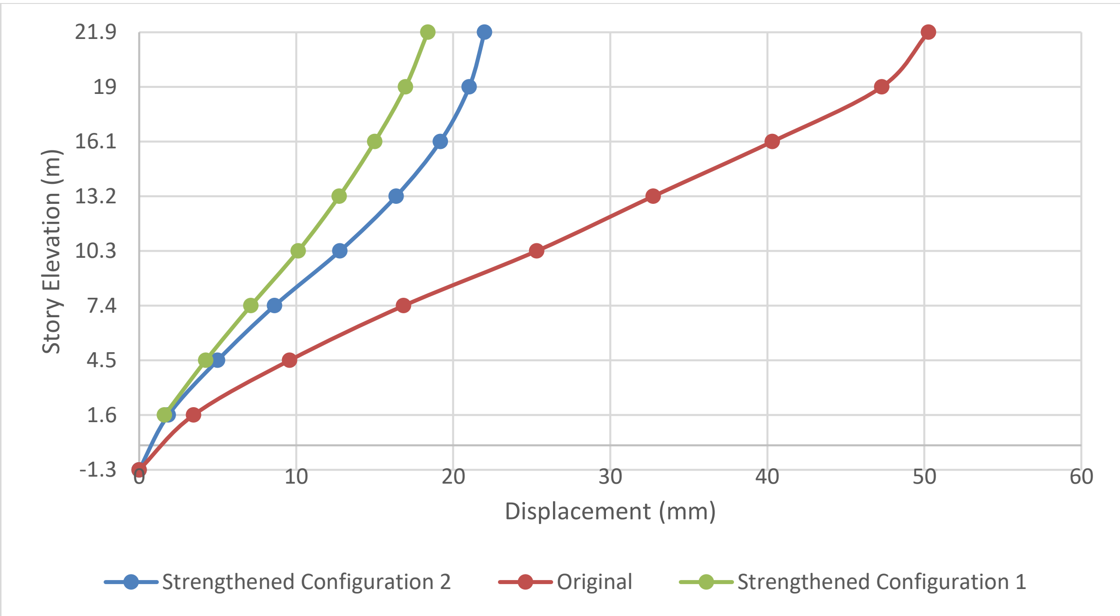

Figure 71.Comparison of stories displacement in Y-direction of 8-story building with configuration 1 and 2 of MS subjected to Duzce X-X Y-Y earthquake

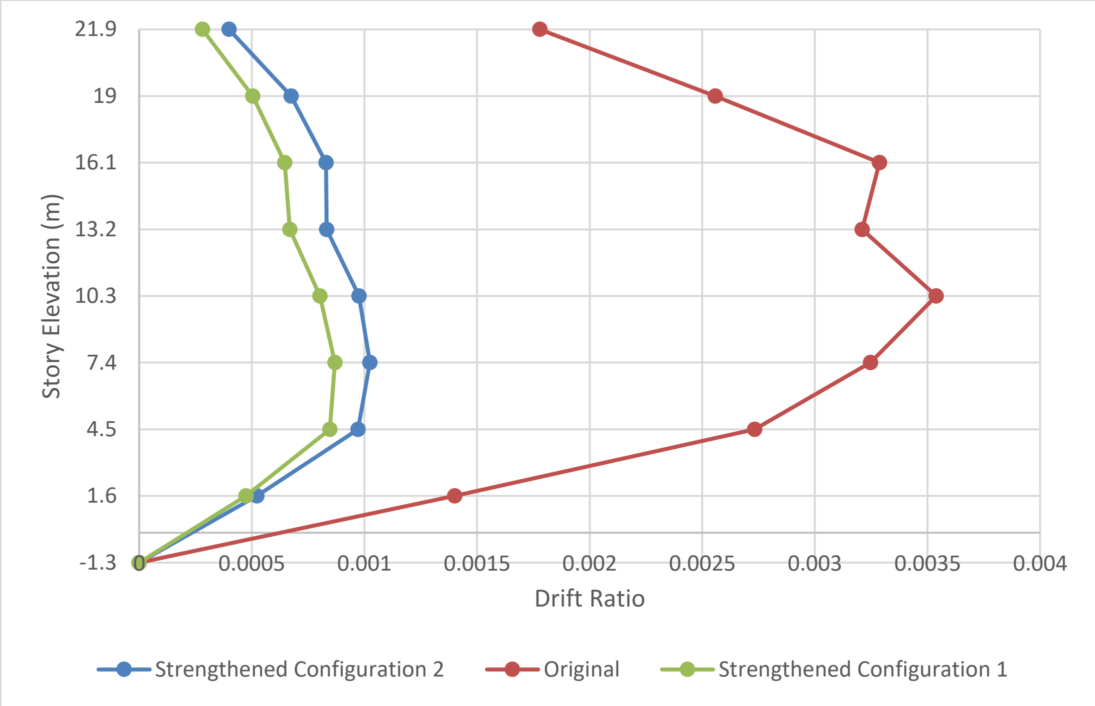

Figure 72. Comparison of stories drift in X-direction of 8-story building with configuration 1 and 2 of MS subjected to Duzce X-X Y-Y earthquake

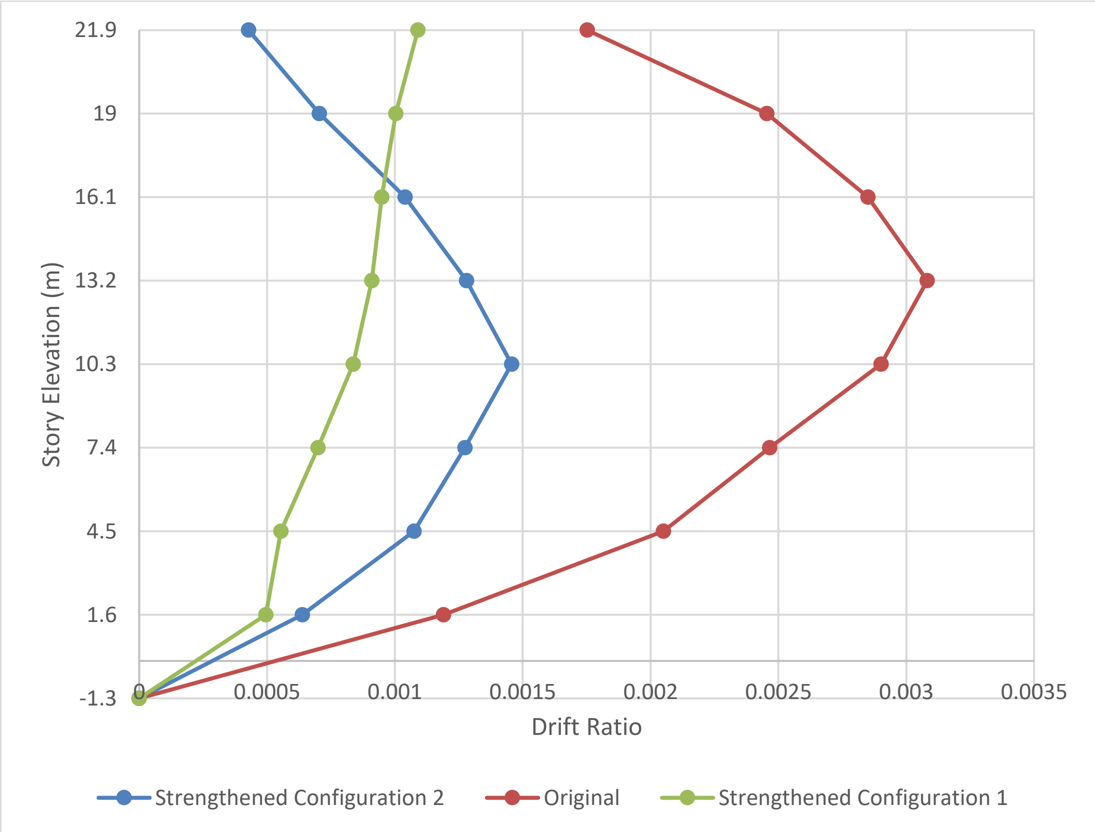

Figure 73. Comparison of stories drift in Y-direction of 8-story building with configuration 1 and 2 of MS subjected to Duzce X-X Y-Y earthquake

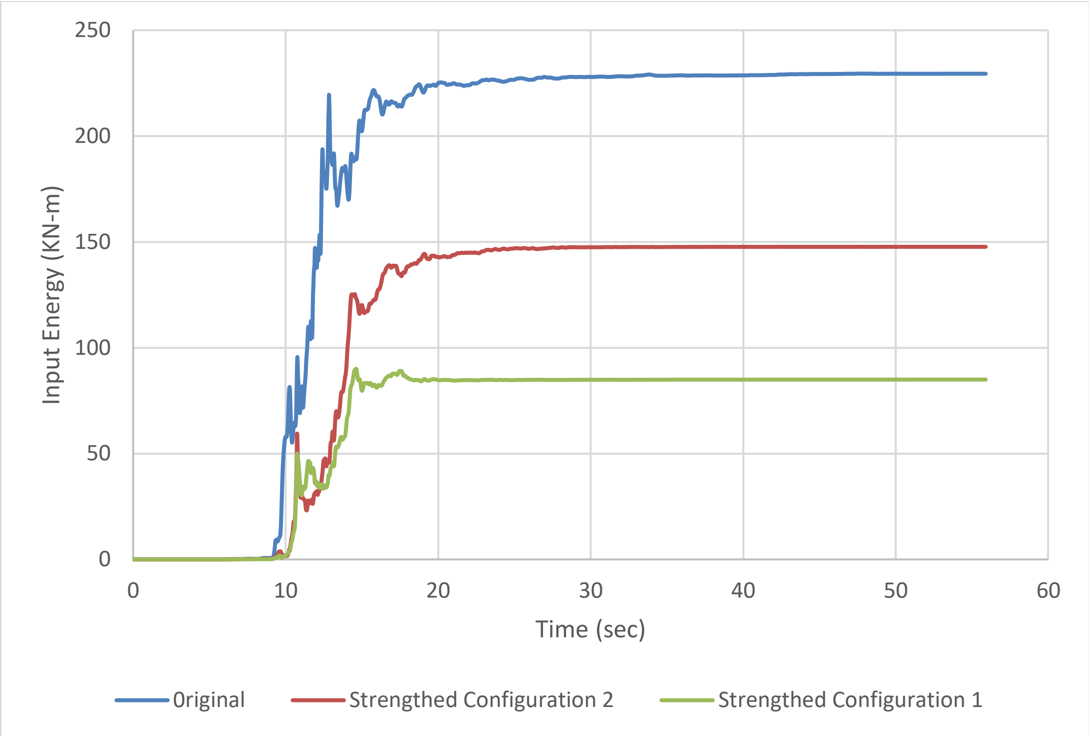

Figure 74. Comparison of input energy of 8-story building with configuration 1 and 2 of MS subjected to Duzce X-X Y-Y earthquake

According to the obtained results of stories response shown in Figures 70 to 74, the strengthening of the 8-Story building by the implementation of SHARK in configurations 1 and 2 showed that both configurations are within the specified limits according to TBEC-2018. However, configuration 1 reduced the displacement, drift, and the input energy more when compared to configuration 2. Furthermore, by considering the cost of the strengthening technique, it can be considered that configuration 2 is more economical. Because less SHARK devices have been applied to the 8-story building. Therefore, the implementation of configuration 2 is recommended to strengthen Deniz building.

4.3.1.4 MAURER SHARK Configuration 1 Applied to 6 Stories of the 8-Story Building Subjected to DUZCE X-X Y-Y

The following results demonstrate story response of the 8-Story bulding strengthened with configuration 1 by the implementation of MAURER SHARK to only 6 of the 8 stories shown in Figure 75.

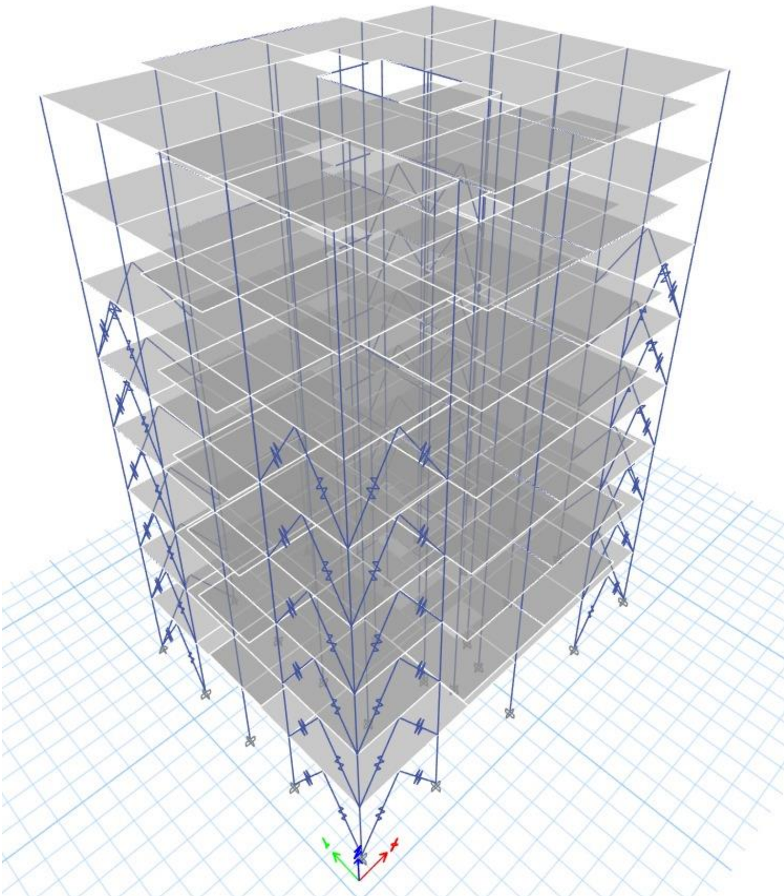

Figure 75. 8-Story building with MAURER SHARK on configuration 1 applied to 6 stories

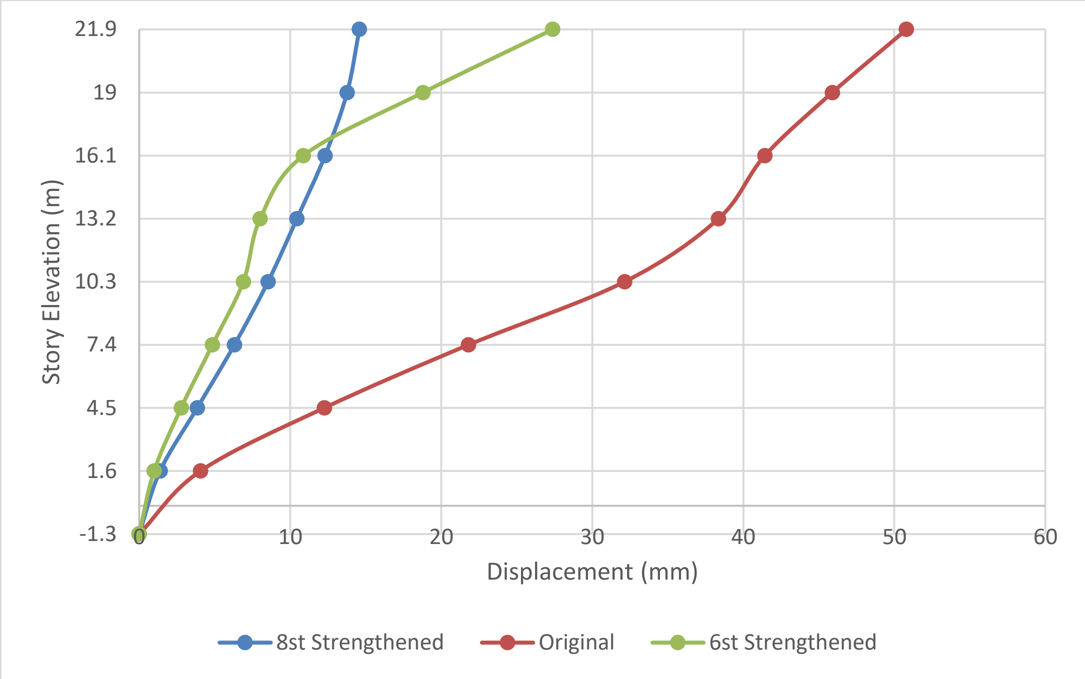

Figure 76. Comparison of stories displacement in X-direction of 8-story building with configuration 1 of MS applied to 6 stories and 8 stories subjected to Duzce X-X Y-Y

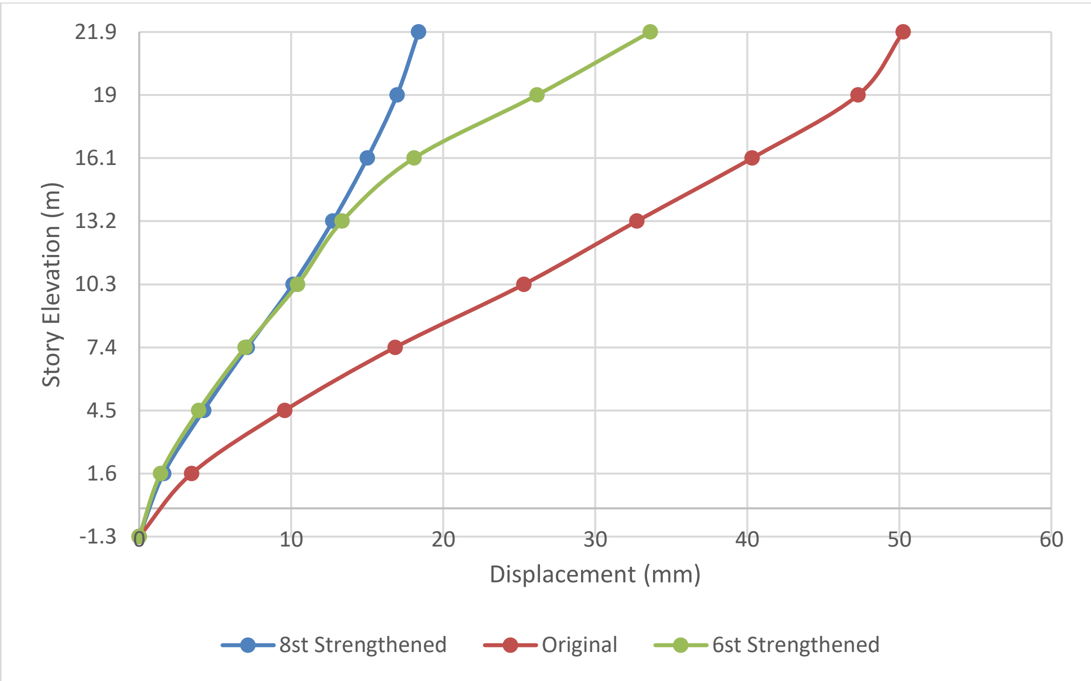

Figure 77. Comparison of stories displacement in Y-direction of 8-story building with configuration 1 of MS applied to 6 stories and 8 stories subjected to Duzce X-X Y-Y

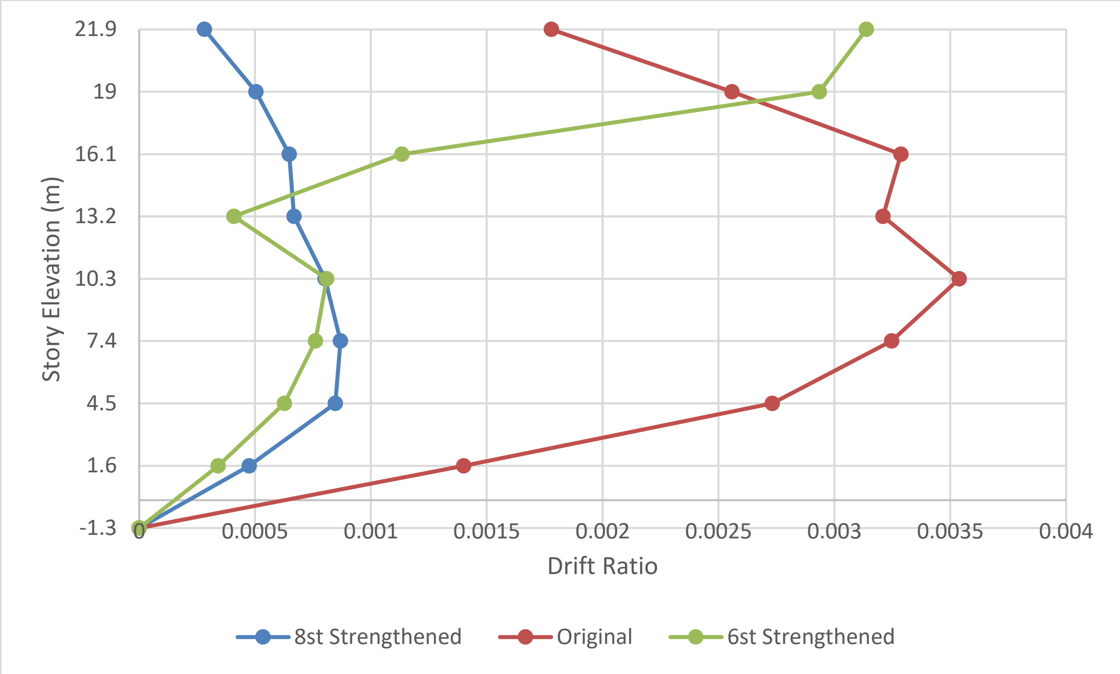

Figure 78. Comparison of stories drift in X-direction of 8-story building with configuration 1 of MS applied to 6 stories and 8 stories subjected to Duzce X-X Y-Y

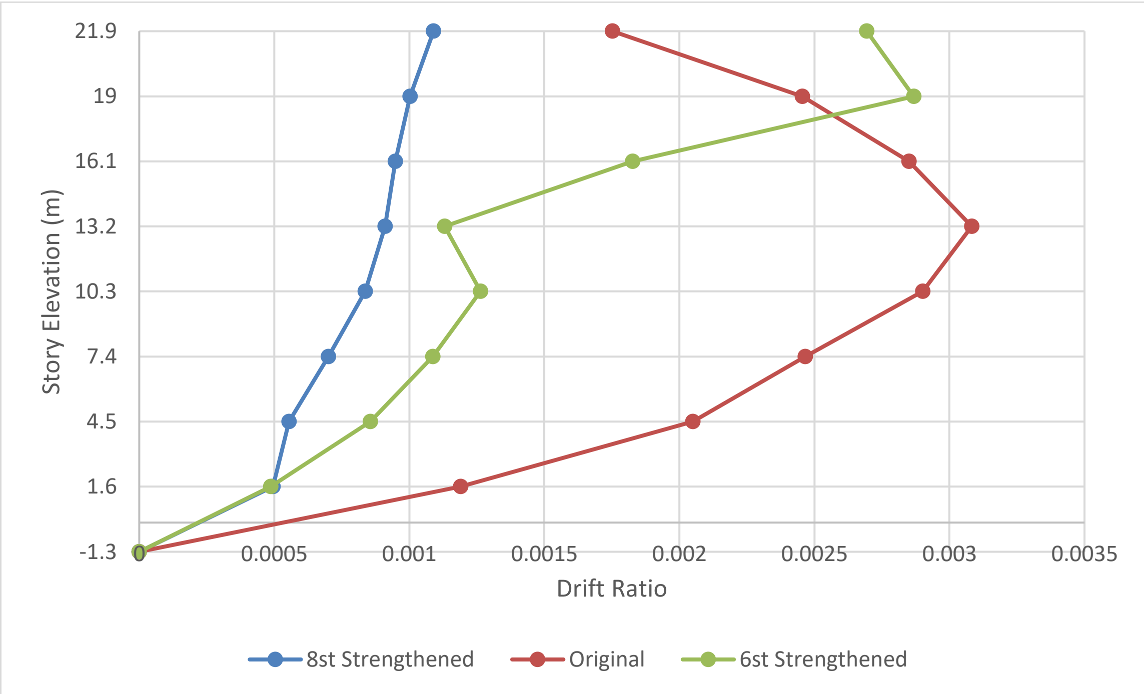

Figure 79. Comparison of stories drift in Y-direction of 8-story building with configuration 1 of MS applied to 6 stories and 8 stories subjected to Duzce X-X Y-Y

According to the results shown in Figures 76 to 79, the implementation of the MAURER SHARK to 6 of the 8-Story building didn't show a good performance for stories 7 and 8 specifically when compared to the strengthened building with the implementation of the MAURER SHARK to the 8 stories. Further the drift of the upper stories resulted to be more than the original building with a sudden strength change. Therefore, the implementation of MAURER SHARK to only 6 of the stories is not recommended. As it can be concluded from the obtained results, applying the energy absorbers only to some of the stories is not providing efficient strengthening. There should be continuous installation of energy absorbers in each story with an acceptable configuration.

Chapter 5

CONCLUSION AND RECOMMENDATIONS

5.1 Conclusion

In this study, the seismic strengthening of multi-story existing RC buildings was carried out by the implementation of MAURER SHARK Hysteretic Energy Dissipation Device (HEDD). The proposed design and configuration have been evaluated through nonlinear time history analyses NLTHA by applying a pair of 11 selected earthquake records on 8-Story RC buildings. The implementation of the SHARK has been carried out in two configurations for the 8-story building by the usage of the specified sizes and values by MAURER and applying it in the ETABS program to achieve the proper behavior of the energy dissipation system against earthquakes. The x- and y- components of the earthquakes were applied to the x- and y-directions of the building, and the y- and x- components of the earthquakes were applied to the x- and y-directions of the building, respectively.

It was observed that the seismic responses of the strengthened structures were significantly higher than the original structures. The levels of input energy decreased considerably, and the structure was able to resist various earthquakes events with less displacement, drift ratio, and acceleration. The following conclusions can be derived from the results of the conducted NLTHA:

- The maximum displacement reduction values of the strengthened buildings are between 70% and 80% in comparison with their original buildings. The reduction is on average about 78% and 72% for the X-direction of the 8-Story building with Configuration 1 and Configuration 2, respectively. However, for the Y-direction resulted in 64% and 62% reduction Configuration 1 and Configuration 2, respectively. The applied configuration and number of stories affect the displacement performance.
- The maximum drift reduction values of the strengthened buildings are between 70% and 80% in comparison with their original buildings. The reduction is on average about 87% and 82% for the X-direction of the 8-Story building with Configuration 1 and Configuration 2, respectively. However, for the Y-direction resulted in 69% and 76% reduction Configuration 1 and Configuration 2, respectively. The applied configuration and number of stories affect the drift performance.
- The maximum acceleration reduction values of the strengthened buildings are between 4% and 20% in comparison with their original buildings. The reduction is on average about 17% and 10% for the X-direction of the 8-Story building with Configuration 1 and Configuration 2, respectively. Furthermore, there were some cases with acceleration increment which can be due to the fact the SHARK performance characteristic may behave like a stiff restrainer in some earthquake events which led to an increment of the story acceleration, this issue can be addressed by the usage of SHARK-Adaptive which can provides effective protection of non-structural components and technological content of the building because of the flexible damper response (minimization of peak floor accelerations) under weak but frequent SLS earthquakes. This

beneficial performance is essential for high technology buildings (e.g., hospitals, police stations, fire stations, data centers, important commercial structures, or emergency management centers) that are required to remain fully operational in the emergency response after an earthquake. Further, it can be due to long-period earthquake, because of the close correlation between the period of the strengthened building and some of the selected earthquakes. Nevertheless, most of the strengthened buildings have shown significantly better seismic performance than the original ones, which approve of the effectiveness of SHARK as an energy dissipation device.

- The input energy of the strengthened building showed a significant decrease as compared to the original building. The reduction is on average about 64% and 70% for the 8-Story building with Configuration 1 and Configuration 2, respectively. It can be concluded that the MAURER SHARK decreased the input energy more for the lower stories' buildings at the specified configuration.
- All the results of the Inter Story Drift Ratio ISDR of the strengthen building are less than the estimated limit according to TBEC-2018.

Based on the above conclusions, the use of the proposed MAURER SHARK, which provides high protection of the structure during severe ULS earthquakes, long-term reliability against wear and fatigue problems, high redundant safety level, easy visual inspection, and easy to replace at low cost, is highly recommended, either for seismic strengthening of the existing buildings or newly designed ones. Finally, it should be emphasized that this study was limited to a few multi-story RC buildings. For more encompassing conclusions, this study should be expanded to encompass several buildings. Further study topics in this area are discussed in the following section.

5.2 Recommendations

The comprehensive analytical work conducted in this research has improved the understanding of earthquake effects on buildings, building behavior, seismic strengthening, and hysteretic energy absorbers. However, some investigation needs to be addressed. Further research in this area is recommended as follows:

- The analyses in this study were carried out using single computer software. Although ETABS is widely used for structural analysis in academia and engineering offices, it is better to compare the results from various software than to rely on one source of information. It is recommended to validate the results of further study with different software.
- In this thesis, Non-linear Time History analysis is performed on a three-dimensional system model and the then the building is strengthened. But here, the building was a simplified model of a real building with basic structural framing which didn't include various elements such as walls, elevator, stair, etc. For further studies, it's highly recommended to analyze the performance of the building with pushover analysis considering the weak zones to investigate more realistic properties of the structure.
- Non-structural elements include things like windows, doors, and other finishing materials were not considered in this study. Therefore, it's highly recommended to consider the implementation of MAURER SHARK based on the placement of non-structural elements and/or suggest removal for some unnecessary windows or doors if there is any.

- When the SHARK experiences minor serviceability limit states (SLS), like other conventional bilinear dampers, the damper primarily operates in its elastic range, acting as a stiff restraint without reducing the input of the earthquake. Therefore, it's recommended to use SHARK-Adaptive configuration to address this issue effectively.
- Applying installation layout 2 shown in Figure 16 is recommended and check how it affects the results.
- Design based on different codes to evaluate the effectiveness of MAURER dissipation device according to specific requirements.
- It’s recommended that to make a study on the cost evaluation of applying the MAURER devices to the buildings.

REFERENCES

Abrahamson, N. A., & Bommer, J. J. (2005). Probability and uncertainty in seismic hazard analysis. *Earthquake spectra*, *21*(2), 603-607.

Agency, F. E. M. (2006). *Techniques for the seismic rehabilitation of existing buildings*. FEMA.

Aiken, I. D., Nims, D. K., Whittaker, A. S., & Kelly, J. M. (1993). Testing of passive energy dissipation systems. *Earthquake spectra*, *9*(3), 335-370.

Al Atik, L., & Abrahamson, N. (2010). An improved method for nonstationary spectral matching. *Earthquake spectra*, *26*(3), 601-617.

Almazán, J. L., Juan, C., Inaudi, J. A., López-García, D., & Izquierdo, L. E. (2007). A bidirectional and homogeneous tuned mass damper: a new device for passive control of vibrations. *Engineering Structures*, *29*(7), 1548-1560.

ASCE. (2007). Seismic rehabilitation of existing buildings.

ASCE. (2014). Seismic evaluation and retrofit of existing buildings.

Benjamin, J. R., & Cornell, C. A. (2014). *Probability, statistics, and decision for civil engineers*. Courier Corporation.

Bondy, K. D. (1996). A more rational approach to capacity design of seismic moment frame columns. *Earthquake Spectra*, *12*(3), 395-406.

Buckle, I. G., & Mayes, R. L. (1990). Seismic isolation: history, application, and performance—a world view. *Earthquake spectra*, *6*(2), 161-201.

Bulut, F., Aktuğ, B., Yaltırak, C., Doğru, A., & Özener, H. (2019). Magnitudes of future large earthquakes near Istanbul quantified from 1500 years of historical earthquakes, present-day microseismicity and GPS slip rates. *Tectonophysics, 764*, 77-87.

Castaldo, P. (2014). *Integrated seismic design of structure and control systems*. Springer.

Çağatay, İ. H. (2005). Experimental evaluation of buildings damaged in recent earthquakes in Turkey. *Engineering Failure Analysis*, *12*(3), 440-452.

Center, P. (2013). Peer ground motion database. Pacific Earthquake Engineering Research Center. *University of California, Berkeley, CA, http://ngawest2. berkeley. edu*.

Chao, S.-H., & Goel, S. C. (2006). Performance based seismic design of special truss moment frames. 4th international conference on earthquake engineering. Taipei. Taiwan, Chao, S.-H., Goel, S. C., & Lee, S.-S. (2007). A seismic design lateral force distribution based on inelastic state of structures. *Earthquake Spectra*, *23*(3), 547-569.

Code, T. B. E. (2018). Disaster and emergency management presidency. *Ministry of Interior, Ankara, Turkey*.

Constantinou, M. C., Soong, T. T., & Dargush, G. F. (1998). Passive energy dissipation systems for structural design and retrofit.

Deb, S. K. (2004). Seismic base isolation–An overview. *Current Science*, 1426-1430.

Demir, S., & Husem, M. (2018). Saw type seismic energy dissipaters: development and cyclic loading test. *Journal of Constructional Steel Research*, *150*, 264-276.

Desai, R., Khurd, V., Patil, S., & Bavane, N. (2016). Behavior of symmetric and asymmetric structure in high seismic zone. *International Journal of Engineering and Techniques*, *2*(6).

Di Cesare, A., & Ponzo, F. C. (2017). Seismic retrofit of reinforced concrete frame buildings with hysteretic bracing systems: design procedure and behaviour factor. *Shock and Vibration, 2017*.

Di Cesare, A., Ponzo, F. C., & Nigro, D. (2014). Assessment of the performance of hysteretic energy dissipation bracing systems. *Bulletin of earthquake engineering*, *12*(6), 2777-2796.

Dolce, M., Cardone, D., Ponzo, F. C., & Valente, C. (2005). Shaking table tests on reinforced concrete frames without and with passive control systems. *Earthquake engineering & structural dynamics*, *34*(14), 1687-1717.

Dooley, K. L., & Bracci, J. M. (2001). Seismic evaluation of column-to-beam strength ratios in reinforced concrete frames. *Structural Journal*, *98*(6), 843-851.

El-Betar, S. A. (2018). Seismic vulnerability evaluation of existing RC buildings. *HBRC journal*, *14*(2), 189-197.

Ellingwood, B. R., & Li, Y. (2009). Counteracting Structural Loads: Treatment in ASCE Standard 7-05. *Journal of structural engineering*, *135*(1), 94-97.

Fardis, M. N. (2005). *Designers' guide to EN 1998-1 and EN 1998-5 Eurocode 8: design of structures for earthquake resistance: general rules, seismic actions, design rules for buildings, foundations and retaining structures*. Thomas Telford Publishing.

Fema, P. (2012). 58-1 (2012) Seismic performance assessment of buildings (volume 1-Methodology). *Federal Emergency Management Agency, Washington*, *1*.

Franco, J., Cahís, X., Gracia, L., & López, F. (2010). Experimental testing of a new anti-seismic dissipator energy device based on the plasticity of metals. *Engineering structures*, *32*(9), 2672-2682.

Gandelli, E., Chernyshov, S., Distl, J., Dubini, P., Weber, F., & Taras, A. (2021). Novel adaptive hysteretic damper for enhanced seismic protection of braced buildings. *Soil Dynamics and Earthquake Engineering*, *141*, 106522.

Gkournelos, P., Triantafillou, T., & Bournas, D. (2021). Seismic upgrading of existing reinforced concrete buildings: A state-of-the-art review. *Engineering Structures*, *240*, 112273.

Goulet, C. A., Haselton, C. B., Mitrani-Reiser, J., Beck, J. L., Deierlein, G. G., Porter, K. A., & Stewart, J. P. (2007). Evaluation of the seismic performance of a code-conforming reinforced-concrete frame building—from seismic hazard to collapse safety and economic losses. *Earthquake Engineering & Structural Dynamics*, *36*(13), 1973-1997.

Gökkaya, K. (2016). Geographic analysis of earthquake damage in Turkey between 1900 and 2012. *Geomatics, Natural Hazards and Risk*, *7*(6), 1948-1961.

Housner, G., Bergman, L. A., Caughey, T. K., Chassiakos, A. G., Claus, R. O., Masri, S. F., . . . Yao, J. T. (1997). Structural control: past, present, and future. *Journal of engineering mechanics*, *123*(9), 897-971.

Hu, Y.-X., Liu, S.-C., & Dong, W. (1996). *Earthquake engineering*. CRC Press.

Inaudi, J. A., & Kelly, J. M. (1995). Mass damper using friction-dissipating devices. *Journal of Engineering Mechanics*, *121*(1), 142-149.

Isik, V., Uysal, I. T., Caglayan, A., & Seyitoglu, G. (2014). The evolution of intraplate fault systems in central Turkey: Structural evidence and Ar-Ar and Rb-Sr age constraints for the Savcili Fault Zone. *Tectonics*, *33*(10), 1875-1899.

Khampanit, A., Leelataviwat, S., Kochanin, J., & Warnitchai, P. (2014). Energy-based seismic strengthening design of non-ductile reinforced concrete frames using buckling-restrained braces. *Engineering Structures*, *81*, 110-122.

Kuntz, G. L., & Browning, J. (2003). Reduction of column yielding during earthquakes for reinforced concrete frames.

Lagaros, N. D., Fragiadakis, M., Papadrakakis, M., & Tsompanakis, Y. (2006). Structural optimization: A tool for evaluating seismic design procedures. *Engineering structures*, *28*(12), 1623-1633.

Liao, W.-C. (2010). *Performance-based plastic design of earthquake resistant reinforced concrete moment frames* University of Michigan].

Marnani, A. B., Zareei, S. A., Rahgozar, M. A., & Behravan, A. (2021). Study on Modern Energy Absorption Systems in Structures Subjected to Earthquake Forces. *Iranian Journal of Science and Technology, Transactions of Civil Engineering*, 1-13.

McGuire, R. K. (2008). Probabilistic seismic hazard analysis: Early history. *Earthquake Engineering & Structural Dynamics*, *37*(3), 329-338.

Moehle, J., & Deierlein, G. G. (2004). A framework methodology for performance-based earthquake engineering. 13th world conference on earthquake engineering,

Mojarab, M., Memarian, H., & Zare, M. (2015). Performance evaluation of the M8 algorithm to predict M7+ earthquakes in Turkey. *Arabian Journal of Geosciences*, *8*(8), 5921-5934.

Mokha, A. S., Amin, N., Constantinou, M. C., & Zayas, V. (1996). Seismic isolation retrofit of large historic building. *Journal of Structural Engineering*, *122*(3), 298-308.

Naeim, F., & Kelly, J. M. (1999). *Design of seismic isolated structures: from theory to practice*. John Wiley & Sons.

Massumi, A., & Absalan, M. (2013). Interaction between bracing system and moment resisting frame in braced RC frames. *archives of civil and mechanical engineering*, *13*(2), 260-268.

MAURER. (2020). MAURER SHARK® Short-Stroke Hysteretic Damper. Retrived from MAURER Retrieved ftom: https://www.maurer.eu/en/products/seismic-devices/dampers/index.html

NEHRP, F. (2006). Techniques for the seismic rehabilitation of existing buildings, FEMA 547. *Building Seismic Safety Council for the Federal Emergency Management Agency*.

Newmark, N. M., & Hall, W. J. (1969). Seismic design criteria for nuclear reactor facilities. In: Report.

Nikos, G. (2012). New strategy for controlling structures collapse against earthquakes. *Natural Science*, *2012*.

Pan, P., Zamfirescu, D., Nakashima, M., Nakayasu, N., & Kashiwa, H. (2005). Base-isolation design practice in Japan: introduction to the post-Kobe approach. *Journal of Earthquake Engineering*, *9*(01), 147-171.

Pekelnicky, R., Engineers, S., Chris Poland, S., & Engineers, N. (2012). ASCE 41-13: Seismic evaluation and retrofit rehabilitation of existing buildings. *Proceedings of the SEAOC*.

Perrone, D., Calvi, P., Nascimbene, R., Fischer, E., & Magliulo, G. (2019). Seismic performance of non-structural elements during the 2016 Central Italy earthquake. *Bulletin of Earthquake Engineering*, *17*(10), 5655-5677.

Pinho, R. (2000). *Selective retrofitting of RC structures in seismic areas* University of London].

Pinkaew, T., Lukkunaprasit, P., & Chatupote, P. (2003). Seismic effectiveness of tuned mass dampers for damage reduction of structures. *Engineering structures*, *25*(1), 39-46.

Prestandard, F. (2000). commentary for the seismic rehabilitation of buildings (FEMA356). *Washington, DC: Federal Emergency Management Agency*, *7*(2).

Priestley, M. N., Calvi, G. M., & Kowalsky, M. J. (2007). *Displacement based seismic design of structures*. Iuss.

Providakis, C. (2008). Effect of LRB isolators and supplemental viscous dampers on seismic isolated buildings under near-fault excitations. *Engineering structures*, *30*(5), 1187-1198.

Rabi, R. R., Bianco, V., & Monti, G. (2021). Energy-based Design Method for Passive Energy Dissipative Bracing Systems.

Reinhorn, A. M., Li, C., & Constantinou, M. (1995). Experimental and analytical investigation of seismic retrofit of structures with supplemental damping: Part. 1-fluid viscous damping devices. In *Experimental and analytical investigation of seismic retrofit of structures with supplemental damping: Part. 1-Fluid viscous damping devices* (pp. (120)-(120)).

Sabelli, R., Mahin, S., & Chang, C. (2003). Seismic demands on steel braced frame buildings with buckling-restrained braces. *Engineering Structures*, *25*(5), 655-666.

Sadek, F., Taylor, A. W., & Chung, R. M. (1996). *Passive energy dissipation devices for seismic applications*. US Department of Commerce, National Institute of Standards and Technology.

Sadhu, A., & Narasimhan, S. (2012). Identification of de-tuning level of tuned-mass-damper system using time-series analysis. *J. Mech. Eng. Autom*, *2*(1), 1-8.

Sahin, C. (2014). Seismic retrofitting of existing structures.

Sahoo, D. R., & Rai, D. C. (2010). Seismic strengthening of non-ductile reinforced concrete frames using aluminum shear links as energy-dissipation devices. *Engineering Structures*, *32*(11), 3548-3557.

Sahoo, D. R., & Rai, D. C. (2013). Design and evaluation of seismic strengthening techniques for reinforced concrete frames with soft ground story. *Engineering structures*, *56*, 1933-1944.

Šipoš, T. K., Hadzima-Nyarko, M., MILIČEVIĆ, I., & GRUBIŠIĆ, M. (2018). Structural performance levels for masonry infilled frames. *Proceedings of the 16th European Conference on Earthquake Engineering, Thessaloniki.*

Skinner, R. I., Robinson, W. H., & McVerry, G. H. (1993). *An introduction to seismic isolation*. Wiley.

Sladek, J. R., & Klingner, R. E. (1983). Effect of tuned-mass dampers on seismic response. *Journal of structural engineering*, *109*(8), 2004-2009.

Soong, T., & Dargush, G. (1999). Passive energy dissipation and active control. *Structural engineering handbook*, 1-28.

Soong, T. T., & Costantinou, M. C. (2014). *Passive and active structural vibration control in civil engineering* (Vol. 345). Springer.

Symans, M., Charney, F., Whittaker, A., Constantinou, M., Kircher, C., Johnson, M., & McNamara, R. (2008). Energy dissipation systems for seismic applications: current practice and recent developments. *Journal of structural engineering*, *134*(1), 3-21.

Symans, M. D., & Constantinou, M. C. (1997). Seismic testing of a building structure with a semi-active fluid damper control system. *Earthquake Engineering & Structural Dynamics*, *26*(7), 759-777.

Tena-Colunga, A., & Nangullasmú-Hernández, H. (2015). Assessment of seismic design parameters of moment resisting RC braced frames with metallic fuses. *Engineering Structures*, *95*, 138-153.

Tsai, K.-C., Chen, H.-W., Hong, C.-P., & Su, Y.-F. (1993). Design of steel triangular plate energy absorbers for seismic-resistant construction. *Earthquake spectra*, *9*(3), 505-528.

Tsionis, G., Apostolska, R., & Tauver, F. (2014). Seismic strengthening of RC buildings. *Luxembourg: Publications Office*.

Veletsos, A., & Newmark, N. M. (1960). Effect of inelastic behavior on the response of simple systems to earthquake motions.

Verde, R. V. (1991). Explanation for the numerous upper floor collapses during the 1985 Mexico City earthquake. *Earthquake engineering & structural dynamics*, *20*(3), 223-241.

Wilkinson, S., & Hiley, R. (2006). A non-linear response history model for the seismic analysis of high-rise framed buildings. *Computers & structures*, *84*(5-6), 318-329.

Yang, T., Moehle, J., Stojadinovic, B., & Der Kiureghian, A. (2009). Seismic performance evaluation of facilities: Methodology and implementation. *Journal of Structural Engineering*, *135*(10), 1146-1154.

Zhang, A., & Ye, Q. (2019). Design and testing of prefabricated steel frame with an innovative re-centering energy dissipative brace. *Engineering Structures*, *201*, 109791.